

JPTM

Journal of Pathology
and Translational Medicine

January 2025
Vol. 59 / No.1
jpatholm.org
pISSN: 2383-7837
eISSN: 2383-7845



*Hemochromatosis and
antibody-mediated
rejection in liver biopsies
after transplantation*

Journal of Pathology and Translational Medicine



Vol. 59, No.1, pp 1-90, January 2025

Aims & Scope

The *Journal of Pathology and Translational Medicine* is an open venue for the rapid publication of major achievements in various fields of pathology, cytopathology, and biomedical and translational research. The Journal aims to share new insights into the molecular and cellular mechanisms of human diseases and to report major advances in both experimental and clinical medicine, with a particular emphasis on translational research. The investigations of human cells and tissues using high-dimensional biology techniques such as genomics and proteomics will be given a high priority. Articles on stem cell biology are also welcome. The categories of manuscript include original articles, review and perspective articles, case studies, brief case reports, and letters to the editor.

Subscription Information

To subscribe to this journal, please contact the Korean Society of Pathologists/the Korean Society for Cytopathology. Full text PDF files are also available at the official website (<https://jpatholm.org>). *Journal of Pathology and Translational Medicine* is indexed by Emerging Sources Citation Index (ESCI), PubMed, PubMed Central, Scopus, KoreaMed, KoMCI, WPRIM, Directory of Open Access Journals (DOAJ), and CrossRef. Circulation number per issue is 50.

Contact the Korean Society of Pathologists/the Korean Society for Cytopathology

Publishers: Kang, Gyeong Hoon, MD; Choi, Yoon Jung, MD, PhD

Editors-in-Chief: Jung, Chan Kwon, MD; Park, So Yeon, MD

Published by the Korean Society of Pathologists/the Korean Society for Cytopathology

Editorial Office

Room 1209 Gwanghwamun Officia, 92 Saemunan-ro, Jongno-gu, Seoul 03186, Korea

Tel: +82-2-795-3094 Fax: +82-2-790-6635 E-mail: office@jpatholm.org

#1508 Renaissancetower, 14 Mallijae-ro, Mapo-gu, Seoul 04195, Korea

Tel: +82-2-593-6943 Fax: +82-2-593-6944 E-mail: office@jpatholm.org

Printed by M2PI

#805, 26 Sangwon 1-gil, Seongdong-gu, Seoul 04779, Korea

Tel: +82-2-6966-4930 Fax: +82-2-6966-4945 E-mail: support@m2-pi.com

Manuscript Editing by InfoLumi Co.

210-202, 421 Pangyo-ro, Bundang-gu, Seongnam 13522, Korea

Tel: +82-70-8839-8800 E-mail: infolumi.chang@gmail.com

Front cover image: Hemochromatosis and antibody-mediated rejection in liver biopsies after transplantation (p. 4, 6)

© 2025 The Korean Society of Pathologists/The Korean Society for Cytopathology

© Journal of Pathology and Translational Medicine is an Open Access journal under the terms of the Creative Commons Attribution Non-Commercial License (<https://creativecommons.org/licenses/by-nc/4.0>).

© This paper meets the requirements of KS X ISO 9706, ISO 9706-1994 and ANSI/NISO Z.39.48-1992 (Permanence of Paper).

Roche Digital Pathology

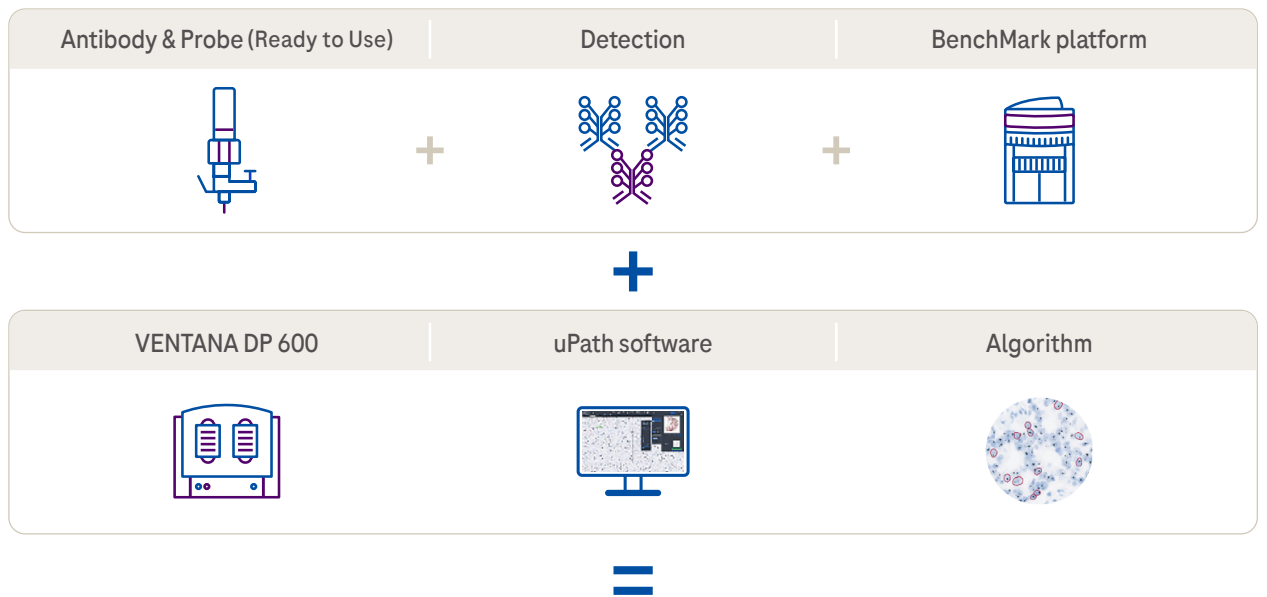


Ventana DP 600 / Ventana DP 200

로슈 슬라이드 스캐너는 트레이 베이스 스캔 방식을 통해, 보다 안정적인 슬라이드 스캔 환경을 제공합니다.

uPath Enterprise Software

uPath Enterprise Software는 뛰어난 성능, 맞춤형 구조 제공을 그리고 디지털화를 통해 판독 업무의 통합 솔루션 지원을 제공합니다.



염색부터 스캔 그리고 분석까지 표준화된 통합 시스템

Editorial Board

Editors-in-Chief

Jung, Chan Kwon, MD (*The Catholic University of Korea, Korea*) <https://orcid.org/0000-0001-6843-3708>
Park, So Yeon, MD (*Seoul National University, Korea*) <https://orcid.org/0000-0002-0299-7268>

Associate Editors

Bychkov, Andrey, MD (*Kameda Medical Center, Japan; Nagasaki University Hospital, Japan*) <https://orcid.org/0000-0002-4203-5696>
Kim, Haeryoung, MD (*Seoul National University, Korea*) <https://orcid.org/0000-0002-4205-9081>
Lee, Hee Eun, MD (*Mayo Clinic, USA*) <https://orcid.org/0000-0001-6335-7312>
Shin, Eunah, MD (*Yongin Severance Hospital, Yonsei University, Korea*) <https://orcid.org/0000-0001-5961-3563>

Editorial Board

Avila-Casado, Maria del Carmen, MD (*University of Toronto, Toronto General Hospital UHN, Canada*)
Bae, Jeong Mo, MD (*Seoul National University, Korea*)
Bae, Young Kyung, MD (*Yeungnam University, Korea*)
Bongiovanni, Massimo, MD (*Lausanne University Hospital, Switzerland*)
Bova, G. Steven, MD (*University of Tampere, Finland*)
Choi, Joon Hyuk (*Yeungnam University, Korea*)
Chong, Yo Sep, MD (*The Catholic University of Korea, Korea*)
Chung, Jin-Haeng, MD (*Seoul National University, Korea*)
Fadda, Guido, MD (*Catholic University of Rome-Foundation Agostino Gemelli University Hospital, Italy*)
Fukushima, Noriyoshi, MD (*Jichi Medical University, Japan*)
Go, Heounjeong (*University of Ulsan, Korea*)
Hong, Soon Won, MD (*Yonsei University, Korea*)
Jain, Deepali, MD (*All India Institute of Medical Sciences, India*)
Kakudo, Kennichi, MD (*Izumi City General Hospital, Japan*)
Kim, Jang-Hee, MD (*Ajou University, Korea*)
Kim, Jung Ho, MD (*Seoul National University, Korea*)
Kim, Se Hoon, MD (*Yonsei University, Korea*)
Komuta, Mina, MD (*Keio University, Tokyo, Japan*)
Lai, Chiung-Ru, MD (*Taipei Veterans General Hospital, Taiwan*)
Lee, C. Soon, MD (*University of Western Sydney, Australia*)
Lee, Hwajeong, MD (*Albany Medical College, USA*)
Lee, Sung Hak, MD (*The Catholic University of Korea, Korea*)
Liu, Zhiyan, MD (*Shanghai Jiao Tong University, China*)
Lkhagvadorj, Sayamaa, MD (*Mongolian National University of Medical Sciences, Mongolia*)
Moran, Cesar, MD (*MD Anderson Cancer Center, U.S.A.*)
Paik, Jin Ho, MD (*Seoul National University, Korea*)
Park, Jeong Hwan (*Seoul National University, Korea*)
Sakhuja, Puja, MD (*Govind Ballabh Pant Hospital, India*)
Shahid, Pervez, MD (*Aga Khan University, Pakistan*)
Song, Joon Seon, MD (*University of Ulsan, Korea*)
Tan, Puay Hoon, MD (*National University of Singapore, Singapore*)
Than, Nandor Gabor, MD (*Semmelweis University, Hungary*)
Tse, Gary M., MD (*The Chinese University of Hong Kong, Hong Kong*)
Yatabe, Yasushi, MD (*Aichi Cancer Center, Japan*)
Zhu, Yun, MD (*Jiangsu Institution of Nuclear Medicine, China*)

Ethic Editor

Choi, In-Hong, MD (*Yonsei University, Korea*)
Huh, Sun, MD (*Hallym University, Korea*)

Statistics Editors

Kim, Dong Wook (*National Health Insurance Service Ilsan Hospital, Korea*)
Lee, Hye Sun (*Yonsei University, Korea*)

Manuscript Editor

Chang, Soo-Hee (*InfoLumi Co., Korea*)

Layout Editor

Jeong, Eun Mi (*M2PI, Korea*)

Website and JATS XML File Producers

Choi, Min Young (*M2PI, Korea*)

Administrative Assistants

Lee, Hye jin (*The Korean Society of Pathologists*)
Kim, Song Yeun (*The Korean Society for Cytopathology*)

Contents

Vol. 59, No.1, January 2025

REVIEWS

- 1** Post-transplant liver biopsies: a concise and practical approach for beginners
Mohamad Beshar Ourfali, David Hirsch, Marianna Scranton, Tony El Jabbour
- 11** Professional biobanking education in Korea based on ISO 20387
Jong Ok Kim, Chungyeul Kim, Sangyong Song, Eunah Shin, Ji-Sun Song, Mee Sook Roh, Dong-chul Kim, Han-Kyeom Kim, Joon Mee Kim, Yeong Jin Choi
- 26** Breast fine-needle aspiration cytology in the era of core-needle biopsy: what is its role?
Ahrong Kim, Hyun Jung Lee, Jee Yeon Kim

ORIGINAL ARTICLES

- 39** Diagnosis of invasive encapsulated follicular variant papillary thyroid carcinoma by protein-based machine learning
Truong Phan-Xuan Nguyen, Minh-Khang Le, Sittiruk Roytrakul, Shanop Shuangshoti, Nakarin Kitkumthorn, Somboon Keelawat
- 50** The combination of CDX2 expression status and tumor-infiltrating lymphocyte density as a prognostic factor in adjuvant FOLFOX-treated patients with stage III colorectal cancers
Ji-Ae Lee, Hye Eun Park, Hye-Yeong Jin, Lingyan Jin, Seung Yeon Yoo, Nam-Yun Cho, Jeong Mo Bae, Jung Ho Kim, Gyeong Hoon Kang
- 60** Comparison of tissue-based and plasma-based testing for *EGFR* mutation in non-small cell lung cancer patients
Yoon Kyung Kang, Dong Hoon Shin, Joon Young Park, Chung Su Hwang, Hyun Jung Lee, Jung Hee Lee, Jee Yeon Kim, JooYoung Na
- 68** PLUNC downregulates the expression of PD-L1 by inhibiting the interaction of DDX17/ β -catenin in nasopharyngeal carcinoma
Ranran Feng, Yilin Guo, Meilin Chen, Ziyang Tian, Yijun Liu, Su Jiang, Jieyu Zhou, Qingluan Liu, Xiayu Li, Wei Xiong, Lei Shi, Songqing Fan, Guiyuan Li, Wenling Zhang

CASE STUDY

- 84** Primary renal *BCOR::CCNB3* sarcoma in a female patient: case report
Somang Lee, Binnari Kim

Post-transplant liver biopsies: a concise and practical approach for beginners

Mohamad Beshar Ourfali^{1*}, David Hirsch^{1*}, Marianna Scranton^{2,3}, Tony El Jabbour¹

¹Department of Pathology and Laboratory Medicine, Hartford Hospital, Hartford, CT, USA

²Connecticut GI, Hartford, CT, USA

³The Comprehensive Liver Center, Hartford Hospital, Hartford, CT, USA

Exposure to post-transplant liver biopsies varies among pathology residencies and largely depends on the institution's training program, particularly if the hospital has a liver transplant program. The interpretation of biopsies from transplanted livers presents its own set of challenges, even for those with a solid understanding of non-transplant medical liver biopsies. In this review, we aim to provide a succinct, step-by-step approach to help you interpret liver transplant biopsies. This article may be beneficial for residents interested in liver pathology, gastrointestinal and liver pathology fellows in the early stages of training, clinical gastroenterology and hepatology fellows, hepatologists and general pathologists who are curious about this niche.

Keywords: Liver transplantation; Graft rejection; Hepatitis, viral, human

INTRODUCTION

Liver transplantation has emerged as a vital therapeutic option for patients with liver failure and/or end-stage liver disease. While it offers significant benefits, it also presents risks and necessitates thorough monitoring to prevent rejection or failure of the transplanted liver. This monitoring is done radiologically and through serial blood liver function tests. The liver function test panel includes alkaline phosphatase, aspartate aminotransferase, alanine aminotransferase, albumin, gamma-glutamyl transferase, bilirubin, prothrombin time, and international normalized ratio. If abnormalities in the liver function tests cannot be explained clinically or radiologically, a biopsy is needed to determine any treatable etiology.

Assessing post-transplant liver biopsies can be challenging because of the wide range of potential pathologies. Breaking down

the assessment of these biopsies into six steps may provide a simplified approach, particularly for beginners. In each step, assess the biopsy for one broad category of etiologies and begin building a differential diagnosis list. After the final step, the comprehensive list of possible diagnoses can be further refined based on the clinical scenario.

STEP 1: DE NOVO DISEASES

De novo liver disease refers to the development of new liver pathology that was not present in the liver before transplantation. To assess this category of entities, begin by disregarding the fact that this is a post-transplant biopsy and assess whether the microscopic findings are pathognomonic of any known liver pathology. Employ the same approach you would use for non-transplant medical liver biopsies. [Table 1](#) summarizes the

Received: August 9, 2024 **Revised:** November 14, 2024 **Accepted:** November 15, 2024

Corresponding Author: Mohamad Beshar Ourfali

Department of Pathology and Laboratory Medicine, Hartford Hospital 80 Seymour Street, Hartford, CT 06106, USA

Tel: +1-860-972-2488, Fax: +1-860-545-2204, E-mail: Mohamad.Ourfali@hhchealth.org

*Mohamad Beshar Ourfali and David Hirsch contributed equally to this work.

This is an Open Access article distributed under the terms of the Creative Commons Attribution Non-Commercial License (<https://creativecommons.org/licenses/by-nc/4.0/>) which permits unrestricted non-commercial use, distribution, and reproduction in any medium, provided the original work is properly cited.

© 2025 The Korean Society of Pathologists/The Korean Society for Cytopathology

pathognomonic histologic findings of the most commonly encountered liver pathologies. These findings are also illustrated in Figs. 1–3.

STEP 2: RECURRENCE OF PRIMARY LIVER DISEASE

In this step, evaluate the primary liver disease that necessitated the transplant. If the disease is prone to recur, examine the biopsy for its distinct histologic features. Incorporate the possibility of disease recurrence into your growing list of differential diagnoses.

Wilson’s disease and alpha-1 antitrypsin deficiency are two primary liver diseases that typically do not recur following liver transplantation. Wilson’s disease arises from a mutation in the *ATP7B* gene, responsible for encoding a copper-transporting ATPase pivotal in excreting excess copper from the liver into bile [1]. Liver transplantation is considered curative as the transplanted liver possesses a functional *ATP7B* gene, facilitating effective regulation of copper metabolism [2]. Alpha-1 antitrypsin deficiency stems from mutations in the *SERPINA1* gene, leading to the production of abnormal alpha-1 antitrypsin protein, which accumulates in hepatocytes, causing inflammation and fibrosis [3]. Liver transplantation is curative for liver dysfunction caused by alpha-1 antitrypsin deficiency as the transplanted liver can produce normal alpha-1 antitrypsin protein [4].

Hereditary hemochromatosis, characterized by increased intestinal iron absorption due to a mutation in the *HFE* gene,

poses a different challenge [5]. It is controversial whether hemochromatosis can recur post-liver transplantation, although it is usually curative [5,6]. Additionally, due to their pathophysiology, primary biliary cholangitis, primary sclerosing cholangitis, autoimmune hepatitis, steatohepatitis, and hepatotropic viral hepatitis are also known to recur after liver transplantation [7-12].

STEP 3: REJECTION

In this step, you should assess the possibility of rejection and include it in the list of potential diagnoses. There are two types of rejection that can occur after liver transplantation: T cell-mediated rejection (TCMR) and antibody-mediated rejection (AMR).

TCMR is more commonly encountered and encompasses acute cellular rejection, chronic ductopenic rejection, and chronic rejection with foam cell arteriopathy. Given its prevalence in clinical practice, it is important to highlight the Banff scoring system. This system is commonly employed for both diagnosing and grading acute cellular rejection. It categorizes the typical histopathological findings of acute cellular rejection into three main areas: portal inflammation, bile duct inflammation, and venous endothelial inflammation. These categories are then graded on a scale ranging from none (0) to severe (3). A cumulative score of 0–1 indicates a negative result for acute cellular rejection, while a score of 2–3 is considered indeterminate or borderline. Mild rejection is denoted by a score of 3–4, moderate rejection by a score of 5–7, and severe rejection by a

Table 1. Common hepatic diseases with their characteristic histological findings

Disease	Characteristic histologic findings
Autoimmune hepatitis	Plasma cell-rich portal inflammation, interface activity, apoptotic hepatocytes, and lobular hepatitis [10]
Primary biliary cholangitis	Lymphocytes-predominant portal inflammation, damaged bile ducts with intraepithelial lymphocytes and epithelioid granulomas [7,10]
Primary sclerosing cholangitis	Edematous portal tracts with bile ductular reaction and neutrophils (early stages) fibrous cholangitis (late stages) [10]
Alcoholic and non-alcoholic steatohepatitis	Steatosis with lobular inflammation and ballooning degeneration with Mallory-Denk bodies [11]
Alpha-1 antitrypsin deficiency	Presence of intrahepatocytic alpha-1 antitrypsin globules visible on PAS-D stain [4]
Hereditary hemochromatosis	Panacinar intrahepatocytic deposition of iron visible on Prussian blue stain [13]
Wilson’s disease	Panacinar intrahepatocytic deposition of copper visible on Rhodanin stain [14]
Hepatitis B virus hepatitis	Lymphocytes-predominant portal inflammation, interface activity, and ground glass hepatocytes inclusion [12]
Hepatitis C virus hepatitis	Lymphocytes-predominant portal inflammation, interface activity, and lymphoid follicles formation [12]

PAS-D, periodic acid–Schiff–diastase.

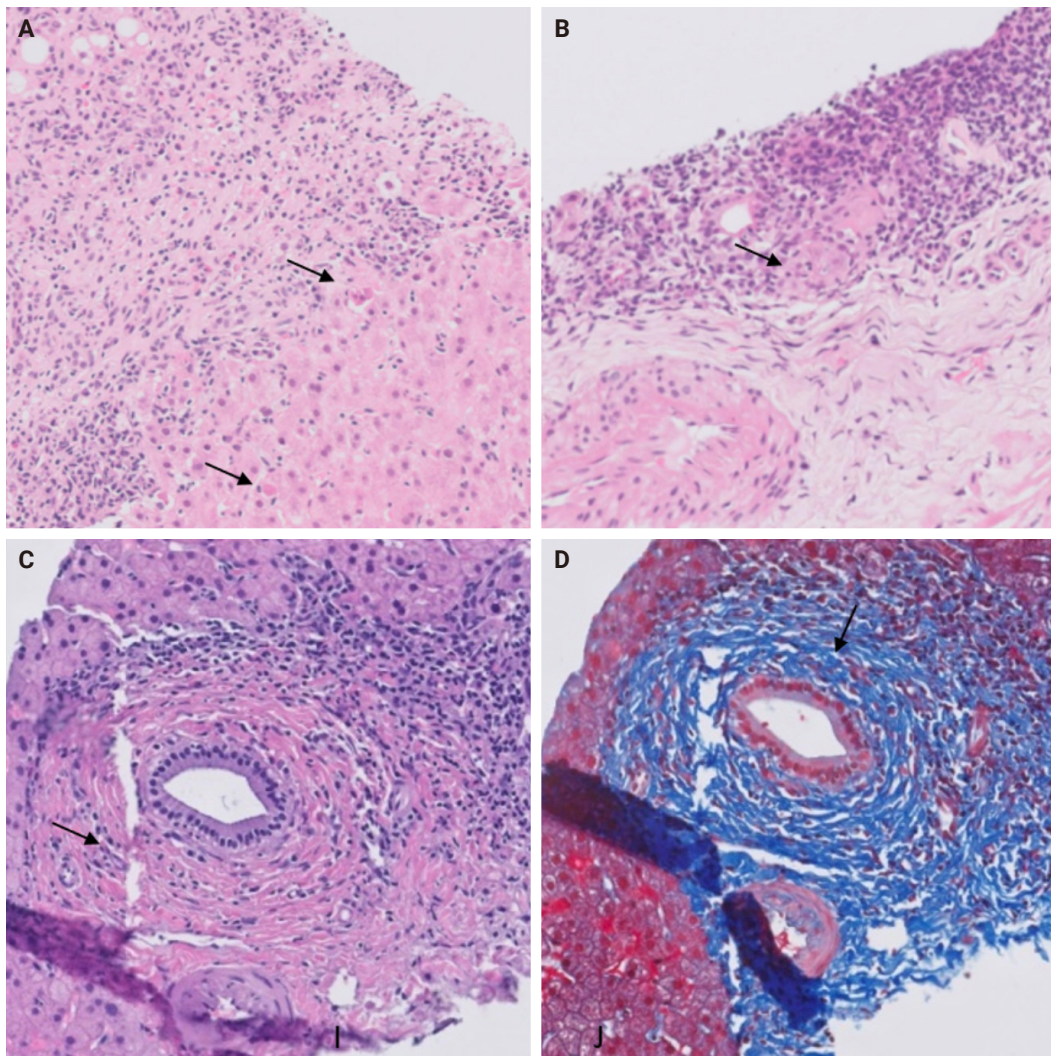


Fig. 1. (A) Autoimmune hepatitis: plasma cell-rich infiltrate with periportal apoptotic hepatocytes (arrows). (B) Primary biliary cholangitis: lymphocyte-rich infiltrate with poorly formed granuloma (arrow). (C, D) Primary sclerosing cholangitis: concentric periductal fibrosis (arrow) (D, Trichrome).

score of 8–9 [15,16].

AMR includes hyperacute AMR (almost eliminated due to its rarity), acute AMR (aAMR), and chronic active AMR. Both of the latter two entities are associated with an elevated serologic titer of donor-specific antibodies, which are antibodies specific to the donor's human leukocyte antigens and C4d deposition in portal microvascular endothelium (portal vein and capillaries) (best seen on C4d immunostain) [16,17].

Plasma cell-rich rejection is a mixed TCMR and aAMR which occurs in patients with original disease other than autoimmune hepatitis [16].

The distinctive histologic features of these rejections are

outlined in Table 2. Figs. 4 and 5 highlight the pathognomonic features of each subtype of rejection.

STEP 4: BLOOD AND BILE FLOW OBSTRUCTION

During liver transplantation, precise vascular and biliary anastomoses are crucial for ensuring the proper function and integration of the transplanted liver into the recipient's body. However, these anastomoses carry the risk of obstruction and failure. Therefore, it is necessary to assess for obstruction or thrombosis of the hepatic artery, hepatic vein, portal vein,

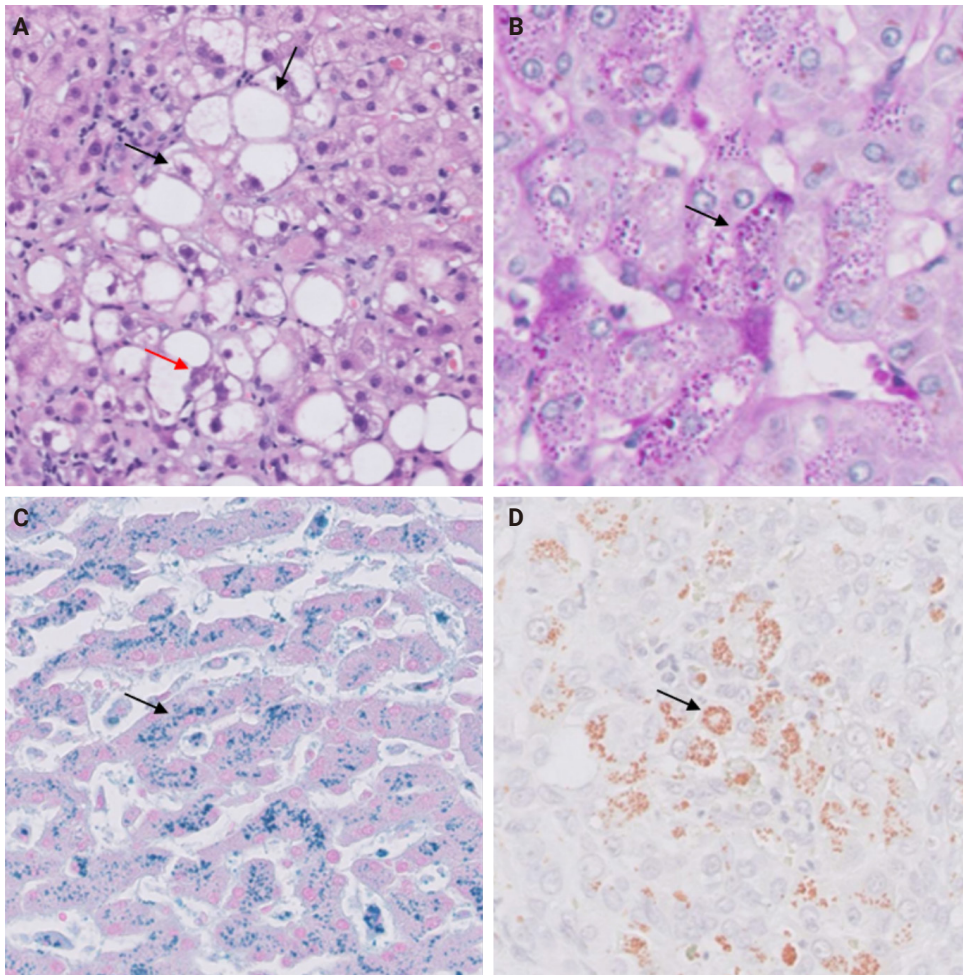


Fig. 2. (A) Steatohepatitis: macrovesicular steatosis with ballooned hepatocytes (black arrows) and Mallory-Denk bodies (red arrow). (B) Alpha-1 antitrypsin deficiency: intrahepatocytic alpha-1 antitrypsin globules (arrow) (periodic acid-Schiff-diastase). (C) Hemochromatosis: intrahepatocytic iron accumulation (arrow) (Perl's stain). (D) Wilson's disease: intrahepatocytic copper accumulation (arrow) (Rhodanine stain).

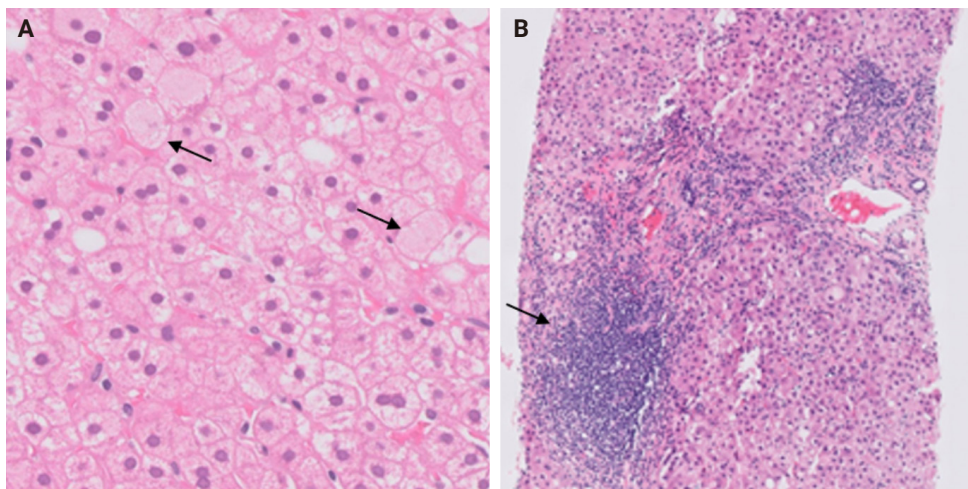


Fig. 3. (A) Hepatitis B virus hepatitis: ground glass hepatocytic inclusion (arrows). (B) Hepatitis C virus hepatitis: lymphoid follicle formation in the portal tract (arrow).

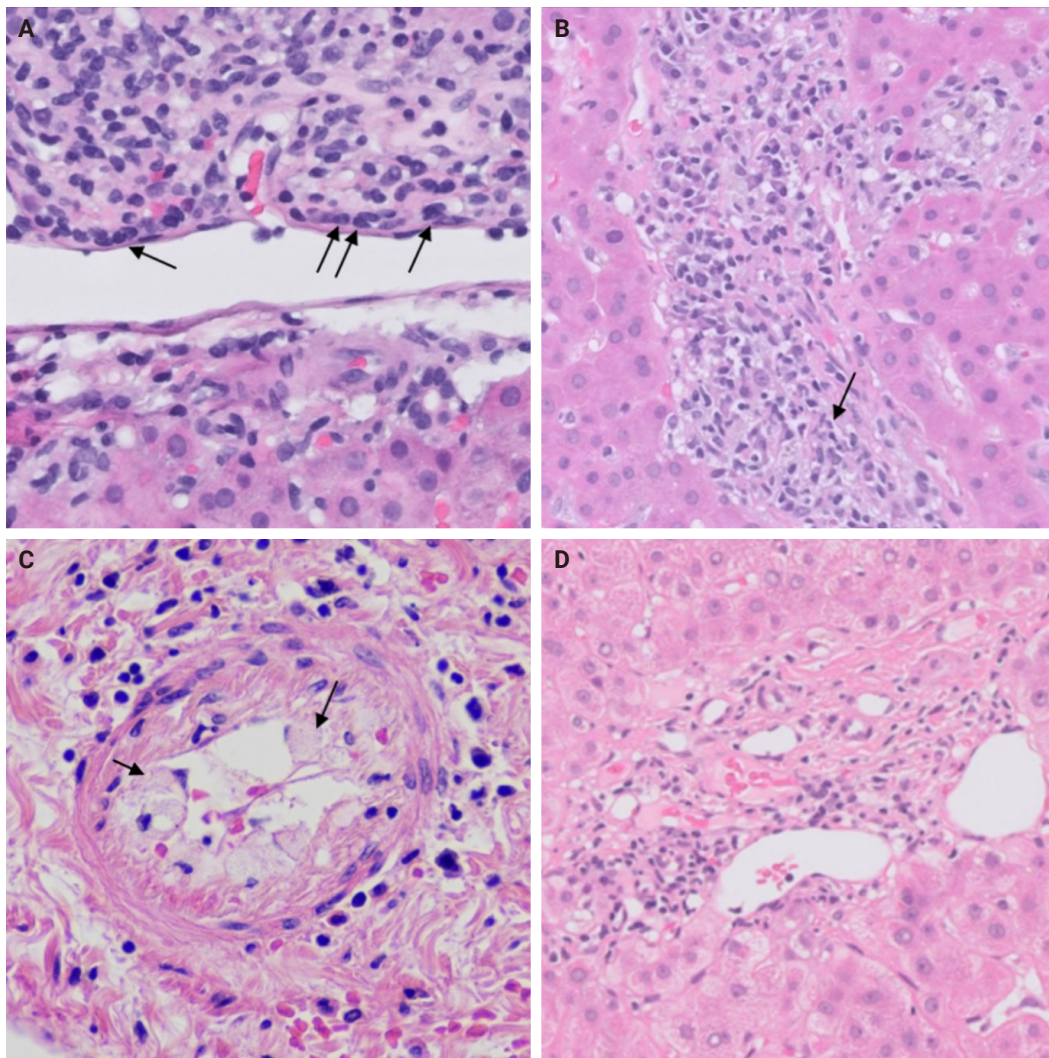


Fig. 4. (A) Acute cellular rejection: endothelitis (arrows). (B) Plasma cell-rich rejection: centrilobular plasma cell-rich inflammatory infiltrate (arrow) (Courtesy of Maria Isabel Fiel MD). (C) Chronic rejection with foam cell arteriopathy: foam cell accumulation in the arterial wall (arrows) (Courtesy of Maria Isabel Fiel MD). (D) Chronic ductopenic rejection: absence of native bile duct in a portal tract.

Table 2. Types of rejection in patients following orthotopic liver transplantation with their characteristic histological findings

Type of rejection	Characteristic histologic findings
Acute cellular rejection	Lymphocytes-rich portal inflammation, bile duct injury, and venous endothelial inflammation (endotheliitis) [15,16]
Chronic ductopenic rejection	Ductopenia (more than half of the portal tracts without native bile ducts), bile ductular reaction, and metaplastic hepatocytes (best seen on CK7 immunostain) [15,16]
Chronic rejection with foam cell arteriopathy	Arteriolar damage with accumulation of foam cells within the vessel walls [15,16]
Acute antibody-mediated rejection	Portal microvascular injury including microvascular endothelial cell enlargement, microvasculitis/capillaritis, capillary dilatation, and microvascular disruption [15,16]
Chronic active antibody-mediated rejection	Mononuclear portal or perivenular inflammation, with interface or perivenular necroinflammatory activity and at least moderate portal/periportal, sinusoidal or perivenular fibrosis [15,16]
Plasma cell-rich rejection	Plasma cell-rich (>30%) portal infiltrate or central infiltrate, with interface or perivenular necroinflammatory activity in patients without history of autoimmune hepatitis [15,16]

CK7, cyokeratin 7.

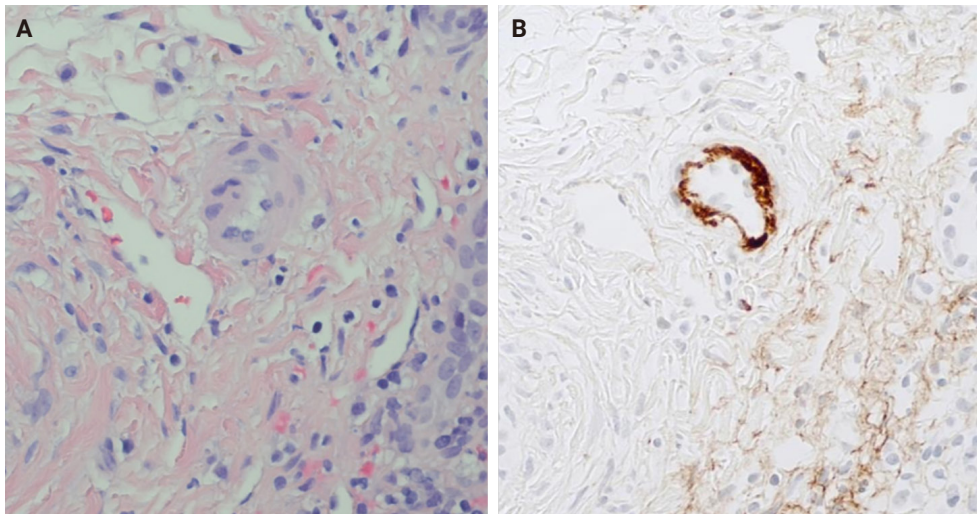


Fig. 5. (A, B) Antibody-mediated rejection: C4d deposition in a hepatic arteriole (B, C4d immunostain).

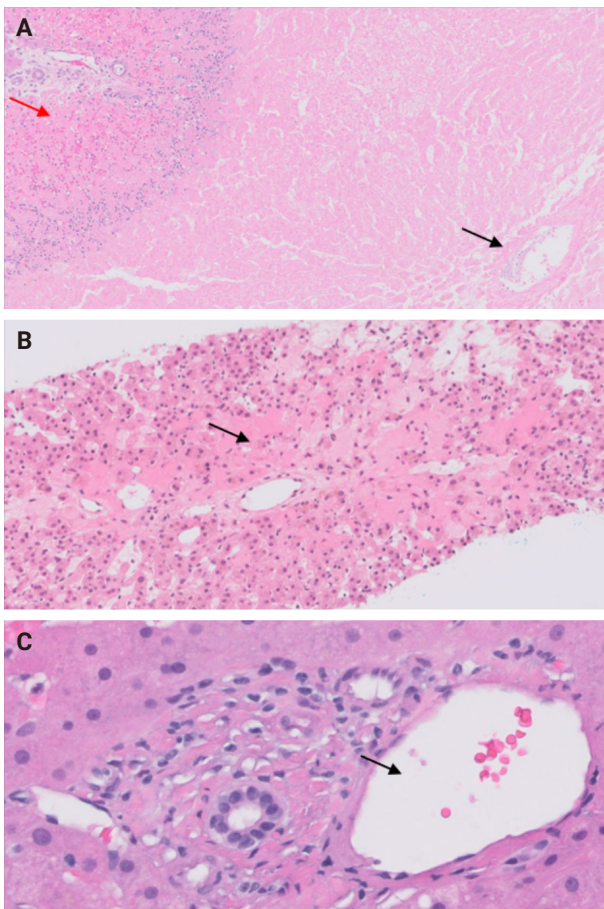


Fig. 6. (A) Hepatic artery thrombosis: centrilobular (black arrow) and periportal coagulative necrosis (red arrow). (B) Hepatic vein thrombosis: centrilobular congestion and necrosis (arrow). (C) Portal vein thrombosis: dystrophic (dilated) portal vein (arrow).

and bile ducts when evaluating a post-transplant liver. [Table 3](#) summarizes the histologic features associated with these clinical scenarios. Additionally, the restoration of blood flow to the transplanted liver after ischemia can lead to liver damage known as reperfusion injury [18]. [Table 3](#) also outlines the histologic characteristics of reperfusion injury [19-23]. All the histologic characteristics are also illustrated in [Figs. 6 and 7](#).

STEP 5: OPPORTUNISTIC NON-HEPATOTROPIC VIRAL INFECTIONS

Following liver transplantation, patients receive immunosuppressive therapy, increasing their susceptibility to various opportunistic infections and/or reactivation of dormant infections, such as cytomegalovirus (CMV), Epstein-Barr virus, and other opportunistic pathogens. Bacterial and fungal infections commonly affect organs other than the liver and often do not require biopsy. However, viral infections can directly involve the liver and may necessitate biopsy to distinguish them from rejection. During this step, the focus is on identifying histologic features specific to non-hepatotropic viral infections, which could also be confirmed by immunostaining. [Table 4](#) provides a summary of the histologic characteristics observed in viral infections following liver transplant [24,25]. Some of these features are shown in [Fig. 8](#).

Table 3. Potential complications of orthotopic liver transplantation with their characteristic histological findings

Complication	Characteristic histologic findings
Hepatic artery thrombosis	Centrilobular (zone 3) necrosis and/or localized coagulative necrosis (could involve zone 1 and zone 2) and possible subsequent ischemic cholangiopathy [19,20]
Hepatic vein thrombosis	Centrilobular (zone 3) congestion and/or necrosis [21]
Portal vein thrombosis	Sinusoidal dilatation, portal veins dystrophy (dilatation, occlusion, and herniation), and possible centrilobular (zone 3) necrosis [22]
Bile duct obstruction	Portal tracts edema with bile ductular reaction and neutrophils [20]
Reperfusion injury	Centrilobular (zone 3) hepatocytes ballooning, cholestasis, and neutrophilic infiltrate with possible subsequent centrilobular (zone 3) hepatocyte necrosis [23]

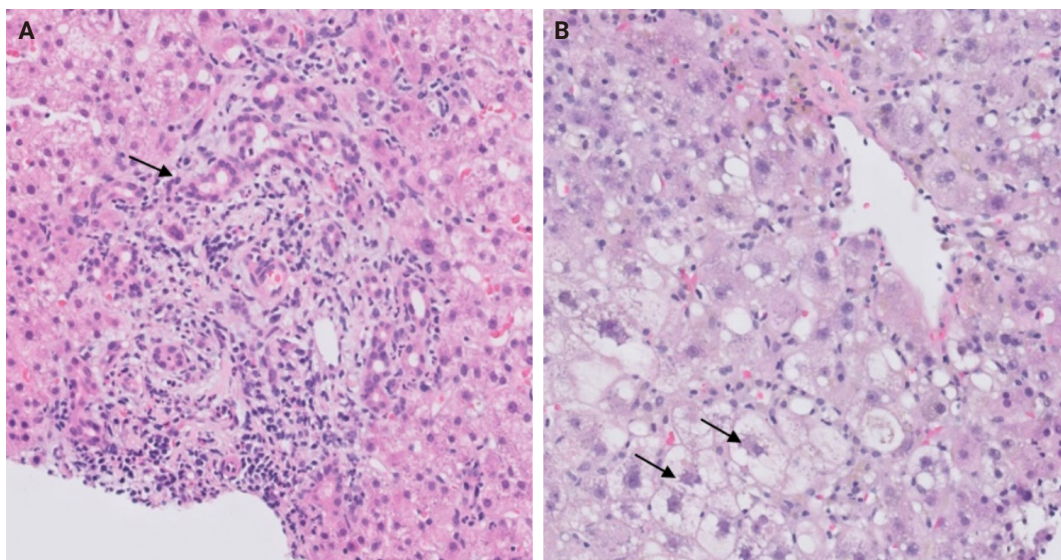


Fig. 7. (A) Bile duct obstruction: portal edema neutrophils and bile ductular reaction (arrow). (B) Reperfusion injury: centrilobular cholestasis and hepatocyte ballooning (arrows).

STEP 6: DRUG-INDUCED LIVER INJURY

Following liver transplantation, patients receive immunosuppressive therapy, medical prophylaxis as well as ongoing treatment for existing comorbidities. Each of these medications have varying degrees of likelihood to cause drug-induced liver injury (DILI) and should be considered as potential offending agents when developing your differential diagnosis. However, diagnosing DILI is challenging due to the diverse histopathological patterns observed, which may overlap with patterns seen in other post-transplant diseases. During this step, it's important to review the patient's medication list to identify any drugs that match any pathognomonic histologic findings observed. The inclusion of DILI in the differential diagnosis may also be reasonable if the histologic findings cannot be explained by other

steps in this evaluation process.

Keep in mind that patients typically receive prophylactic antimicrobial medications and immunosuppressants in the post-operative period, many of which can induce DILI. In terms of antiviral medications, valganciclovir (Valcyte) is indicated for CMV prophylaxis for the first 3–6 months post-transplantation in all patients [26]. For antibiotic coverage, prophylaxis against *Pneumocystis jirovecii* pneumonia is typically administered for 12 months after transplantation [26]. Trimethoprim/sulfamethoxazole is the most common medication used; however, atovaquone or dapsone can be used as an alternative in patients with a sulfa allergy [26]. In patients with latent tuberculosis, prophylactic isoniazid is warranted for 9 months duration [26]. Finally, fungal prophylaxis is indicated in low-risk patients for 1 month after transplant but may be used for longer duration in higher risk patients [26]. This is typically accomplished with

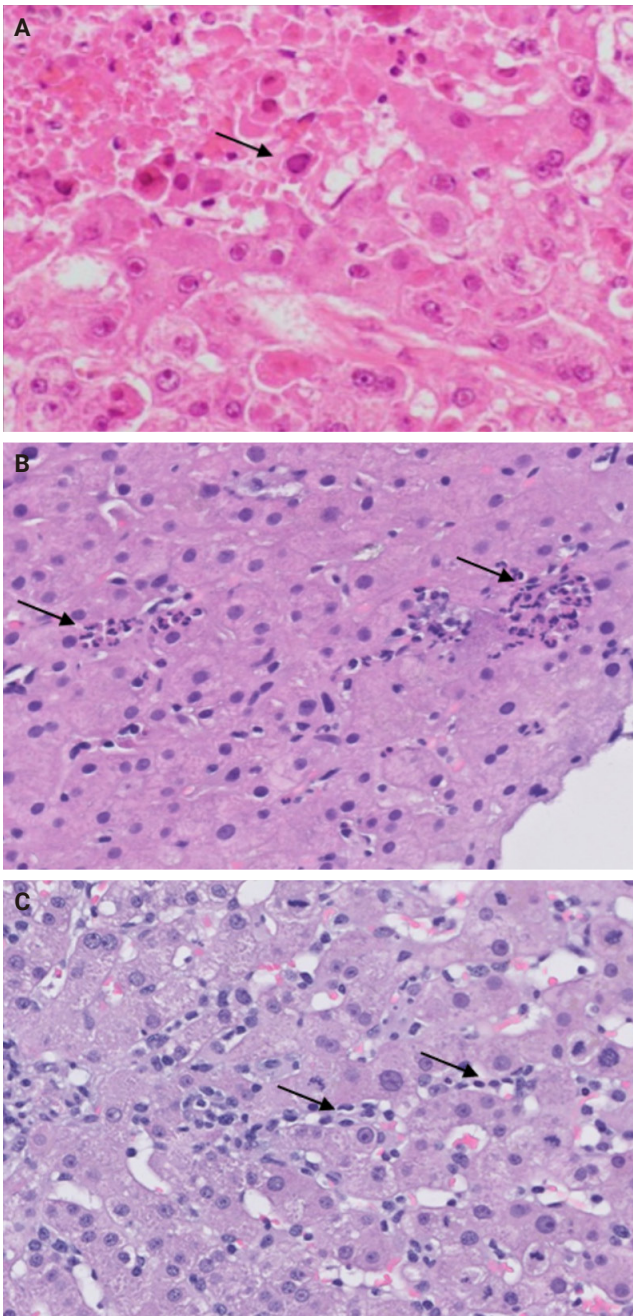


Fig. 8. (A) Herpes simplex virus hepatitis: nuclear inclusion (arrow) (Courtesy of Hwa Jeong Lee, MD). (B) Cytomegalovirus: neutrophilic microabscess (arrows). (C) Epstein-Barr virus hepatitis: sinusoidal mildly atypical lymphocytic infiltrate (arrows).

clotrimazole, fluconazole, or itraconazole [26]. Commonly used medications for immunosuppression and antimicrobial prophylaxis, along with their likelihood of causing DILI, are listed in Table 5.

A rare manifestation of DILI is the development of pseudo-

Table 4. Non-hepatotropic viral hepatitis with their characteristic histological findings

Virus	Characteristic histologic findings
Cytomegalovirus	Scattered foci of apoptotic hepatocytes with neutrophilic microabscesses and rare nuclear inclusions [24]
Human simplex virus	Non-zonal necrosis of the hepatocytes with viral cytopathic effect in the remaining hepatocytes [24]
Epstein-Barr virus	Prominent sinusoidal mildly atypical lymphocytic infiltrate with rare hepatocytic/parenchymal necrosis [24]
Adenovirus	Non-zonal necrosis with smudge cells (cells with basophilic nuclei and indistinct chromatin) [25]

Table 5. Common immunosuppressants and antimicrobial prophylactic medications with their corresponding likelihood of causing DILI, according to the NIH

Medication	Likelihood score ^a of DILI [27]
Immunosuppressants	
Glucocorticoids	A
Calcineurin inhibitors	C
Everolimus	E
Mycophenolate	D
Sirolimus	C
Azathioprine	A
Anti-thymocyte globulin	D
Basiliximab	E
Antimicrobial prophylaxis	
Valganciclovir	C
Valacyclovir	D
Trimethoprim-sulfamethoxazole	A
Atovaquone	D
Dapsone	A
Clotrimazole	E
Fluconazole	B
Itraconazole	B
Isoniazid	A

DILI, drug-induced liver injury; NIH, National Institutes of Health.

^aLikelihood scoring: A, well established cause of liver injury; B, highly likely cause of liver injury; C, probable rare cause of clinically apparent liver injury; D, possible rare cause of clinically apparent liver injury; E, unproven and also unlikely cause of clinically apparent liver injury.

ground-glass inclusions, which can occur with immunosuppressive therapy. These inclusions can mimic the appearance of hepatitis B inclusions but will be negative for hepatitis B virus surface antigen [28]. These inclusions are highlighted in Fig. 9.

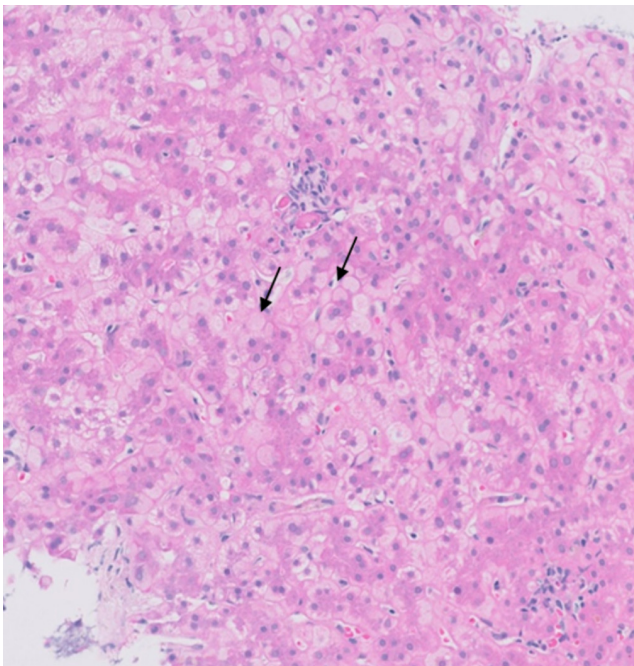


Fig. 9. (A) Drug-induced liver injury: pseudo-ground-glass inclusion secondary to polypharmacy (arrows).

CONCLUSION

Evaluation of post-transplant liver biopsies presents a unique challenge in pathology training, influenced significantly by institutional exposure and the presence of specialized liver transplant programs. By emphasizing key diagnostic considerations such as de novo diseases, disease recurrence, rejection, vascular complications, viral infections, and DILI, our structured, step-by-step approach outlined in this review aims to facilitate a systematic interpretation of these biopsies, bridging the knowledge gap for pathologists at various stages of their careers.

Ethics Statement

Institutional Review Board approval was waived due to the use of retrospective, de-identified data. This study adhered to the guidelines enacted by the Office of Human Research Protection that is supported by the U.S. Department of Health & Human Services. All information included in this report is de-identified and no personal details that may be used to identify the patient are included in this report.

Availability of Data and Material

Data sharing not applicable to this article as no datasets were generated or analyzed during the study.

Code Availability

Not applicable.

ORCID

Mohamad Beshar Ourfali

<https://orcid.org/0009-0009-5511-3284>

David Hirsch

<https://orcid.org/0009-0000-7783-8029>

Marianna Scranton

<https://orcid.org/0000-0001-8149-2462>

Tony El Jabbour

<https://orcid.org/0000-0002-6823-1919>

Author Contributions

Conceptualization: TEJ. Investigation: DH, MBO, TEJ, MS. Project administration: TEJ, MBO, DH, MS. Resources: TEJ. Supervision: TEJ. Visualization: TEJ, MBO, DH. Writing—original draft: MBO, DH, MS. Writing—review & editing: TEJ, DH, MBO, MS. Approval of final manuscript: all authors.

Conflicts of Interest

The authors declare that they have no potential conflicts of interest.

Funding Statement

No funding to disclose.

Acknowledgments

Hwa Jeong Lee, MD for contributing a case of herpes simplex virus hepatitis. Maria Isabel Fiel, MD for contributing a case of chronic rejection with foam cell arteriopathy.

REFERENCES

1. Wu F, Wang J, Pu C, Qiao L, Jiang C. Wilson's disease: a comprehensive review of the molecular mechanisms. *Int J Mol Sci* 2015; 16: 6419-31.
2. Catana AM, Medici V. Liver transplantation for Wilson disease. *World J Hepatol* 2012; 4: 5-10.
3. Fromme M, Schneider CV, Trautwein C, Brunetti-Pierri N, Strnad P. Alpha-1 antitrypsin deficiency: a re-surfacing adult liver disorder. *J Hepatol* 2022; 76: 946-58.
4. Mitchell EL, Khan Z. Liver disease in alpha-1 antitrypsin deficiency: current approaches and future directions. *Curr Pathobiol Rep* 2017; 5: 243-52.
5. Dobrindt EM, Keshi E, Neulichedl J, et al. Long-term outcome of orthotopic liver transplantation in patients with hemochromatosis: a summary of a 30-year transplant program. *Transplant*

- Direct 2020; 6: e560.
6. Shubin AD, De Gregorio L, Hwang C, MacConmara M. Combined heart-liver transplantation in a case of haemochromatosis. *BMJ Case Rep* 2021; 14: e241508.
 7. Schreiber I, Regev A. Recurrent primary biliary cirrhosis after liver transplantation: the disease and its management. *Med-GenMed* 2006; 8: 30.
 8. Visseren T, Erler NS, Polak WG, et al. Recurrence of primary sclerosing cholangitis after liver transplantation: analysing the European Liver Transplant Registry and beyond. *Transpl Int* 2021; 34: 1455-67.
 9. Harputluoglu M, Caliskan AR, Akbulut S. Autoimmune hepatitis and liver transplantation: Indications, and recurrent and de novo autoimmune hepatitis. *World J Transplant* 2022; 12: 59-64.
 10. Faisal N, Renner EL. Recurrence of autoimmune liver diseases after liver transplantation. *World J Hepatol* 2015; 7: 2896-905.
 11. Shetty A, Giron F, Divatia MK, Ahmad MI, Kodali S, Victor D. Nonalcoholic fatty liver disease after liver transplant. *J Clin Transl Hepatol* 2021; 9: 428-35.
 12. Jothimani D, Venugopal R, Vij M, Rela M. Post liver transplant recurrent and de novo viral infections. *Best Pract Res Clin Gastroenterol* 2020; 46-47: 101689.
 13. Salomao MA. Pathology of hepatic iron overload. *Clin Liver Dis (Hoboken)* 2021; 17: 232-7.
 14. Mazhar A, Piper MS. Updates on Wilson disease. *Clin Liver Dis (Hoboken)* 2023; 22: 117-21.
 15. Choudhary NS, Saigal S, Bansal RK, Saraf N, Gautam D, Soin AS. Acute and chronic rejection after liver transplantation: what a clinician needs to know. *J Clin Exp Hepatol* 2017; 7: 358-66.
 16. Demetris AJ, Bellamy C, Hubscher SG, et al. 2016 Comprehensive update of the Banff Working Group on Liver Allograft Pathology: introduction of antibody-mediated rejection. *Am J Transplant* 2016; 16: 2816-35.
 17. Lee BT, Fiel MI, Schiano TD. Antibody-mediated rejection of the liver allograft: an update and a clinico-pathological perspective. *J Hepatol* 2021; 75: 1203-16.
 18. Rampes S, Ma D. Hepatic ischemia-reperfusion injury in liver transplant setting: mechanisms and protective strategies. *J Biomed Res* 2019; 33: 221-34.
 19. Lee M, Agostini-Vulaj D, Gonzalez RS. Evaluation of histologic changes in the livers of patients with early and late hepatic artery thrombosis. *Hum Pathol* 2019; 90: 8-13.
 20. Gupta NB. *Liver biopsy made easy*. New Delhi: Jaypee Brothers Medical Publishers, 2017.
 21. Nakhleh RE. Pathology and differential diagnosis of hepatic venous outflow impairment. *Clin Liver Dis (Hoboken)* 2017; 10: 49-52.
 22. Terada T, Hosono M, Nakanuma Y. Microvasculature in the small portal tracts in idiopathic portal hypertension: a morphological comparison with other hepatic diseases. *Virchows Arch A Pathol Anat Histopathol* 1989; 415: 61-7.
 23. Geramizadeh B, Hassani M, Kazemi K, Shamsaifar AR, Malek-Hosseini SA. Value of histopathologic findings of post-reperfusion liver needle biopsies. *Int J Organ Transplant Med* 2018; 9: 168-72.
 24. Dancygier H. Viral infections by nonhepatotropic viruses. In: Dancygier H, ed. *Clinical hepatology*. Berlin: Springer, 2010; 823-30.
 25. Zheng N, Wang Y, Rong H, Wang K, Huang X. Human adenovirus associated hepatic injury. *Front Public Health* 2022; 10: 878161.
 26. Lucey MR, Terrault N, Ojo L, et al. Long-term management of the successful adult liver transplant: 2012 practice guideline by the American Association for the Study of Liver Diseases and the American Society of Transplantation. *Liver Transpl* 2013; 19: 3-26.
 27. Livertox: clinical and research information on drug-induced liver injury [Internet]. Bethesda: National Institute of Diabetes and Digestive and Kidney Diseases, 2012 [cited 2024 Jul 31]. Available from: <http://www.ncbi.nlm.nih.gov/books/NBK547852/>.
 28. Fischer AK, Baba H, Lainka E, et al. Rapid development of pseudo-ground-glass bodies in liver transplants. *Histopathology* 2024; 85: 190-2.

Professional biobanking education in Korea based on ISO 20387

Jong Ok Kim¹, Chungyeul Kim², Sangyong Song³, Eunah Shin⁴, Ji-Sun Song⁵, Mee Sook Roh⁶, Dong-chul Kim⁷, Han-Kyeom Kim⁸, Joon Mee Kim⁹, Yeong Jin Choi¹⁰

¹Department of Pathology, Daejeon St. Mary's Hospital, College of Medicine, The Catholic University of Korea, Daejeon, Korea

²Department of Pathology, Korea University College of Medicine, Seoul, Korea

³Department of Pathology, Samsung Medical Center, Sungkyunkwan University School of Medicine, Seoul, Korea

⁴Department of Pathology, Yongin Severance Hospital, Yonsei University College of Medicine, Yongin, Korea

⁵Department of Pathology, Ewha Womans University Seoul Hospital, Ewha Womans University College of Medicine, Seoul, Korea

⁶Department of Pathology, Dong-A University College of Medicine, Busan, Korea

⁷Pathology Division, Seoul Clinical Laboratories, Yongin, Korea

⁸Professor Emeritus of Pathology, Medical College Korea University, HiLab, HANARO Medical Foundation, Seoul, Korea

⁹Department of Pathology, Inha University School of Medicine, Incheon, Korea

¹⁰Department of Hospital Pathology, Seoul St. Mary's Hospital, College of Medicine, The Catholic University of Korea, Seoul, Korea

To ensure high-quality bioresources and standardize biobanks, there is an urgent need to develop and disseminate educational training programs in accordance with ISO 20387, which was developed in 2018. The standardization of biobank education programs is also required to train biobank experts. The subdivision of categories and levels of education is necessary for jobs such as operations manager (bank president), quality manager, practitioner, and administrator. Essential training includes programs tailored for beginner, intermediate, and advanced practitioners, along with customized training for operations managers. We reviewed and studied ways to develop an appropriate range of education and training opportunities for standard biobanking education and the training of experts based on KS J ISO 20387. We propose more systematic and professional biobanking training programs in accordance with ISO 20387, in addition to the certification programs of the National Biobank and the Korean Laboratory Accreditation System. We suggest various training programs appropriate to a student's affiliation or work, such as university biobanking specialized education, short-term job training at unit biobanks, biobank research institute symposiums by the Korean Society of Pathologists, and education programs for biobankers and researchers. Through these various education programs, we expect that Korean biobanks will satisfy global standards, meet the needs of users and researchers, and contribute to the advancement of science.

Keywords: Biological specimen banks; Standardization; Education; International organization

INTRODUCTION

Biobanking is the collection of a large number of biospecimens containing personal and health information, mainly for health and medical research [1]. Biobank samples include not only

classical archive specimens such as tissues, blood, nucleic acids, and microbiomes, but also virtual specimens such as images and data. In the current global situation, it is imperative to emphasize ethical and legal considerations and to standardize processes. The International Organization for Standardization

Received: September 4, 2024 **Revised:** October 29, 2024 **Accepted:** November 4, 2024

Corresponding Author: Joon Mee Kim, MD, PhD

Department of Pathology, Inha University Hospital, Inha University School of Medicine, 27 Inhang-ro, Jung-gu, Incheon 22332, Korea

Tel: +82-32-890-3981, Fax: +82-42-220-9843, E-mail: jmk@path@inha.ac.kr, jkim@catholic.ac.kr

Yeong Jin Choi, MD, PhD

Department of Hospital Pathology, Seoul St. Mary's Hospital, College of Medicine, The Catholic University of Korea, 222 Banpo-daero, Seocho-gu, Seoul 06591, Korea

Tel: +82-2-2258-1616, Fax: +82-2-2258-1627, E-mail: mdyjchoi@catholic.ac.kr

This is an Open Access article distributed under the terms of the Creative Commons Attribution Non-Commercial License (<https://creativecommons.org/licenses/by-nc/4.0/>) which permits unrestricted non-commercial use, distribution, and reproduction in any medium, provided the original work is properly cited.

© 2025 The Korean Society of Pathologists/The Korean Society for Cytopathology

(ISO) documents for biobanking (ISO 20387:2018) define biobanks as legal entities or parts of a legal entity, so the whole biobanking process (acquisition and storage, including collection, preparation, and preservation; testing; analysis; and distribution) must be performed within adequate legal boundaries [2]. To establish and administrate biobanks, there is an urgent need to develop and disseminate educational training programs in accordance with ISO 20387. In Republic of Korea, a pilot project for KS J ISO 20387-accredited certification has been implemented, and three institutions have acquired Korea Laboratory Accreditation Scheme (KOLAS) accreditation. The number of institutions seeking ISO 20387 certification in Republic of Korea is increasing, as is the demand for education on biobanking standards. Although an education system or program is mandatory to comply with global standards, specified infrastructure for biobanking personnel in Republic of Korea is insufficient. In this article, we briefly review ISO 20387, KS J ISO 20387, and both international and Korean educational programs for biobanking and offer suggestions for professional programs based on KS J ISO 20387.

OVERVIEW OF ISO 20387

The ISO is a global network of national standards bodies (foremost standards organizations in their countries) composed of 170 members, one per represented country. The name ISO is derived from the Greek *iso*, meaning equal. Though the acronym originally differed across languages, called the IOS in England and the Organization International Denormalization in France, the founders decided to use ISO globally to represent equality, whatever the country and language. The ISO was established in 1946 to support global trade by developing and publishing international standards, driving inclusive and equitable economic growth, advancing innovation, and promoting health and safety to achieve a sustainable future (ISO mission). Currently, there are about 13,500 ISO standards [3].

A *conformity assessment* demonstrates whether a product or service, process, claim, system, or person meets the relevant requirements (ISO/IEC 1700). *Accreditation* is the publication of an official certification by a third party to indicate that a conformity assessment body is qualified to perform a particular conformity assessment task (KSQ ISO IEC 17000) [4]. The International Laboratory Accreditation Cooperation (ILAC) is an international organization of accreditation bodies for calibration laboratories, testing laboratories, medical testing

laboratories and inspection bodies, proficiency testing providers, reference material products, and biobanks. The ILAC can secure the international equivalence of conformity assessments in individual countries based on an agreement under ISO/IEC 17011. The ILAC-Mutual Recognition Arrangement (ILAC-MRA) demonstrates the equivalent competence of conformity assessment bodies. In other words, the accrediting bodies of each country participate in regional and international agreements to assess and certify conformity assessment and demonstrate their eligibility internationally.

ISO 20387 was developed in 2018 to promote confidence in biobanking. It specifies general requirements for biobank competence, impartiality, and consistency, including quality control requirements, to ensure the appropriate collection of biological materials and data. The Republic of Korea introduced ISO 20387 and enacted KS J ISO 20387 in 2019. The development of standard operating procedures (SOPs) for the collection, processing, and storage of samples and data based on ISO 20387 has an important impact on the quality control and future use of bioresources. SOPs are mandatory for the efficient use of bioresources, including human-derived materials. Experts with a biobanking standards education based on ISO 20387 are needed to standardize bioresource quality. ISO 20387 became the exclusive accreditation standard for ILAC in October 2018, following its publication in August of that year (ILAC GA 22.19). In October 2020, biobanking (ISO 20387) activities were included as an Asia Pacific Accreditation Cooperation (APAC)-MRA (Level 3, APAC GA Ballot 2020-02). In November 2021, ISO 20387 was introduced in the ILAC-MRA scope, and related document updates were promoted (ILAC GA resolution 25.09, 2021-11) [5,6]. Then, American Association for Laboratory Accreditation launched a biobanking accreditation program based on ISO 20387 in January 2019. Because biobanks are important research infrastructure for bio businesses, research and discussions about specialized biobanking education are being conducted in Republic of Korea.

OVERVIEW OF KS J ISO 20387

The KOLAS is an accreditation body that evaluates and performs accreditation work on inspection bodies and calibration tests in Republic of Korea under the Framework Act on National Standards and Regulations. The KOLAS has signed an international MRA with ILAC for testing, calibration, and medical testing laboratories, but it has not yet signed an MRA relating

to biobanks. To achieve such expansion, KS J ISO 20387 was enacted by the KOLAS in Republic of Korea in December 2019. KS J ISO 20387:2019, aligned with ISO 20387, *Biotechnology — Biobanking — General requirements for biobanking*, was published as the Korean Industrial Standard in 2019, to promote trust in the operation of biological resource banks. This standard ensures that collected bioresources and associated data are of appropriate quality, and it ensures the eligibility, fairness, and consistent operation of bioresource banks. KS J ISO 20387 consists of general, structural, resource, and process requirements, in addition to quality control systems and annexes. The general requirements involve matters such as impartiality and confidentiality. Resource requirements involve personnel; facilities/dedicated areas and environmental conditions; externally provided processes, products, and services; and equipment. The process requirements include the collection, reception, distribution, transport, and traceability of biological material and associated data, as well as the preparation, preservation, and storage of biological material, quality control, validation and verification of methods, and the management of information and data, nonconforming output, reports, and complaints. The quality management system is based on ISO 9001 and provides two options. Option A lists the minimum requirements for implementing a quality management system in biobanks according to the *principles* of ISO 9001. Option B allows biobanks to establish and maintain a quality management system under the *implemented requirements* of ISO 9001. Under these regulations, it is necessary to introduce and be aware of the ISO 9001 system in KS J ISO 20387:2018.

In October 2022, three institutions, the Korean National Institute of Health (National Biobank of Korea), the National Culture Collection for pathogens, and the Korean Institute of Radiological & Medical Science, received KOLAS accreditation certification [7].

CURRENT STATUS OF OVERSEAS BIOBANKING EDUCATION

In Europe and the Americas, professional biobanking education has expanded since the 2010s in recognition of the need for specialized training and to meet the demand for experts in the growing bioindustry. Biobanking education is largely divided into degree programs and job training courses (Table 1) [8-17]. Degree programs in universities exist mainly in Europe, with six-degree courses available as of 2022.

King's College London in the United Kingdom offers a Master's degree in research biobanking and offers 5-month practical training sessions. The program focuses on the collection and storage of oncology-related bioresources, as well as bioresource preparation, preservation, and staining techniques. Through this course, students can learn how to handle and analyze DNA and tumor cells, but only six to eight first-year students are accepted each year, limiting this opportunity for education [17].

The Master's degree program for biobanking at the Medical University of Graz in Austria offers a five-semester, part-time, English online learning course. The course uses a biobanking curriculum for job training with comprehensive topics comprising introduction and basic knowledge of biobanking, ethics and law, collection and management of samples, risk management and biobanking, biobanking IT, sustainability, budgeting and business planning, epidemiology, quality management and quality control, management and communication, strategy and development, research methods I, research methods II, design and implementation of clinical studies, international biobanking, and managing multidisciplinary teams [8]. Another educational focus includes courses on building and operating biobanks. The Medical University of Graz also offers various 2-day and 4-day biobanking courses [8]. The Université d'Azur in France offers a specialized Master's degree in biobank data management, involving practice-oriented education that includes field practice in a biobank and comprehensive programs on biobanking processes [10].

Lyon Catholic University in France offers a 2-year Master's program that involves both field classes and practice. This degree teaches skills in biobank management and biology for use in positions of responsibility in biobanks [11]. The Universidad Católica de Valencia in Spain teaches field classes for 1 year as a Master's degree [12]. The University of Milano-Bicocca has developed a comprehensive Master's-level curriculum, including 40 online series (webinars), training programs, and staff exchange programs, by integrating with existing curriculums for three semesters.

In addition to universities, network-style organizational institutions such as associations and academic societies offer biobanking job training courses. The Integrated Biobank of Luxemburg, which uses proficiency tests certified by the International Society for Biological and Environmental Repositories (ISBER), offers a three-week seminar for up to 35 students each year in conjunction with the University of Luxembourg [13,17]. The European Biobank Network of human-derived biobanks in

Table 1. Overseas biobanking education

Type	Educational institution	Training courses	Characteristics	Education method	Education period
College degree programs	King's College London (England)	Master's degree in biobanking	Two 5-month practical training sessions, six to eight new students a year Focus on the collection and storage of oncology-related bioresources and sample preparation, preservation, and dyeing technology	Field class, practice	1 yr
	Medical University of Graz (Austria)	Master's degree in biobanking	Online-learning courses in English	Online and in-person seminars (in English)	Five semesters
	Université d'Azur (France)	Master's degree in biobank data management	Overall job training for biobanking, including comprehensive issues 2nd and 4th semesters: internship 1st semester, learn human health-agro-environment, quality in biobanking, bioethics in biobanking, safety and security in biobanking, project management, and technical practice at the biobank Côte d'Azur	Field classes	2 yr
	Lyon Catholic University (France)	Master's degree	3rd semester, biobankonomics, big data for biobanking, networking in biobanking, professional integration, communication and marketing, and success stories in biobanking	Field classes, practice	2 yr
	Universidad Catolica de Valencia (Spain)	Master's degree	Biobank management and biology	Field classes	1 yr
	University of Milano-Bicocca (Italy)	Master's degree	Comprehensive curriculum	-	Three semesters
Network-type job training courses	IBBL-Luxembourg University Link	-	On-site biobanking job training	Field classes	3 wk
	Medical University of Graz	Certificate	Data collection, preservation, and data management of samples Theoretical and practical training workshops	Field classes	3 days, 5 days
	BBMRI-ERIC, European Biobank network	Certificate, Master's degree	Annual biobank week conference with information exchange, presentation, and discussions Research infrastructure training program leading to Master's degree at the University of Milano-Bicocca	Staff exchange, webinars, training programs	3–18 mo
	College of American Pathologists (CAP)		Coordinated research infrastructure building enduring life-science services (CORBEL) Systematic and professional education for medical laboratory technologists	Field classes, online	-
			Accredited as a high-quality bioresource provider		
Online-based bio-bank e-learning	ISBER/in partnership with the Canadian Tissue Repository Network	Certificate	Online education and webinar about bioresources and biobanking by pathologists' society	Online	20–30 hr
	CTRNet, UBC Office of Biobank Education and Research	-	Collaboration with ISBER Basic biobanking education program based on ISBER best practices in conjunction with the University of British Columbia for students and research technicians	-	-

BBMRI-ERIC, Biobanking and Biomolecular Resources Research Infrastructure-European Research Consortium; ISBER, International Society for Biological and Environmental Repositories.

Europe holds a Global Biobank Week Conference once a year to exchange information and discuss presentations related to biobanks.

The Biobanking and Biomolecular Resources Research Infrastructure–European Research Infrastructure Consortium (BBMRI-ERIC) is the largest pan-European service-driven infrastructure in health research [18]. The BBMRI-ERIC has operated educational infrastructure projects since 2015. In 2020, with the support of Horizon, it developed a related policy framework recognizing the importance of biobanking education and training. The Research Infrastructure Training Program (RItrain) defines the competencies required by research institutions from initial preparation to the operational stage, links those competency-specific requirements to existing training courses, and culminates in a Master's degree at the University of Milano-Bicocca. The RItrain project is operated by a consortium of leading European research infrastructure institutions such as the European Bioinformatics Institute and the European Clinical Research Infrastructure Network [18].

The Coordinated Research Infrastructure Building Enduring Life-science Service (CORBEL) project has the same nature as RItrain but seeks to build shared services between biological and medical research infrastructures, including the European Marine Biological Resource Center (EMBRC). EMBRC is part of the European Strategic Forum on Research Infrastructure, comprising cross-infrastructure science workflows and a common suite of services in response to the needs of specific users and research infrastructures. The EMBRC is part of a transnational access program and provides standardized services, an innovation desk, a working group on quality management, and training. The CORBEL project focuses on data management and integration, physical access, ethics, and innovation and develops and operates education and training programs through staff exchanges and webinars [19].

The College of American Pathologists (CAP) offers a systematic and professional online and offline curriculum for clinical pathologists and operates an educational program to earn CAP Biobank accreditation. This accreditation is a peer evaluation model that allows students to share knowledge and best practices with other biobank experts through education. If a biobank acquires this accreditation, it will be recognized as an institution that provides high-quality biomaterials. An example of a CAP webinar related to biobanking is the “Biospecimens and Biorepositories for the Community Pathologist” [17].

ISBER, a global biobanking organization, offers online

training courses on the general operation and management of biobanking, dealing with major issues in establishing, maintaining, and accessing biobanking services. The education program includes nine online modules designed to provide “how-to” knowledge for researchers and biobankers and “what is” knowledge for stakeholders (e.g., the public, ethics board members). The nine modules are the overview of research biobanking; governance; ethics, privacy, and security; facility design and safety; quality management and process improvement; informed consent; biospecimen collection and processing; biospecimen storage and distribution; and data systems and records management (Table 2). Module 1 covers general management applicable to overall biobanking, and modules 2 through 9 detail specific biobanking processes [16]. In addition, ISBER provides information about institutions and curriculums that offer biobanking education by country (Table 1). Annual meetings and symposiums have been held for more than 20 years. ISBER offers opportunities for academia, industry, and pharmaceutical companies to learn, connect, discuss, and collaborate with biobankers from six continents, along with education programs on various topics through in-person and online/hybrid gatherings [15].

The Canadian Task Repository Network (CTRNet), jointly with ISBER, offers basic online courses on general operational management of biobanks and standardized biospecimen research methods. These are in-depth courses based on the National Cancer Institute and ISBER operation guidelines in conjunction with the University of British Columbia for researchers, undergraduates, graduate and doctoral students, and research technicians dealing with human-derived specimens (Table 1) [17,20].

Our examination of the status of overseas biobanking education showed that a small number of educational institutions/associations has been providing systematic biobanking education, including practical training and theoretical courses, for a considerable period of time. Those educational programs were developed and distributed with technical and legislative support.

CURRENT STATUS OF BIOBANKING EDUCATION IN REPUBLIC OF KOREA

Within the life research resource management implementation plan, the registration agencies of each ministry operated training and education programs for human resources from 2012 to 2023. The Ministry of Science, ICT, and Future Planning

Table 2. ISBER details on the online module of the biobanking operation management course

Module	Training course	Description
1	Basics of biobanking	Provide an overview of the establishment, maintenance, and use of biobanks
2	Governance	Concept of biobank governance, structure, model development, access and release process management model, and stakeholder interests
3	Ethics, privacy, and security	Ethics, personal information protection, and security standards related to research and biobanking The role of the ethics review board in the operation of biobanks Considerations for the development of security standards related to the use of bioinformation Ethical principles in terms of biobanking procedures and organizational operations
4	Facility design and safety	Physical requirements for biobanks Necessary security measures for the protection of bioinformation and data in facilities Need for backup devices and systems Securing the safety of a biobank's workforce
5	Quality management and process improvement	Defining the quality management role of biobanks Definition of the quality management system Implementation of the quality management system Establishment and maintenance of standard operating procedures for biobanks Importance of process monitoring and continuous improvement
6	Informed consent	Purpose and principles of informed consent Types of informed consent Special considerations in the informed consent process Withdrawal of consent procedures and related documents Considerations for obtaining parental permission and pediatric consent
7	Biospecimen collection and processing	Different types of biospecimens Important considerations for obtaining and processing biospecimens Various processing methods for each biospecimen Considerations for labeling biospecimens
8	Biospecimen storage and distribution	Understanding research support through biospecimen distribution Required steps for biospecimen transport Objectives of material transfer agreements (MTAs) Steps for biospecimen distribution and reception documentation
9	Data systems and records management	Requirements for annotating biospecimens Considerations for choosing databases for biobanks Overview of data types, data standards, data quality, and data access policies Mechanisms for data protection

Source: International Society for Biological and Environmental Repositories (ISBER), <https://www.isber.org> [16].

(currently the Ministry of Science and ICT) conducted workshops on microbial classification, identification, culture technology, sample collection, and preservation, and the Ministry of Oceans and Fisheries held workshops on seaweed collection, classification, and conservation. However, those were one-off educational opportunities focused on specific processes (mainly collection and preserving) in biobank operations. On the other hand, the Korean Disease Control and Prevention Agency under the Ministry of Health and Welfare has regularly offered comprehensive education by segmenting courses for biobank

practitioners into foundational and advanced levels [17]. A new training course for KOLAS biobank assessors began in 2022.

Korean Biobank Project, Korean Disease Control and Prevention Agency

The Ministry of Health and Welfare and the Korean Disease Control and Prevention Agency (formerly the Korean Centers for Disease Control and Prevention) established the Comprehensive Information and Management System for Health and Medical Bioresources in 2007, to secure the collection and use

of human resources at the national level.

In the first phase of the Korean Biobank project (2008–2012), 100 professors and researchers associated with the biobank were trained twice under the theme “Biobank and Bioethics.” The program started with education on bioethics and safety laws related to biobanks and their regularization. That was followed by systemized basic and in-depth education programs. In 2012, the project offered basic courses for new employees (having worked less than 1 year) of 17 human biosource regional banks located at university hospitals and in-depth courses for those who had worked for more than 1 year or had completed the basic courses in the previous year. In addition, the trainees practiced preserving, dyeing, separating, and identifying pathogens using a pathogen management system. Since 2009, the National Biobank of Korea has offered step-by-step training to strengthen the job capabilities of biobank operators [21–23].

In the second phase of the project (2013–2015), the frequency and importance of basic and in-depth training were increased to strengthen the job capabilities of practitioners. Training on the National Biobank Information Management System (BIMS) was conducted independently and regularly. Furthermore, in 2014, the Korean Biobank project offered basic education for new employees and workers of less than 1 year from not only the 17 biobanks at university hospitals, but also those from 55 other biobanks of human-derived products approved by the Ministry of Health and Welfare. This training covered the basic management of biobanks, such as a biobank overview, an introduction to the Korean Biobank project (including BIMS 3.0), ethics related to biobanks and biosources, and the management of biobanks under the Bioethics and Safety Act. A total of 59 trainees completed these training courses [24,25]. Beginning in July 2014, BIMS hands-on education was conducted regularly, and education participation surveys targeting biobank practitioners were conducted every month. As a result, customized education could be offered to users. The training included an introduction to the system’s basic structure and function, biological resource collection, safety inspection, distribution, medical information registration method, resource and medical information batch processing, and basic searches of biosources [25]. BIMS is used by the National Biobank of Korea and the human biosource regional banks at 17 university hospitals (Korean Biobank Network). In 2015, it was extended to 18 new biobanks outside the Korean Biobank Network to facilitate the operation of Korean human-derived biobanks. BIMS 3.0 hands-on education has been conducted every month since July 2015,

and the curriculum was divided into two courses: elementary education and advanced/in-depth education. As of the end of December 2015, education had been offered five times, with 65 trainees participating in the elementary education program and 89 participating in the in-depth education program [26]. In addition, the *Basic Textbook for Human Materials Banking Practitioners* [24] was published and contains the following chapters: overview of biobanking, Korean Biobank Project, biobank ethics and law, Biosources Information Management [BIMS 3.0, One-Stop System Main Function Introduction], biosource quality management (blood, body fluids, tissues, nucleic acids), storage equipment and high-pressure gas safety education, and biobank laboratory safety management [24].

In the third phase of the Korean Biobank project (2016–2020), four educational programs offered monthly hands-on training courses on biosource management for practitioners, biosource quality management, additional courses on biosource quality management, and the operation and update of BIMS. In 2017, the project initiated a biosource quality management program to improve the management ability of new workers by training them to handle human specimens. Three biobanks at university hospitals (Ajou University Hospital, Keimyung University Dongsan Hospital, and Cheonbuk National University Hospital) oversaw this training. Practical training was offered once for 5–6 students, and a total of 80 students completed 13 sessions by the end of 2020 [27–30]. Apart from training on DNA and RNA extraction and quality management using cell lines operated by biobanks, students practiced collection, preservation, RNA extraction (automated equipment and manual methods), and quality management methods for biosources collected by biobanks. In November 2020, Ajou University Hospital and Keimyung University Dongsan Hospital ran three training sessions on quality control using a series of training courses, such as extracting RNA from tissues, measuring quality control values, and analyzing the results [30].

In the fourth phase (2021–2025), the 2021 standard software revision of BIMS (HuBis_Sam) was distributed to 61 of the 75 domestic biobanks to improve biosource management efficiency and user convenience. To carry out the “education and certification support for enhancing expertise” task, the project considered a domestic accreditation system for ISO 20387:2018, an advanced test of biosource quality management proficiency, and the development of biobank education programs [31]. In September 2021, the National Biobank of Korea launched an online education program to revitalize and standardize bio-

bank operations. As a result, four courses and 13 sessions of the National Biobank of Korea's online training began in 2022, and included biobank overview and trends, bioresource management and provision procedures, bioresource collection and assessment of quality control errors, bioresource management facilities and equipment operation, safety management of human resource storage rooms and accident response, and BIMS (HuBis_Sam). In 2022, 326 trainees completed those courses (Table 3) [32].

The National Biobank of Korea regularly holds trainings, forums, and symposiums for continuous education and promotion of biobank experts. In addition, to diversify public relations channels and actively communicate with researchers through mobile-oriented services, the Kakao Talk channel of the National Biobank of Korea (channel name: the National Biobank of Korea of Central Disease Control Headquarters) has been operated since 2021 [30].

Korean National Research Resource Center Project

The Korean National Research Resource Center (KNRRC) originated as a Ministry of Science and Technology specialization promotion project in 1995 and is currently operating as a research resource support project under the Ministry of Science and ICT/National Research Foundation of Korea. It comprises a central research resource center, five base centers, five national purpose-based research resource banks, and 31 research resource banks. It has specialized research resources in various fields, such as bioresources, animals, plants, microorganisms, and fusion materials. The organization helps to discover, collect, and store resources that are difficult for individual researchers to secure. From 2008 to 2019, yearly educational workshops and symposiums were held. For the efficient operation of research resource banks, KNRRC offered training for workers at 30 biobanks. In 2018, educational training was offered on the standardization and certification preparation process necessary for biobank operation [33].

KOLAS biobank education based on KS J ISO 20387

The KOLAS biobank curriculum is for assessors and workers and is divided into new assessor training, internal auditor education, general training, training for special topics, and refresher training. The KOLAS biobank employee training is for practitioners, quality managers, and technical managers. The KOLAS training program, "KS J ISO 20387 Operation Practice _ [KOLAS] KS J ISO 20387 Operation Practice (Biobank)," is

mandatory for staff members, quality managers, and technical managers of a biobank. The purpose is to improve the quality of biobank operations by informing students about the KS J ISO 20387 requirements. These requirements need to be met for authorized institutions to establish a management system and perform tasks in compliance. The training is expected to demonstrate to students the system operator role of the KOLAS, enhance operational capabilities by aligning with KS J ISO 20387 requirements, and maintain and improve in-house quality management systems. The training is completed over 3 days (20 hours) and is organized as follows:

Day 1: Biobank accreditation system, international trends, and KS J ISO 20387 requirements.

Day 2: KS J ISO 20387 requirements, the operation status of biobanks.

Day 3: Method validation, verification, and KOLAS accreditation criteria.

The KS J ISO 20387 Operation Practice_ [KOLAS] KS J ISO 20387 Operation Practice (Biobank) course began in 2023 and offered online lectures in February and July. It is available on the Korea Conformity Laboratories website (<https://www.kcl.re.kr/site/program/education/eduschedule.do?menuid=007002001>) [34].

The training course for assessors is divided into (1) new assessor training and (2) lead assessor training. The new assessor training courses are specified in ILAC-G3 (assessor training guidelines used by accredited organizations) and APAC CBC-002 (assessor curriculum guidelines) documents. Biobank assessors must complete the ISO-IEC-17025 and ISO 20387 courses including training on KS Q ISO/IEC 17011, KS Q ISO 19011, KS Q ISO/IEC 17025, measurement uncertainty, and KS J ISO 20387 (Tables 4, 5) [2,7,35]. The program also includes an introduction to accreditation systems, international trends in conformity assessment systems, the importance of quality assurance and quality management concepts, the standards and interpretation of each accreditation scheme, assessment techniques and practices, metrological traceability, measurement uncertainty, qualification criteria and registration procedures for assessors, and the qualification requirements of KS Q ISO/IEC 17011.6.1.2. The new training course for KOLAS biobank assessors opened in 2022. Maintenance training courses for assessors are currently in preparation for future inclusion in the curriculum [7]. Internal auditors must complete internal auditor training courses (in-person, 3 days [20 hours]) and employee refresher training courses (online) [7].

Table 3. Practical training by the National Biobank of Korea (Ministry of Health and Welfare/Korea Centers for Disease Control and Prevention)

1st phase (2008–2012)	2nd phase (2013–2015)	3rd phase (2016–2020)	4th phase (2021–2025)
2009	2013	2017	2021
First biobank practitioner training for working professors and researchers in the Korean Biobank Network (KBN) (offered two times)	Biobank practitioner training at KBN units – Basic training – In-depth training – Publishing basic textbooks for practitioners at biobanks	Bioresource management training Bioresource quality management training Add training courses on the quality management of human tissue resources BIMS hands-on training	Revised BIMS Distribution of standard software (HuBis_Sam)
2010	2014	2018	2022
Biobank practitioner training – Basic training – In-depth training Pathogen resource bank practical training – Pathogen Management System (PIMS) – Pathogen preservation and dyeing practice	Basic training for the management of biobanks Bio Information Management System (BIMS) practical training	Biobank manager training Practical training for bioinformation users BIMS training Bioresource distribution desk training Practical training for quality management Practical training for blood-derived resource quality management Practical training for tissue resource quality management	Start e-learning education
2011	2015	2019	2023
Biobank practitioner training – Basic training – In-depth training Pathogen resource bank training – PIMS – Separation and identification of pathogen resources	Regular training courses of BIMS 3.0 practice – Monthly courses – Basic/in-depth training Bioresource management training – Basic training – In-depth training – Target expansion to all biobanks approved by the Ministry of Health and Welfare	Biobank practitioner training Biobank practitioner workshop Practical training for users of bioinformation systems Bioinformation system basic/in-depth course Bioresource distribution desk basic course Practical training for tissue resource quality management	The second session of the biobank manager practical training course
2012	-	2020	-
Practitioner training for 17 KBN biobanks	-	Practical training for tissue resource quality management	-
Start regular training for practitioners	Increase in the frequency of training	Overview	Distribution of standard software (HuBis_Sam)
Systematization of educational programs	Independent operation and expansion of BIMS education Expanding training targets in 2015	Separate operation of four training programs Expansion of BIMS education	Development of online education content for biobank manager practical training course in 2022

Table 4. Content of KOLAS training related to ISO 20387

Training type	Module	Courses	Content and structure
Assessor training	1. New assessor training	ISO 17025 (40 hr)	Ethics education International mutual accreditation and conformity assessment system Trends in international conformity assessment and KS Q ISO/IEC 1701 Assessment techniques and skills KS Q ISO 19011 guidelines Certified information integration system KS Q ISO/IEC 17025 requirements description and understanding Nonconformity cases and application practice Roleplay, case assessment Report writing practice Course evaluation
		Measurement uncertainty (20 hr)	Theory of statistics Measurement uncertainty assessment overview Bottom-up and top-down approaches Measurement uncertainty assessment case practice ISO 5725 overview Course evaluation
		ISO 20387 (16 hr)	Bioethics, biosafety ethics education KOLAS biobank accreditation system and international trends according to KS Q ISO/IEC 17011 KS J ISO 20387 requirements: description and understanding Current status and cases of biobank operation Method validation and verification overview Requirement application practice Course evaluation
	2. Lead assessor training	-	Scheduled
Practitioner training	1. New training (20 hr)	-	Ethics education KOLAS biobank accreditation system and international trends KS J ISO 20387 requirements: description and understanding Metrological traceability and overview of SI units Current status and case of biobank operation Method validation and verification overview KOLAS accreditation criteria Course evaluation (60 points or higher)
		2. Maintenance (5 hr, once every 3 yr)	-
Internal auditor training	-	-	KS Q ISO 19011 management system review guidelines Case analysis (practice) Theory 50%, practice 50%

KOLAS, Korea Laboratory Accreditation Scheme.

COMPOSITION OF PROPOSED PROFESSIONAL EDUCATION PROGRAMS BASED ON KS J ISO 20387

The composition of biobanking education based on KS J ISO 20387 is divided into general, structure, resource, process, and quality management system requirements, as shown in Table 5 [35]. For the establishment, maintenance, and quality control of biobanking, we suggest that biobanking practices based on KS J ISO 20387 be applied, and that professional education programs for training professionals include the following.

First, the general operation management course, which deals with quality management, risk management, ethics, and the law of biobanking (based on KS J ISO 20387) is unified into a common education program applicable to all biobanks.

Second, the course about managing bioresources, such as human-derived resources, animals, plants, and microorganisms, applies to resources based on KS J ISO 20387 and provides preservation methods, quality control methods, and deposit sales units.

Third, professional biobanking education from biobanks should be offered with various and systematic curriculums. Training courses should be divided according to the tasks of the operating manager (bank president), quality control manager, practitioner in charge of bioresources from deposit to sale, and an administrative officer in charge of education, and

they should offer a systematic step-by-step curriculum. This program will subdivide educational categories and levels for customized education, including beginner, intermediate, and advanced grades with various educational content.

Fourth, biobanks based on KS J ISO 20387:2018 must be familiar with ISO 9001:2015 to operate the quality management system, so they should offer training courses related to ISO 9001:2015 for quality management systems and certification. They must also be familiar with ISO 17025:2017 for general requirements about the competence of testing and calibration laboratories and accreditation, with ISO 17043:2010 for proficiency test providers, and with ISO 13528:2015 for statistical methods used in proficiency testing by interlaboratory comparison.

Fifth, the expected effect and use plan for professional curriculum developed based on KS J ISO 20387 for biobanking encourages continuous contribution of the Korea Accreditation Support Center, which provides education on assessment specifications for biobank certification that meets the requirements of the international standard. Therefore, it operates under ISO/IEC 17024: 2012 Conformity Assessment–General requirements for models operating certifications of persons, which sets out the principles and requirements for institutions that regularly provide standards training for biobank members and certify surveyor qualifications. In addition, when government-related institutions want to establish professional education institutions for biobanks and provide common standard

Table 5. KS J ISO 20387–based professional training plan

Category	Description	Key content
Basics of biobanking	Overview of the scope, citation standards, terms and definitions, and establishment, maintenance, and use of biobanks	-
General requirements	General requirements such as operating procedures, fairness, and confidentiality	General principles
Structural requirements	The legal status of bioresources, the authority and obligations of banks and members, governance	Organizational structure, responsibilities, authority, legal identity
Resource requirements	Biobank requirements according to components: general matters; personnel (general matters, eligibility, eligibility assessment, and training); facilities/applicable areas and environmental conditions; outside processes; management of products and services; equipment, etc.	Resource management
Process requirements	Biobank requirements according to processes: general matters; collection, receipt, distribution, transportation, tracking, preparation, preservation, and storage of bioresources and related data; quality control of bioresources and data; validation and verification of methods; management of information and data; requirements for nonconforming result reports, complaints, etc.	Material and material information management
Requirements for quality management system	Options, documentation and management of quality management systems, records management, actions to risks and opportunities, improvements, response to nonconforming results, internal audits, and quality management review	Quality management system

education applicable to pan-ministerial biobanks, the Biobank Research Association can cooperate as a specialized institution for establishing an educational system.

Sixth, the following method for providing domestic professional education programs is proposed (Table 6).

- KS J ISO 20387-based SOPs and various educational contents should be developed considering the operational status of each institution and the composition of the national governance system.
- Despite the growing demand for biobanking experts, no university in Republic of Korea offers a biobanking degree program. A biobanking degree program could synergize the knowledge and practices of general biobanking professional education by offering professional on-site/online biobanking education at a university and awarding a Master's degree within 2 years.
- Universities or other institutions could provide specialized courses and certifications for data quality education through approximately 6 months of on-site and online training. Universities or other institutions with short- and long-term courses could offer certificates through molecular and genetic education classes and practical training during 3 days to 6

- months of on-site practice and field classes.
- A one- to two-day elementary education program that is mandatory for beginners could be administered online (e-learning, webinar, online learning, podcast, etc.), and courses requiring practical training such as quality control and preservation methods could be conducted on-site.
- One- to two-day job training in the form of workshops, seminars, or webinars could be provided for biobanking practitioners to respond to changing biobanking technology and help manage quality control according to the type of biological resources.
- One- to two-day in-depth (advanced) courses at the biobank level could be provided through field classes and hands-on training (in-person seminar format).
- The Korean Society of Pathology Biobank Research Group could continue holding symposiums for pathologists on site and online. Symposium program files have been uploaded annually to the website of the Biobank Research Association of the Korean Society of Pathologists for biobankers and researchers.

Table 6. A proposal for KS J ISO 20387-based professional education programs

Education institution	Characteristics	Completion of training courses	Training method	Period
National Biobank of Korea	SOP renewal based on KS J ISO 20387	-	On-site, online	All the time
	Development and application of international biobanking standards	-	On-site, online	All the time
	Operation of a professional human resource training program	Certificate	On-site, online	All the time
University or other institution of specialized education	Common biobanking professional education	Diploma/certificate	On-site, online	2 yr
	Data quality training	Diploma/certificate	On-site, online	6 mo
	Molecular and genetic education classes and practical training	Certificate	On-site, field classes, practice, course education (short course, long course)	3 days-6 mo
Domestic regional biobanks	Elementary education for beginners	Certificate	E-learning, webinars, podcasts	1-2 days
	Job training for biobanking practitioners	Certificate	Workshops, seminars, webinars	1-2 days
	Group-type in-depth (advanced) courses	Certificate	Field classes and hands-on training	1-2 days
Biobank Study Group of the Korean Society of Pathologists	Symposiums	-	On-site, online	1 day
	Lectures on biobanking	-	Online	All the time
	Education for biobankers and researchers	-	Online	All the time

SOP, standard operating procedure.

EXPECTED EFFECTS OF BIOBANKING EDUCATION IN REPUBLIC OF KOREA

There is a high demand for professional biobanking education, as evidenced by the number of people who completed the National Biobank of Korea's e-learning course in 2022. Domestic accreditation of KS J ISO 20387:2018 for high-quality managed bioresources is now required. For this, systematic governance and professional job training are mandatory. Education programs for biobank members, such as operating managers, quality managers, practitioners, and administrators, can facilitate this accreditation. These programs will benefit health and medical research and related industries.

Nonetheless, there are several limitations to implementing the proposed education programs.

- Because no universities in Republic of Korea currently provide programs related to biobanking, continuous interest, commitment, and financial support are required to establish academic biobank courses at the university level.
- Domestic Regional Biobanks are considered the best institutions actively implementing educational programs because they receive national support. It is necessary to encourage these banks to actively implement educational programs for researchers in their regions.
- The Biobank Study Group of the Korean Society of Pathologists needs to continue to implement the education programs it has provided to date.
- Due to the diverse range of job types within biobanks, it is challenging to implement educational programs within a single integrated system. The educational programs for assessors and practitioners provided by KOLAS pertain to many ISO-related programs; however, their focus on biobanking education is limited. As a result, it is challenging to establish a system based on KS J ISO 20387 after receiving practical training and evaluation related to this standard.
- It is desirable for assessor trainers to have practical experience working in and managing biobanks. The participation of doctors, including pathologists, as assessor trainees is low so far, but it is anticipated that pathologists will eventually engage more actively as assessors.

CONCLUSION

Biobank work will become more specialized and systemized

through international certification, and continual and professional education is an essential element for qualified biobank personnel. Biobank education programs need to include an appropriate range of training opportunities to meet the various needs of biobank employees. These could include in-person and online education programs. Certification of completed education courses is necessary to verify the expertise of qualified biobank operators.

The support of tertiary institutions is needed to establish a Master's degree and education program in the field of biobanking that can be implemented at the universities mentioned in this paper.

Ethics Statement

Not applicable.

Availability of Data and Material

All data generated or analyzed during the study are included in this published article (and its supplementary information files).

Code Availability

Not applicable.

ORCID

Jong Ok Kim	https://orcid.org/0000-0002-3632-2998
Chungyeul Kim	https://orcid.org/0000-0002-9636-5228
Sangyong Song	https://orcid.org/0000-0001-5540-6823
Eunah Shin	https://orcid.org/0000-0001-5961-3563
Ji-Sun Song	https://orcid.org/0009-0007-7116-8141
Mee Sook Roh	https://orcid.org/0000-0002-5676-5569
Dong-chul Kim	https://orcid.org/0000-0002-4710-6449
Han-Kyeom Kim	https://orcid.org/0000-0001-6750-8528
Joon Mee Kim	https://orcid.org/0000-0003-1355-4187
Yeong Jin Choi	https://orcid.org/0000-0002-0744-3854

Author Contributions

Conceptualization: HKK. Formal analysis: JOK, JMK. Investigation: CK, SS, ES, JSS, MSR, DCK. Resources: JOK, JMK. Supervision: JMK, YJC. Writing—original draft: JOK, JMK. Writing—review & editing: JOK, JMK, YJC. Approval of final manuscript: all authors.

Conflicts of Interest

E.S., a contributing editor of the *Journal of Pathology and Translational Medicine*, was not involved in the editorial evaluation

or decision to publish this article. All remaining authors have declared no conflicts of interest.

Funding Statement

The Korean Society for Pathologists provided research funding to the Korean Biobank Study Group.

Acknowledgments

We thank to Choonghyun Lee and Kirham Lee in Korea Conformity Laboratories for their advice in writing this article.

REFERENCES

- Annaratone L, De Palma G, Bonizzi G, et al. Basic principles of biobanking: from biological samples to precision medicine for patients. *Virchows Arch* 2021; 479: 233-46.
- ISO 20387 Biotechnology–Biobanking–General requirements for biobanking [Internet]. Geneva: International Organization for Standardization, 2018 [cited 2024 Jan 26]. Available from: <https://www.iso.org/standard/67888.html>.
- Members [Internet]. Geneva: International Organization for Standardization, 2020 [cited 2024 Jan 9]. Available from: <https://www.iso.org/members.html>.
- ISO/IEC 17000:2020(en) [Internet]. Geneva: International Organization for Standardization, 2020 [cited 2024 Jan 26]. Available from: <https://www.iso.org/standard/73029.html>.
- Yoo KO. Overview of the biobank accreditation system (ISO 20387) and KOLAS policy direction. Daejeon: Korea Bioinformatics Center, 2022.
- About ILAC [Internet]. Vejen: International Laboratory Accreditation Cooperation, 1977 [cited 2024 Jan 28]. Available from: <https://ilac.org/about-ilac/>.
- KOLAS education [Internet]. Eumseong: Korea Laboratory Accreditation Scheme, 2001 [cited 2023 Jan 27]. Available from: <https://www.knab.go.kr/usr/edu/inf/RqinsKolasEduSumryInfo.do>.
- Medical University of Graz. International Biobanking Education [Internet]. Graz: Medical University of Graz, 2015 [cited 2023 Jan 11]. Available from: <https://www.medunigraz.at/en/international-biobanking-education>.
- King's College London [Internet]. London: King's College London, 1829 [cited 2020 Jan 11]. Available from: <https://www.kcl.ac.uk/>.
- Universite Cote D'azur. MSc biobanks and complex data management [Internet]. Nice: University Administrative Center, 2002 [cited 2023 Jan 10]. Available from: <https://univ-cotedazur.eu/search?beanKey=&page=&l=1&RH=1410659255029&q=M-Sc+Biobanks+%26+Complex+Data+Management>.
- Lyon Catholic University. Biobank management | graduate [Internet]. Lyon: Lyon Catholic University, 1875 [cited 2024 Jan 25]. Available from: <https://www.ucl.fr/en/academics/our-programmes/biobank-management-graduate/>.
- Universidad Catolica de Valencia. Postgraduate programmes [Internet]. Valencia: Universidad Catolica de Valencia, 2020 [cited 2024 Jan 28]. Available from: <https://www.ucv.es/eng/studies/postgraduate-programmes>.
- Castellanos-Uribe M, May ST, Betsou F. Integrated BioBank of Luxembourg-University of Luxembourg: University Biobanking Certificate. *Biopreserv Biobank* 2020; 18: 7-9.
- BBMRI.at. Courses and educational events [Internet]. Graz: Biobanking and BioMolecular Resources Research Infrastructure, 2023 [cited 2023 Jan 11]. Available from: <https://bbmri.at/courses>.
- ISBER. Events [Internet]. Vancouver: ISBER, 2023 [cited 2023 Jan 21]. Available from: <https://www.isber.org/page/events>.
- Biobank Resource Centre. Essentials of biobanking course [Internet]. Vancouver: ISBER, 2023 [cited 2023 Jan 11]. Available from: <https://biobanking.org/webs/education>.
- Nam S, Lee S. The necessity for standardized biobanking education. *J Stand Certif Saf* 2018; 8: 35-51.
- Litton JE. Launch of an infrastructure for health research: BBMRI-ERIC. *Biopreserv Biobank* 2018; 16: 233-41.
- CORBEL: coordinated research infrastructures building enduring life-science [Internet]. Paris: European Marine Biological Resource Centre, 2015 [cited 2023 Jan 3]. Available from: <https://www.embrc.eu/collaborative-projects/corbel>.
- Essentials of biobanking [Internet]. Vancouver: Canadian Tissue Repository Network, 2023 [cited 2023 Jan 11]. Available from: <https://www.ctrnet.ca/en/education/>.
- Annual report 2009 (11-1352159-000006-10), Korea Biobank Project. Cheongju: Division of Biobank for Health Science, Korea National Institute of Health, 2010.
- 2010 Annual report of National Biobank of Korea (11-1352159-000046-10). Cheongju: Division of Biobank for Health Science, National Biobank of Korea, 2011.
- 2011 Annual report on National Biobank of Korea (11-1352159-000070-10). Cheongju: Division of Biobank for Health Science, National Biobank of Korea, 2012.
- 2013 Annual report on National Biobank of Korea (11-1352159-000070-10). Cheongju: Division of Biobank for Health Science, National Biobank of Korea, 2014.

25. 2014 Annual report on National Biobank of Korea (11-1352159-000070-10). Cheongju: Division of Biobank for Health Science, National Biobank of Korea, 2015.
26. 2015 Annual report on National Biobank of Korea (11-1352159-000070-10). Cheongju: Division of Biobank for Health Science, National Biobank of Korea, 2016.
27. 2017 Annual report on the National Biobank of Korea. Cheongju: Division of Biobank for Health Science, National Biobank of Korea, 2018.
28. 2018 Annual report on the National Biobank of Korea (#11-1352159-000070-01). Cheongju: Division of Biobank for Health Science, National Biobank of Korea, 2019.
29. 2019 Annual report on the National Biobank of Korea (#11-1352159-000070-10). Cheongju: Division of Biobank for Health Science, National Biobank of Korea, 2020.
30. 2020 Annual report on the National Biobank of Korea (#11-1352159-000070-10). Cheongju: Division of Biobank for Health Science, National Biobank of Korea, 2021.
31. Annual report on National Biobank of Korea (2019) [Internet]. Cheongju: National Institute of Health, 2020 [cited 2023 Jan 13]. Available from: <https://nih.go.kr/>.
32. Human resources manager practical training course (2020-1st session) [Internet]. Jincheon: Government e-learning Platform, 2023 [cited 2023 Jan 22]. Available from: <https://kdca.nhi.go.kr/crs/schedule/crsScheduleList.do>.
33. Lee YH. The microorganisms and industry. Seoul: Korea National Research Resource Center, 2010; 8-12.
34. Korea Conformity Laboratories. KCL/Training/Consulting/Proficiency Korea [Internet]. Seoul: Korea Conformity Laboratories, 1998 [cited 2023 Jan 27]. Available from: <https://www.kcl.re.kr/site/program/education/eduschedule.do?menuid=007002001>.
35. KS J ISO 20387:2018 Biotechnology–Biobanking–General requirements for biobanking. Seoul: Korean Standards Association, 2019.

Breast fine-needle aspiration cytology in the era of core-needle biopsy: what is its role?

Ahrong Kim^{1,2*}, Hyun Jung Lee^{1,3*}, Jee Yeon Kim^{1,3}

¹Department of Pathology, Pusan National University School of Medicine, Yangsan, Korea

²Department of Pathology, Biomedical Research Institute, Pusan National University Hospital, Busan, Korea

³Department of Pathology, Research Institute for Convergence of Biomedical Science and Technology, Pusan National University Yangsan Hospital, Yangsan, Korea

Fine-needle aspiration cytology (FNAC) has long been recognized as a minimally invasive, cost-effective, and reliable diagnostic tool for breast lesions. However, with the advent of core-needle biopsy (CNB), the role of FNAC has diminished in some clinical settings. This review aims to re-evaluate the diagnostic value of FNAC in the current era, focusing on its complementary use alongside CNB, the adoption of new approaches such as the International Academy of Cytology Yokohama System, and the implementation of rapid on-site evaluation to reduce inadequate sample rates. Advances in liquid-based cytology, receptor expression testing, molecular diagnostics, and artificial intelligence are discussed, highlighting their potential to enhance the diagnostic accuracy of FNAC. Despite challenges, FNAC remains a valuable diagnostic method, particularly in low-resource settings and specific clinical scenarios, and its role continues to evolve with technology.

Keywords: Cytology; Breast; Diagnostic techniques; Biomarkers, Tumor

INTRODUCTION

Fine-needle aspiration cytology (FNAC) is a widely known and cost-effective diagnostic tool that is simple to perform and carries a low complication rate. Having no absolute contraindications, FNAC has a high diagnostic accuracy and was once commonly used in clinical practice [1-3]. Before the development of breast screening programs, the primary reason for patients visiting breast clinics was palpable breast lesions, and FNAC was the primary diagnostic method [4]. When a malignancy was diagnosed on FNAC, the diagnosis was confirmed by incisional biopsy and frozen section in the operating field, followed by surgical excision.

However, with advances in breast screening programs, a significant increase has been observed in the detection of non-

palpable breast lesions [5,6]. In conjunction with the development of radiology and the need to evaluate biomarkers for determining the feasibility of preoperative targeted therapies, core-needle biopsy (CNB) has become the preferred method [7,8]. As a result, the role of FNAC in diagnosing breast lesions has diminished, with its diagnostic use decreasing dramatically in clinical settings. Only in low- and middle-income countries, does FNAC remain the primary diagnostic tool for breast pathology [9-11].

While the use of FNAC in the diagnosis of breast lesions has decreased, it remains relevant in situations requiring a rapid and minimally invasive diagnostic test. FNAC is still used when CNB is challenging due to the location of the lesion, or when assessing small axillary lymph nodes or distant metastatic lesions. Ancillary tests such as immunocytochemical staining can

Received: October 2, 2024 **Revised:** October 26, 2024 **Accepted:** November 1, 2024

Corresponding Author: Jee Yeon Kim, MD, PhD

Department of Pathology, Pusan National University School of Medicine, 49 Busandaehak-ro, Mulgeum-eup, Yangsan 50612, Korea
Tel: +82-55-360-1861, Fax: +82-55-360-1865, E-mail: jeykim@pusan.ac.kr

*Ahrong Kim and Hyun Jung Lee contributed equally to this work.

This is an Open Access article distributed under the terms of the Creative Commons Attribution Non-Commercial License (<https://creativecommons.org/licenses/by-nc/4.0/>) which permits unrestricted non-commercial use, distribution, and reproduction in any medium, provided the original work is properly cited.

© 2025 The Korean Society of Pathologists/The Korean Society for Cytopathology

also be performed on cytology samples. Imprint cytology continues to be used for frozen-section diagnoses. It has been reported that mRNA and DNA extracted from FNAC samples are of a higher quality compared with those from formalin-fixed paraffin-embedded (FFPE) tissue, making them suitable for molecular pathology analysis [12,13]. Recent reports suggest that FNAC may have advantages over CNB in digital pathology systems using artificial intelligence (AI) [14].

Given that CNB is now the primary diagnostic tool for breast lesions in developed countries, we aim to review the evolving role of FNAC in breast lesion diagnosis.

TRENDS IN DIAGNOSIS OF BREAST LESIONS

The decline in breast FNAC

After its introduction by Martin and Ellis [15] in New York in the 1930s, breast FNAC evolved significantly at the Karolinska Institute in Sweden over the 1950s and became a primary diagnostic tool for palpable breast lesions, particularly in the United States [16-18]. From the 1980s onward, the techniques and diagnostic applications of breast FNAC continued to improve, making it a safe, economical, and accurate diagnostic method [19,20]. FNAC offers particular advantages in cases involving small lesions and those just beneath the skin or above the chest wall, as well as in patients with breast implants and those taking anticoagulants [21,22].

However, the effectiveness of FNAC depends on the skill and experience of the physician performing the aspiration and the cytopathologist interpreting the results. As breast screening mammography became more popular with the development of innovative localization devices and advances in radiology, the demand for FNAC changed. The high rate of inadequate specimens, difficulties distinguishing in situ from invasive lesions, challenges diagnosing certain lesion categories (e.g., papillary breast lesions, atypical hyperplasia, and lobular carcinoma), and lower diagnostic accuracy for non-palpable lesions and those smaller than 10 mm contributed to the global decline in FNAC use. The rising incidence of false-positive cases and resulting legal actions also contributed to its reduced use [7,8]. Although attempts have been made to address these challenges through image-guided aspiration and the implementation of the triple test (cytology combined with clinical and radiological imaging), the trend in developed countries, including Korea, has shifted toward CNB as the preferred diagnostic method. However,

FNAC remains in use in low- and middle-income countries [9-11].

With CNB now the preferred diagnostic method for breast lesions, clinicians have fewer opportunities to practice FNAC skills, and cytopathologists have fewer chances to interpret FNAC results [23]. This has led to a vicious cycle in which the number of poor-quality smears increases, reducing diagnostic accuracy and prompting more clinicians to choose CNB, ultimately resulting in the abandonment of FNAC [24,25].

The role of CNB

Since its introduction in the late 1990s, the use of CNB has increased significantly, and it is now the primary diagnostic method for evaluating palpable breast lesions and category 4 lesions under the Breast Imaging Reporting and Data System (BI-RADS) [8]. Compared with FNAC, CNB is more expensive, complex, and invasive. It is associated with a higher risk of complications, such as bleeding and hematoma formation, localized infections (up to 2.0% in CNB vs. up to 0.2% in FNAC), skin tethering due to malignant cell seeding along the needle tract (up to 50.0% of CNB cases), and penetration of the pneumothorax or chest wall (1 in 10,000 for FNAC vs. 5 in 10,000 for CNB) [26,27]. Patients often report more pain during or after CNB procedures, a response that can be attributed to the large gauge of needle used. CNB typically involves needles ranging from 14- to 20-gauge, with external diameters of 2.1 to 0.9 mm, compared with FNAC, which uses smaller 22- to 25-gauge needles with an external diameter of 0.7 mm. Despite these drawbacks, CNB offers greater diagnostic accuracy, particularly in cases of non-palpable or calcified lesions, and can more reliably differentiate between in situ and invasive carcinomas. CNB also yields a larger sample volume, which makes possible additional assessments, such as tumor grading, and the evaluation of predictive markers, such as hormone receptors and human epidermal growth factor receptor 2 (HER2) status [28]

NEW APPROACHES TO OVERCOME FINE-NEEDLE ASPIRATION CYTOLOGY LIMITATIONS

Despite the increasing use of CNB, FNAC remains a cost-effective method for diagnosing breast lesions. Numerous studies have compared the diagnostic accuracy of CNB and FNAC, with FNAC sensitivity reportedly ranging from 43.8% to

97.5%—higher when performed by experienced cytopathologists, although sensitivity tends to be lower for atypical or suspicious lesions. Specificity of FNAC ranges from 89.8% to 100%, with a positive predictive value (PPV) as high as 99.3% and a negative predictive value (NPV) of 96.2%. In comparison, CNB typically achieves a sensitivity of 85.0% to 100% and a specificity between 86.0% and 100%, generally showing higher sensitivity and specificity than FNAC, particularly in the evaluation of non-invasive and suspicious lesions. CNB is often preferred over FNAC in cases of suspected malignancy due to its superior diagnostic accuracy and predictive values [7,8]. However, recent comparative studies suggest that the diagnostic outcomes between the two methods do not differ significantly. One study reported that FNAC achieves similar sensitivity (97.0% vs. 97.0%), specificity (94.0% vs. 96.0%), diagnostic accuracy (95.0% vs. 96.0%), and NPV (98.0% vs. 96.0%) when compared with CNB, while offering fewer complications [21].

A new reporting system, the International Academy of Cytology Yokohama System

Introduction of International Academy of Cytology Yokohama System

Since 2016, the International Academy of Cytology (IAC) Yokohama System has been recommended for breast cytology diagnosis. The system involves reporting breast cytology in five categories based on the risk of malignancy (ROM): “insufficient/inadequate,” “benign,” “atypical,” “auspicious of malignancy,” and “malignant.” Each category uses clear descriptive terms and provides definitions, ROM, and a management algorithm. The system outlines key diagnostic cytological features for lesions within each category, supported by illustrations [29].

Categories, ROM, and summary of recommended managements

The “insufficient/inadequate” category is characterized by a paucity of cells, poor smearing, or suboptimal fixation, rendering cytomorphological diagnosis unfeasible. The recommended ROM for this category ranges from 2.6% to 4.8%. When clinical and imaging findings are uncertain or suspicious, a repeat FNAC or CNB is recommended. In cases of imaging findings that appear benign, a repeat FNAC is advised. The “benign” category only applies when cytological findings are unequivocal, and a specific benign diagnosis may be given. With a recommended ROM of 1.4% to 2.3%, further tissue biopsy is

unnecessary if the clinical and imaging findings are benign (i.e., the “triple test” is concordant). If clinical or imaging findings are ambiguous or suspicious, a repeat FNAC or CNB should be performed. “Atypical” is defined by cytological features that are predominantly benign but include rare findings potentially associated with malignancies. The recommended ROM for this category is 13.0% to 15.7%. If atypia can be attributed to technical issues, repeat FNAC is warranted. If the smear quality is adequate but atypia persists, a repeat FNAC or CNB is recommended. The “suspicious of malignancy” category includes lesions with definitive malignant cellular features, although insufficient in quantity or quality for a malignant diagnosis. Describing the suspected malignancy is encouraged. The recommended ROM for this category ranges from 84.6% to 97.1%, and CNB is mandatory after reviewing clinical and imaging findings. The “malignant” category includes smears with clear malignant cytological features, and the type of malignancy should be described if possible. The recommended ROM for this category is 99.0% to 100%. Discrepancies between clinical/imaging findings and cytology necessitate a CNB. If the “triple test” indicates malignancy, definitive treatment should proceed [20,29].

Published data of diagnostic accuracy of IAC Yokohama System

Many studies of the use of the IAC Yokohama System’s five-tier reporting framework and its application across institutions have been conducted. Based on those published between 2019 and 2021, the sensitivity, specificity, PPV, NPV, and diagnostic accuracy of each category were analyzed (Table 1) [30-44]. Diagnostic accuracy varied depending on the exclusion of categories such as “insufficient,” “atypical,” or “suspicious for malignancy.” Studies published in 2019 showed considerable heterogeneity, with diagnostic accuracies ranging from 68.2% to 95.0%, whereas studies published after 2020 demonstrated accuracies that had improved to between 82.7% and 99.4%. This may be likely attributable to accumulated experience with the IAC Yokohama System [45]. Agrawal et al. [39] retrospectively analyzed all cases of breast masses evaluated using FNAC and their histologic correlations in 321 cases. Sensitivities for the “atypical,” “suspicious for malignancy,” and “malignant” categories were 98.2%, 96.0%, and 86.7%, respectively. Specificities for the same categories were 59.5%, 91.9%, and 100%, respectively. The ROMs for the “benign,” “atypical,” “suspicious for malignancy,” and “malignant” categories were estimated at 8.3%

Table 1. Studies included in the review with diagnostic accuracy of the International Academy of Cytology Yokohama System for breast cytology diagnosis

Study	Sensitivity (%)	Specificity (%)	PPV (%)	NPV (%)	Diagnostic accuracy (%)
Nigam et al. (2021) [30]	73.6–92.5	81.5–98.5	80.3–97.5	79.5–93.0	85.6–89.0
Agrawal et al. (2021) [31]	86.1–99.1	99.3–99.6	99.5–99.1	89.9–99.3	93.6–99.4
Sundar et al. (2022) [32]	90.8–98.9	85.0–98.9	76.1–97.5	95.7–99.3	89.5–96.2
Agrawal et al. (2021) [33]	91.5–98.9	61.9–99.1	89.3–99.7	78.3–94.6	90.1–95.2
Wong et al. (2021) [34]	82.7–99.0	94.3–100	85.8–100	94.3–99.7	95.5–98.0
Dixit et al. (2021) [35]	95.0	99.5	98.3	98.6	98.5
Ahuja et al. (2021) [36]	79.2–97.2	86.0–100	77.0–100	90.9–98.5	89.6–96.4
Marabi et al. (2021) [37]	69.5–72.5	98.9–99.2	93.1–94.8	93.7–94.3	93.8–94.1
Oosthuizen et al. (2021) [38]	63.0–88.9	83.6–100	72.7–100	84.6–93.9	-
Agarwal et al. (2021) [39]	86.7–98.2	59.5%–100	88.0–100	71.2–91.7	88.6–95.0
De Rosa et al. (2020) [40]	93.7–98.9	46.3–90.8	80.5–95.8	86.6–95.1	82.7–92.8
Apuroopa et al. (2020) [41]	95.9	97.9	96.8	97.6	98.6
Wong et al. (2019) [42]	92.0–98.9	62.1–97.8	71.1–97.6	92.7–98.3	80.2–95.0
McHugh et al. (2019) [43]	79.5–84.6	75.2–85.1	68.8–77.5	86.6–88.3	78.9–82.9
Montezuma et al. (2019) [44]	83.3–98.3	54.8–99.8	49.2–99.5	93.0–98.6	68.2–94.7

PPV, positive predictive value; NPV, negative predictive value.

(range, 2.3% to 20.0%), 17.2% (range, 5.8% to 35.8%), 77.8% (range, 57.7% to 91.4%), and 100% (range, 98.1% to 100%), respectively, demonstrating a favorable cytological-histologic correlation. The IAC Yokohama System primarily recommends basing reports on direct smears, and studies have found strong interobserver agreement [46]. Folarin et al. [47] also reported excellent interobserver agreement in liquid-based cytology (LBC) evaluations.

The “atypical” category

In the absence of a standardized cytology reporting system, the clinical decision-making impact of “atypical” diagnoses varies, but has yet to be clearly analyzed. Without standardized guidelines, clinicians tend to base “atypical” diagnoses on sample type and individual judgment. A standardized reporting system allows cytopathologists, clinicians, and patients to mutually understand what an “atypical” diagnosis entails, reducing the unnecessary use of this category, minimizing confusion or patient anxiety, and fostering effective communication between cytopathologists and clinicians. The five-tier IAC Yokohama System is considered an appropriate standardized reporting system for breast-lesion FNAC. However, much discussion has occurred regarding the “atypical” category, which continues to pose challenges [20,44,48]. How clinicians within each institution interpret and respond to the “atypical” category is a critical factor. Additional explanations, such as “favor benign” or “can-

not exclude malignancy,” can help convey the level of concern and limitations regarding an “atypical” diagnosis, drawing on the relationship between pathologists and clinicians. Multidisciplinary discussions can initiate these conversations, although it may take time for clinicians to become familiar with a new reporting system [49]. It is particularly important for institutions to use prospective ROM categories in a manner consistent with their chosen reporting system to ensure structured management (Table 2) [30-44,50,51].

Limitations of the IAC Yokohama System

This new structured standardized reporting system, which is based on the ROM, would improve the performance, interpretation, and reporting of breast FNAC and clarify communication between cytopathologists and clinicians. The suggested management algorithm will benefit patient and provide diagnostic options. Nevertheless, diagnostic pitfalls persist. Pauci-cellular smears can lead to false-negative diagnoses, particularly for lobular carcinoma. Complex sclerosing lesions, fibroadenomas, and papillomas can exhibit worrisome features, resulting in false-positive diagnoses. Benign inflammatory lesions such as fat necrosis, and rare entities such as collagenous spherulosis, may also cause diagnostic challenges. Ductal carcinoma in situ may lead to both false-negative and false-positive diagnoses, particularly in distinguishing high-grade lesions from invasive carcinoma, highlighting the limita-

Table 2. Studies included in review with comparing the ROM for each diagnostic category of the International Academy of Cytology Yokohama System for breast cytology diagnosis

Study	ROM of inadequate (%)	ROM of benign (%)	ROM of atypical (%)	ROM of suspicious of malignancy (%)	ROM of malignant (%)
Nigam et al. (2021) [30]	50.0	7.3	40.0	83.3	97.5
Agrawal et al. (2021) [31]	16.0	0.7	23.3	94.1	100
Sundar et al. (2022) [32]	38.0	0.6	21.9	100	97.0
Agrawal et al. (2021) [33]	30.0	5.0	25.0	71.0	99.7
Wong et al. (2021) [34]	13.6	0.4	25.0	85.7	100
Tejeswini et al. (2021) [50]	22.2	5.3	26.3	100	100
Saranghi et al. (2021) [51]	33.3	0.4	37.5	96.0	100
Dixit et al. (2021) [35]	33.3	0.5	13.3	83.3	100
Ahuja et al. (2021) [36]	5.0	1.5	17.4	81.8	100
Marabi et al. (2021) [37]	8.8	0.5	22.6	89.2	100
Oosthuizen et al. (2021) [38]	11.0	3.0	28.0	56.0	100
Agarwal et al. (2021) [39]	60.9	8.3	17.2	77.8	100
De Rosa et al. (2020) [40]	-	4.9	20.7	78.7	98.8
Apuroopa et al. (2020) [41]	5.0	1.2	12.5	93.7	100
Wong et al. (2019) [42]	2.6	1.7	15.7	84.6	99.5
McHugh et al. (2019) [43]	0	12.0	25.0	46.0	91.0
Montezuma et al. (2019) [44]	4.8	1.4	13.0	97.1	100

ROM, risk of malignancy.

tions of cytology in certain cases [52].

FNAC with rapid on-site evaluation

In cytology, rapid on-site evaluation (ROSE) assists in evaluating the cytomorphological features of fine-needle aspiration (FNA) smears or biopsy touch preparations [53]. ROSE reduces the number of “insufficient/inadequate” samples in breast cytology to less than 1%, and concordance between on-site diagnoses and final diagnoses is high [54]. ROSE also helps determine whether additional FNAC attempts are necessary, and after assessing the ROSE results, further sampling from the lesion can be performed for ancillary tests [54]. During ROSE, the consistency of the lesion/mass (soft, firm, or hard), changes in lesion size after aspiration, color of the aspirated fluid (bloody, clear, or green, etc.), consistency of the aspirated fluid (viscous, watery, or mucinous, etc.), and cellularity are evaluated [54]. Schoellnast et al. [55] emphasized the importance of having a cytopathologist evaluate the quality of the specimen on-site. They reported that FNAC without on-site cytopathological evaluation does not yield superior sensitivity and specificity compared with CNB. When on-site evaluations were performed, the average non-diagnostic rate of FNAC decreased from 20.0% to 0.1%, and diagnostic accuracy increased

to 96.0% [53,56,57].

Wong et al. [42] reported statistically significant differences in the “inadequate” and “malignant” categories when comparing FNAC with ROSE. IAC Yokohama System also recommends the use of ROSE where possible to reduce the rate of insufficient and/or inadequate samples in FNAC. They found that ROSE reduced the proportion of inadequate samples from 17.1% to 4.0% and increased the proportion of malignant samples from 17.9% to 39.0%, with statistically significant differences. ROSE is recommended to reduce the proportion of “inadequate” and “atypical” categories and increase the diagnoses of “suspicious of malignancy” and “malignant,” allowing for immediate classification for additional biopsy when necessary [25,42]. Suciú et al. [58] analyzed the diagnostic accuracy of the on-site cytopathology advance report (OSCAR) for breast masses classified by the American College of Radiology BI-RADS. Their findings demonstrated a sensitivity of 97.4%, specificity of 95.0%, and diagnostic accuracy of 96.5%. The OSCAR procedure proved to be a reliable diagnostic approach, particularly in multidisciplinary, integrated, one-stop clinics where an interventional cytopathologist can efficiently identify patients who require CNB [58].

Agrawal et al. [31], who classified breast lesions using the

IAC categories, reported overall sensitivity and specificity of 99.1% and 99.3%, respectively, with ROSE significantly enhancing the diagnostic outcomes. ROSE reduced the rate of “insufficient” cases ($p < .001$) and improved the concordance between cytopathology and histopathology from 76.9% to 90.2%. The ROM progressively increased from the “insufficient” to the “malignant” categories, with this trend becoming more pronounced when ROSE was applied. Studies have found that, with ROSE, the ROM in the “insufficient” category was reduced from 0%–60.9% to 0%–11.0% [42]. Bharti et al. [59] suggested that standardized guidelines for ROSE are essential for its broader implementation and to reduce the rate of the “insufficient/inadequate” category. However, under the current healthcare system in Korea, inadequate reimbursements and the labor-intensive nature of the procedure have prevented the widespread adoption and made it difficult to implement in secondary and tertiary hospitals.

Combined approach of FNAC followed by CNB

FNAC and CNB are both useful diagnostic methods, each with distinct advantages and limitations. Several studies have suggested that these two techniques can be used complementarily rather than separately. One study reported that the sensitivity for breast cancer diagnosis was 80% when FNAC was used alone, 88.0% when CNB was used alone, but 100% when both techniques were applied [60]. While the use of FNAC has gradually declined and been replaced by CNB in many institutions, Nassar [8] emphasized the importance of FNAC and the utility of newer techniques that could help overcome its limitations compared with CNB. One of the major disadvantages of FNAC is the relatively high rate of inadequate samples compared with CNB. In studies of non-palpable breast lesions, Salami et al. [61] reported that 22.0% of FNAC samples were inadequate, while Ibrahim et al. [62] found an even higher rate of 58.7%. To address these limitations, Joudeh et al. [63] proposed performing CNB immediately after ensuring an adequate FNAC sample in the same setting. This approach allows both tests to be completed in a single visit, making it convenient for the patient, and the combined samples from FNAC and CNB enable a more accurate diagnosis, reducing the need for additional invasive procedures and improving cost efficiency. They also suggested that, when CNB is performed in the same setting as FNAC, adding a touch imprint would provide even more diagnostic information.

The combination of FNAC and CNB can increase overall

diagnostic accuracy, particularly in small lesions, and provide more material for additional ancillary studies. FNAC and CNB together allow for better interpretation of morphology and structure, increase sensitivity and specificity compared with either method alone, and offer greater convenience to patients. This approach can provide greater satisfaction to clinicians who may hesitate to rely solely on cytological data. It also gives pathologists who rely on histological diagnoses the opportunity to build more experience with cytology, making it a valuable approach to handling complex malignancies such as composite malignancies.

Sustova and Klijanienko [64] evaluated the diagnostic accuracy of FNAC and CNB in palpable breast tumors. While CNB had greater diagnostic accuracy for benign tumors (94.7% for FNAC vs. 100% for CNB), FNAC was more accurate when dealing with malignant tumors (95.6% for FNAC vs. 94.7% for CNB). The diagnostic correlation between FNAC and CNB for malignant tumors was strong, and the unsatisfactory category was lower for FNAC (2.7% for FNAC vs. 4.9% for CNB). Only 0.4% of cases had unsatisfactory results from both FNAC and CNB, and when the two methods were combined, sensitivity reached 99.8%. Based on these findings, Sustova and Klijanienko [64] concluded that combining FNAC and CNB is the optimal approach to diagnosing palpable breast tumors, and they recommended it as a standard diagnostic method.

FNA using LBC

According to the College of American Pathologists' National Breast FNA Biopsy Practice Survey, approximately 40% of laboratories reported using LBC for breast FNA [65]. Multiple studies have reported that FNA using conventional smears and LBC are comparably accurate in detecting malignant tumors [45,66,67]. Folarin et al. [47] emphasized the utility of LBC, particularly given the relative decline in breast FNAC and the lack of ROSE for assessments. They evaluated the reproducibility of the IAC Yokohama System for reporting breast FNA using LBC, reporting substantial to almost perfect agreement among reviewers ($\kappa = 0.73$ – 0.91) and concordance with histopathologic follow-up ($\kappa = 0.66$ – 0.85). The use of LBC reduced the rate of inadequate samples compared with conventional cytology, although the categories with the lowest agreement were “inadequate” and “atypical.” The lower concordance in the atypical category was attributed primarily to low cellularity or incomplete structural features.

Proposed diagnostic algorithm

Silva et al. [68] recommended a stepwise diagnostic approach in a multidisciplinary setting. The first step involves mammography and ultrasound imaging, followed by FNAC. In rare cases, cytologically benign but highly cellular lesions undergo further evaluation with CNB. If malignant cells are detected in FNAC, CNB of the breast tumor is performed along with FNAC of the axillary lymph nodes, and treatment planning is based on staging.

A diagnostic algorithm that combines FNAC with CNB has been recognized as an effective approach to improved diagnostic accuracy in breast lesions and providing better information in uncertain cases. This approach starts with an initial evaluation using FNAC to rapidly assess malignant, benign, or atypical cells. If the FNAC results are atypical or suspicious, or if the patient or physician desires a definitive diagnosis, CNB is performed for further tissue sampling. This method improves the accuracy of breast lesion diagnosis while minimizing patient discomfort [7,8,69]. This diagnostic algorithm can be an effective strategy to reduce unnecessary surgeries or additional tests, while ensuring rapid and accurate diagnosis of malignant lesions.

BEYOND THE CYTOLOGY IN BREAST FINE-NEEDLE ASPIRATION

Immunocytochemical stains in breast FNAC

While it was known that receptor expression could not be reliably assessed in cytological specimens, several studies published since the 2000s have demonstrated the successful evaluation of receptor expression in FNAC samples [70,71]. Studies have confirmed that estrogen receptor (ER) and progesterone receptor (PR) analyses can be accurately performed on FNAC smears. Durgapal et al. [72] reported a 99.0% diagnostic accuracy for immunocytochemical analysis performed on FNAC samples compared to immunohistochemistry, with 100% concordance between immunocytochemistry and fluorescence in situ hybridization (FISH) techniques. Vohra et al. [73] analyzed the correlation between expression of these markers in cell blocks obtained from FNAC and tissue blocks, showing excellent agreement for ER and HER2 and “moderate agreement” for PR. Cytological preparations differ from tissue fixed in formalin in that they are alcohol-fixed, which can lead to differences in tissue structure and cellular composition [74]. Additionally, the lack of tissue architecture in cytological spec-

imens can affect the interpretation of immunocytochemical staining [75]. Extensive validation studies have been conducted for immunocytochemical staining, including comparisons with paired surgical or core biopsy specimens and/or clinical data, to account for factors that could affect interpretation [76].

Pinto and Schmitt [77] conducted extensive validation of four immunostains (ER, PR, HER2/neu, and Ki-67) on primary breast lesions and cytological specimens. Studies applying a 1% cutoff for ER- and PR-positivity have shown concordance rates ranging from 80% to 99% [73,78,79]. Vohra et al. [73] reported more than 98% concordance between HER2 immunocytochemistry and HER2 FISH performed on cell blocks. Studies using Ki-67 immunostaining with a 20% cutoff reported concordance rates of 85%–90% [80,81].

For axillary metastases, studies of tissue sections from FFPE samples have shown high (greater than 95%) concordance rates for hormone receptor status between primary tumors and axillary lymph node metastases. For HER2, concordance was slightly lower but still above 85% [82,83]. Although few studies have examined receptor expression in metastatic breast cancer, Pareja et al. [84] reported finding similar concordance between primary breast lesions and metastatic sites. However, some discordance was observed, with most cases involving loss of hormone receptor positivity in axillary lymph node FNACs from initially hormone receptor-positive primary tumors. This phenomenon, known as receptor loss, is often seen following endocrine therapy and could explain discrepancies in studies in which biopsy data from both primary and metastatic sites are separated by treatment intervals [85]. Nevertheless, it is essential to consider potential sampling errors or low cellularity before prematurely attributing negative results to treatment effects [86]. With the approval of trastuzumab-deruxtecan for HER2-low metastatic breast cancer, the interobserver variability in HER2 immunostaining interpretation of cytological specimens from metastatic sites has been evaluated. Discrepancies were observed in approximately 30% of cases, highlighting the need for standardization in interpretation [87].

Molecular study using cytology samples

Generally, non-formalin-fixed cytological material is more suitable for molecular testing than formalin-fixed tissue or cell blocks. This is because such samples tend to preserve high-quality nucleic acids that are stable and easy to extract [88]. Most molecular tests are now conducted on FFPE samples, largely because these tests have been validated on FFPE

samples. Although cytological samples are underutilized in molecular pathology [88,89], several studies have shown that cytological preparations, such as smears and LBC, perform equally well or better than FFPE samples in molecular testing [89,90]. With proper sample collection and careful validation of molecular tests, cytological samples can be a valuable resource for molecular diagnostics.

FNAC samples can be particularly useful for biomarker evaluation or discovery, as they often contain a higher proportion of tumor cells compared with CNB or surgically excised tissue [91]. FNAC samples have been used successfully for genomic testing across a variety of tumor types, yielding reliable results [92]. Park et al. [93] identified novel cancer biomarkers using high-throughput proteomic analysis of FNAC samples from breast cancer, demonstrating results comparable to those obtained from tissue.

LBC improves sample quality by reducing contamination and artifact formation and can preserve residual material for additional molecular analyses. LBC reportedly provides high-quality DNA suitable for genetic testing and plays a key role in identifying actionable mutations in breast cancer [94]. Akahane et al. [95] reported that high-quality DNA and RNA were obtained from cells preserved in various LBC fixatives, detecting expected genetic mutations and fusion genes. The use of residual LBC specimens for genomic analysis, including gene fusion analysis, is especially useful for obtaining preoperative genomic information.

Although cytomorphologic evaluations using tissue-touch imprints during ROSE or intraoperative consultation are valuable, few studies have explored their use in molecular testing, and next-generation sequencing in particular. Aydin Mericoz et al. [96] suggested that touch imprint slides could serve as an alternative when neoplastic cells are scarce or when nucleic acid quality is compromised by decalcification in permanent biopsy specimens. They recommended routine use of touch imprints in all bone biopsies, with digital scans made for reference and original slides reserved for DNA/RNA-based molecular research.

Cell block (and blood clot) preparations are reliable sources of stored material for molecular testing. FISH is one of the most commonly performed tests in routine practice. In breast cancer, FISH can be used to detect specific gene fusions, such as *MYB-NFIB*, or to assess the level of *HER2* amplification [97,98].

Although most molecular tests are performed on FFPE tissue samples, several well-established molecular diagnostic tests and

both commercial and laboratory-developed tests can be performed on cytological samples [88].

Digital pathology and AI

Modern whole-slide scanners, capable of capturing high-resolution and stacked images, have enabled the development of digital tools for cytopathology and AI models [99]. The use of whole-slide imaging (WSI) in cytopathology has lagged behind that in histopathology. Ren et al. [100] scanned glass slides of intraoperative touch imprint cytology from the axillary sentinel lymph nodes of patients with breast cancer using two different WSI scanners. They compared intraobserver and interobserver agreement, accuracy, potential causes of diagnostic errors, scanning times, and review times between WSI and light microscopy (LM). When comparing LM slides with WSI digital slides, intraobserver and interobserver agreement was high. LM accuracy averaged 98.06%, slightly higher than that of WSI (96.8%–97.8%). Most diagnostic errors were due to false negatives, typically arising from cases with few cancer cells or confusion between cancer cells and histiocytes or lymphocytes. The Ren et al.'s study [100] suggested that WSI may serve as a practical option for intraoperative touch imprint cytological diagnosis of sentinel lymph nodes when experienced pathologists are unavailable.

Deep learning algorithms for detecting lymph node metastases from tissue sections have shown promising results [101]. As digital cytopathology and AI continue to evolve, future capabilities may include not only cytological diagnosis but integrated structural reporting, possibly even replacing certain molecular tests [102,103].

CONCLUSION

We reviewed the role of breast FNAC in the diagnosis of breast lesion. Despite the increasing use of CNB, FNAC remains a cost-effective, minimally invasive, and safe diagnostic method of evaluating breast lesions with a significant degree of accuracy, particularly when performed by experienced practitioners.

To overcome the limitations and declining use of breast FNAC, new approaches have been attempted. A new standardized reporting system, the IAC Yokohama System, based on the ROM can improve the diagnostic skill and interpretation of breast FNAC, as well as communication between cytopathologists and clinicians. The introduction of ROSE has substantially reduced the number of inadequate samples, further enhanc-

ing FNAC's diagnostic value. A combination of FNAC and CNB can significantly enhance diagnostic accuracy. Together, these techniques allow for more comprehensive evaluation, particularly when the initial FNAC result is "indeterminate" or "atypical."

The ongoing integration of advanced technologies, such as LBC, molecular testing using FNAC samples, and digital pathology supported by WSI and AI, is transforming the landscape of cytological diagnostics. These innovations allow for more precise molecular profiling, superior sample preservation, and enhanced diagnostic accuracy, making FNAC a relevant and valuable tool, even in the modern era of breast pathology. As these technologies continue to evolve, FNAC's role may expand, providing a cost-effective, efficient, and less-invasive option for breast cancer diagnosis, particularly in multidisciplinary settings where rapid, reliable diagnoses are critical for treatment planning.

Ethics Statement

Not applicable.

Availability of Data and Material

Data sharing not applicable to this article as no datasets were generated or analyzed during the study.

Code Availability

Not applicable.

ORCID

Ahrong Kim <https://orcid.org/0000-0003-2317-8920>
 Hyun Jung Lee <https://orcid.org/0000-0002-2995-6060>
 Jee Yeon Kim <https://orcid.org/0000-0002-0503-984X>

Author Contributions

Conceptualization: JYK, AK, HJL. Resources: JYK. Writing—original draft: JYK. Writing—review & editing: JYK, AK, HJL. Approval of final manuscript: all authors.

Conflicts of Interest

The authors declare that they have no potential conflicts of interest.

Funding Statement

No funding to declare.

REFERENCES

- Gupta DK, Mooney EE, Layfield LJ. Fine-needle aspiration cytology: a survey of current utilization in relationship to hospital size, surgical pathology volume, and institution type. *Diagn Cytopathol* 2000; 23: 59-65.
- Ly A, Ono JC, Hughes KS, Pitman MB, Balassanian R. Fine-needle aspiration biopsy of palpable breast masses: patterns of clinical use and patient experience. *J Natl Compr Canc Netw* 2016; 14: 527-36.
- Farras Roca JA, Tardivon A, Thibault F, et al. Diagnostic performance of ultrasound-guided fine-needle aspiration of nonpalpable breast lesions in a multidisciplinary setting: the Institut Curie's experience. *Am J Clin Pathol* 2017; 147: 571-9.
- Ciatto S, Cariaggi P, Bulgaresi P, Confortini M, Bonardi R. Fine needle aspiration cytology of the breast: review of 9533 consecutive cases. *Breast* 1993; 2: 87-90.
- Elmore JG, Barton MB, Moceri VM, Polk S, Arena PJ, Fletcher SW. Ten-year risk of false positive screening mammograms and clinical breast examinations. *N Engl J Med* 1998; 338: 1089-96.
- Fornage BD, Faroux MJ, Simatos A. Breast masses: US-guided fine-needle aspiration biopsy. *Radiology* 1987; 162: 409-14.
- Willems SM, van Deurzen CH, van Diest PJ. Diagnosis of breast lesions: fine-needle aspiration cytology or core needle biopsy? A review. *J Clin Pathol* 2012; 65: 287-92.
- Nassar A. Core needle biopsy versus fine needle aspiration biopsy in breast: a historical perspective and opportunities in the modern era. *Diagn Cytopathol* 2011; 39: 380-8.
- Tikku G, Umap P. Comparative study of core needle biopsy and fine needle aspiration cytology in palpable breast lumps: scenario in developing nations. *Turk Patoloji Derg* 2016; 32: 1-7.
- Mremi A, Pallangyo A, Mshana T, et al. The role of clinical breast examination and fine needle aspiration cytology in early detection of breast cancer: a cross-sectional study nested in a cohort in a low-resource setting. *Womens Health (Lond)* 2024; 20: 17455057241250131.
- Khorsandi N, Balassanian R, Vohra P. Fine needle aspiration biopsy in low- and middle-income countries. *Diagn Cytopathol* 2024; 52: 426-32.
- Uzan C, Andre F, Scott V, et al. Fine-needle aspiration for nucleic acid-based molecular analyses in breast cancer. *Cancer* 2009; 117: 32-9.
- Lee HB, Joung JG, Kim J, et al. The use of FNA samples for whole-exome sequencing and detection of somatic mutations in breast cancer surgical specimens. *Cancer Cytopathol* 2015; 123:

- 669-77.
14. Islam R, Tarique M. Artificial intelligence (AI) and nuclear features from the fine needle aspirated (FNA) tissue samples to recognize breast cancer. *J Imaging* 2024; 10: 201.
 15. Martin HE, Ellis EB. Aspiration biopsy. *Surg Gyn Obst* 1934; 59: 578-89.
 16. Bauermeister DE. The role and limitations of frozen section and needle aspiration biopsy in breast cancer diagnosis. *Cancer* 1980; 46: 947-9.
 17. Masood S. Core needle biopsy versus fine-needle aspiration biopsy: are there similar sampling and diagnostic issues? *Breast J* 2003; 9: 145-6.
 18. Cobb CJ, Raza AS. Obituary: "alas poor FNA of breast: we knew thee well!". *Diagn Cytopathol* 2005; 32: 1-4.
 19. Pinto DG, Tse G, Tan PH, Schmitt F. Aspiration techniques. In: Tse G, Tan PH, Schmitt F, eds. *Fine needle aspiration cytology of the breast: atlas of cyto-histologic correlates*. Berlin: Springer, 2023; 21-31.
 20. Field AS, Raymond WA, Richard MT, et al. Introduction and overview. In: Field AS, Raymond WA, Schmitt F, eds. *The International Academy of Cytology Yokohama System for reporting breast fine needle aspiration biopsy cytopathology*, Berlin: Springer, 2020; 1-9.
 21. Moschetta M, Telegrafo M, Carluccio DA, et al. Comparison between fine needle aspiration cytology (FNAC) and core needle biopsy (CNB) in the diagnosis of breast lesions. *G Chir* 2014; 35: 171-6.
 22. Ballo MS, Sneige N. Can core needle biopsy replace fine-needle aspiration cytology in the diagnosis of palpable breast carcinoma: a comparative study of 124 women. *Cancer* 1996; 78: 773-7.
 23. Berner A, Sauer T. Fine-needle aspiration cytology of the breast. *Ultrastruct Pathol* 2011; 35: 162-7.
 24. El Chamieh C, Vielh P, Chevret S. Statistical methods for evaluating the fine needle aspiration cytology procedure in breast cancer diagnosis. *BMC Med Res Methodol* 2022; 22: 40.
 25. Field AS, Raymond WA, Rickard M, Schmitt F. Breast fine needle aspiration biopsy cytology: the potential impact of the International Academy of Cytology Yokohama System for reporting breast fine needle aspiration biopsy cytopathology and the use of rapid on-site evaluation. *J Am Soc Cytopathol* 2020; 9: 103-11.
 26. Hoorntje LE, Schipper ME, Kaya A, Verkooijen HM, Klinkenbijn JG, Borel Rinkes IH. Tumour cell displacement after 14G breast biopsy. *Eur J Surg Oncol* 2004; 30: 520-5.
 27. Kazi M, Parshad R, Seenu V, Mathur S, Haresh KP. Fine-needle aspiration cytology (FNAC) in breast cancer: a reappraisal based on retrospective review of 698 cases. *World J Surg* 2017; 41: 1528-33.
 28. Litherland JC. Should fine needle aspiration cytology in breast assessment be abandoned? *Clin Radiol* 2002; 57: 81-4.
 29. Field AS, Raymond WA, Rickard M, et al. The International Academy of Cytology Yokohama System for reporting breast fine-needle aspiration biopsy cytopathology. *Acta Cytol* 2019; 63: 257-73.
 30. Nigam JS, Kumar T, Bharti S, Sinha R, Bhadani PP. The International Academy of Cytology standardized reporting of breast fine-needle aspiration biopsy cytology: a 2 year's retrospective study with application of categories and their assessment for risk of malignancy. *Cytojournal* 2021; 18: 27.
 31. Agrawal N, Kothari K, Tummidi S, Sood P, Agnihotri M, Shah V. Fine-needle aspiration biopsy cytopathology of breast lesions using the International Academy of Cytology Yokohama System and rapid on-site evaluation: a single-institute experience. *Acta Cytol* 2021; 65: 463-77.
 32. Sundar PM, Shanmugasundaram S, Nagappan E. The role of the IAC Yokohama System for reporting breast fine needle aspiration biopsy and the ACR Breast Imaging-Reporting and Data System in the evaluation of breast lesions. *Cytopathology* 2022; 33: 185-95.
 33. Agrawal S, Anthony ML, Paul P, et al. Prospective evaluation of accuracy of fine-needle aspiration biopsy for breast lesions using the International Academy of Cytology Yokohama System for reporting breast cytopathology. *Diagn Cytopathol* 2021; 49: 805-10.
 34. Wong YP, Vincent James EP, Mohammad Azhar MA, et al. Implementation of the International Academy of Cytology Yokohama standardized reporting for breast cytopathology: an 8-year retrospective study. *Diagn Cytopathol* 2021; 49: 718-26.
 35. Dixit N, Trivedi S, Bansal VK. A retrospective analysis of 512 cases of breast fine needle aspiration cytology utilizing the recently proposed IAC Yokohama System for reporting breast cytopathology. *Diagn Cytopathol* 2021; 49: 1022-31.
 36. Ahuja S, Malviya A. Categorization of breast fine needle aspirates using the International Academy of Cytology Yokohama System along with assessment of risk of malignancy and diagnostic accuracy in a tertiary care centre. *J Cytol* 2021; 38: 158-63.
 37. Marabi M, Aphivatanasiri C, Jamidi SK, et al. The International Academy of Cytology Yokohama System for Reporting Breast Cytopathology showed improved diagnostic accuracy. *Cancer Cytopathol* 2021; 129: 852-64.
 38. Oosthuizen M, Razack R, Edge J, Schubert PT. Classification of male breast lesions according to the IAC Yokohama System for

- reporting breast cytopathology. *Acta Cytol* 2021; 65: 132-9.
39. Agarwal A, Singh D, Mehan A, et al. Accuracy of the International Academy of Cytology Yokohama System of breast cytology reporting for fine needle aspiration biopsy of the breast in a dedicated breast care setting. *Diagn Cytopathol* 2021; 49: 195-202.
 40. De Rosa F, Migliatico I, Vigliar E, et al. The continuing role of breast fine-needle aspiration biopsy after the introduction of the IAC Yokohama System for reporting breast fine needle aspiration biopsy cytopathology. *Diagn Cytopathol* 2020; 48: 1244-53.
 41. Apuroopa M, Chakravarthy VK, Rao DR. Application of Yokohama System for reporting breast fine needle aspiration cytology in correlation with histopathological and radiological findings. *Ann Pathol Lab Med* 2020; 7: A210-5.
 42. Wong S, Rickard M, Earls P, Arnold L, Bako B, Field AS. The International Academy of Cytology Yokohama System for reporting breast fine needle aspiration biopsy cytopathology: a single institutional retrospective study of the application of the system categories and the impact of rapid onsite evaluation. *Acta Cytol* 2019; 63: 280-91.
 43. McHugh KE, Bird P, Sturgis CD. Concordance of breast fine needle aspiration cytology interpretation with subsequent surgical pathology: an 18-year review from a single sub-Saharan African institution. *Cytopathology* 2019; 30: 519-25.
 44. Montezuma D, Malheiros D, Schmitt FC. Breast fine needle aspiration biopsy cytology using the newly proposed IAC Yokohama System for reporting breast cytopathology: the experience of a single institution. *Acta Cytol* 2019; 63: 274-9.
 45. Nikas IP, Vey JA, Proctor T, et al. The use of the International Academy of Cytology Yokohama System for reporting breast fine-needle aspiration biopsy. *Am J Clin Pathol* 2023; 159: 138-45.
 46. Layfield LJ, Wang G, Yang ZJ, Gomez-Fernandez C, Esebua M, Schmidt RL. Interobserver agreement for the International Academy of Cytology Yokohama System for reporting breast fine-needle aspiration biopsy cytopathology. *Acta Cytol* 2020; 64: 413-9.
 47. Polarin O, Kim D, Gokozan HN, et al. Interobserver agreement and risk of malignancy using the International Academy of Cytology Yokohama System for reporting breast FNA biopsy in a liquid-based exclusive cohort. *Cancer Cytopathol* 2024; 132: 320-6.
 48. Hoda RS, Brachtel EF. International Academy of Cytology Yokohama System for reporting breast fine-needle aspiration biopsy cytopathology: a review of predictive values and risks of malignancy. *Acta Cytol* 2019; 63: 292-301.
 49. VandenBussche CJ, Baloch ZW. The cytologic diagnosis of "atypical": criteria and controversies. *Diagn Cytopathol* 2022; 50: 143-5.
 50. Tejeswini V, Chaitra B, Renuka IV, Laxmi K, Ramya P, Sowjanya KKS. Effectuation of International Academy of Cytology Yokohama reporting system of breast cytology to assess malignancy risk and accuracy. *J Cytol* 2021; 38: 69-73.
 51. Sarangi S, Rao M, Elhence PA, et al. Risk stratification of breast fine-needle aspiration biopsy specimens performed without radiologic guidance by application of the International Academy of Cytology Yokohama System for reporting breast fine-needle aspiration cytopathology. *Acta Cytol* 2021; 65: 483-93.
 52. Gomes Pinto D, Schmitt FC. Overcoming pitfalls in breast fine-needle aspiration cytology: a practical review. *Acta Cytol* 2024; 68: 206-18.
 53. Cai G, Adeniran AJ. Overview. In: Cai G, Adeniran AJ, eds. *Rapid on-site evaluation (ROSE)*. Berlin: Springer, 2019; 3-11.
 54. Hernandez A, Brandler TC, Cangiarella JF. Breast. In: Cai G, Adeniran AJ, eds. *Rapid on-site evaluation (ROSE)*. Berlin: Springer, 2019; 61-92.
 55. Schoellnast H, Komatz G, Bisail H, et al. CT-guided biopsy of lesions of the lung, liver, pancreas or of enlarged lymph nodes: value of additional fine needle aspiration (FNA) to core needle biopsy (CNB) in an offsite pathologist setting. *Acad Radiol* 2010; 17: 1275-81.
 56. Silverman JF, Finley JL, O'Brien KE, et al. Diagnostic accuracy and role of immediate interpretation of fine needle aspiration biopsy specimens from various sites. *Acta Cytol* 1989; 33: 791-6.
 57. Nasuti JF, Gupta PK, Baloch ZW. Diagnostic value and cost-effectiveness of on-site evaluation of fine-needle aspiration specimens: review of 5,688 cases. *Diagn Cytopathol* 2002; 27: 1-4.
 58. Suci V, El Chamieh C, Soufan R, et al. Real-world diagnostic accuracy of the On-Site Cytopathology Advance Report (OSCAR) procedure performed in a multidisciplinary one-stop breast clinic. *Cancers (Basel)* 2023; 15: 4967.
 59. Bharti JN, Nigam JS, Rath A, Pradeep I. Insufficient/inadequate category in breast cytology: are the standardized guidelines of rapid on-site evaluation available to reduce its rate? *Diagn Cytopathol* 2023; 51: 321-4.
 60. Poole GH, Willsher PC, Pinder SE, Robertson JF, Elston CW, Blamey RW. Diagnosis of breast cancer with core-biopsy and fine needle aspiration cytology. *Aust N Z J Surg* 1996; 66: 592-4.
 61. Salami N, Hirschowitz SL, Nieberg RK, Apple SK. Triple test approach to inadequate fine needle aspiration biopsies of palpable breast lesions. *Acta Cytol* 1999; 43: 339-43.
 62. Ibrahim AE, Bateman AC, Theaker JM, et al. The role and histological classification of needle core biopsy in comparison with

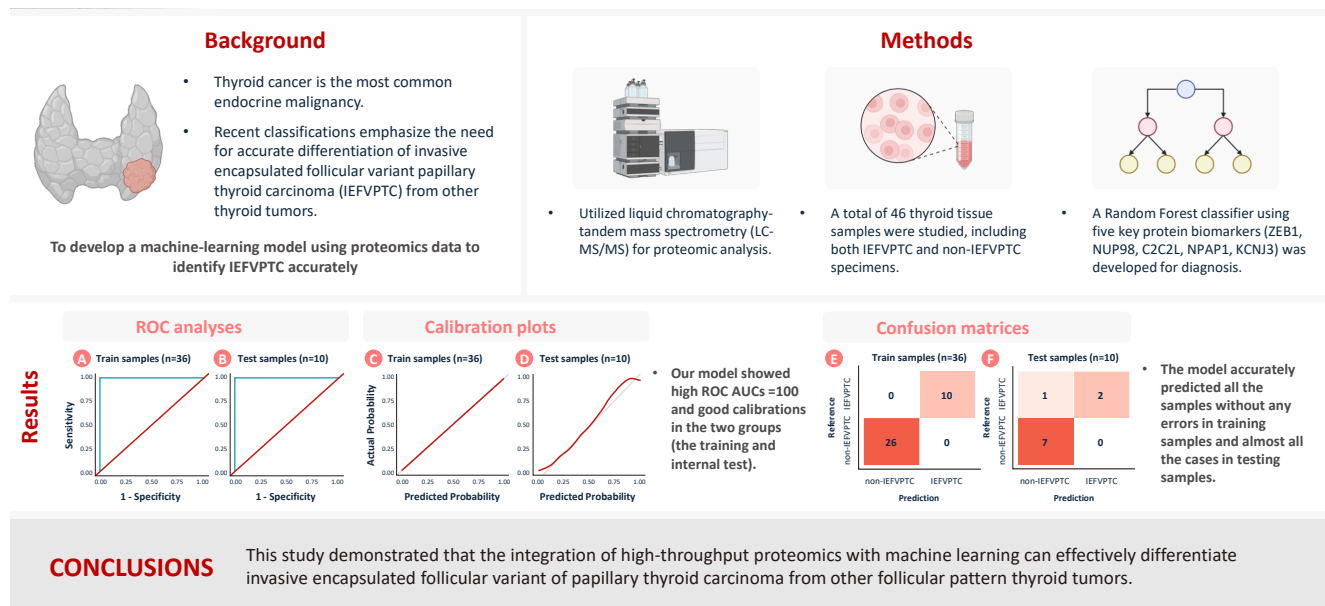
- fine needle aspiration cytology in the preoperative assessment of impalpable breast lesions. *J Clin Pathol* 2001; 54: 121-5.
63. Joudeh AA, Shareef SQ, Al-Abadi MA. Fine-needle aspiration followed by core-needle biopsy in the same setting: modifying our approach. *Acta Cytol* 2016; 60: 1-13.
 64. Sustova P, Klijanienko J. Value of combined use of fine-needle aspiration and core needle biopsy in palpable breast tumors performed by pathologist: Institut Curie experience. *Diagn Cytopathol* 2020; 48: 71-7.
 65. Li Z, Souers RJ, Tabbara SO, Natale KE, Nguyen LN, Booth CN. Breast fine-needle aspiration practice in 2019: results of a College of American Pathologists national survey. *Arch Pathol Lab Med* 2021; 145: 825-33.
 66. Gerhard R, Schmitt FC. Liquid-based cytology in fine-needle aspiration of breast lesions: a review. *Acta Cytol* 2014; 58: 533-42.
 67. Ryu HS, Park IA, Park SY, Jung YY, Park SH, Shin HC. A pilot study evaluating liquid-based fine needle aspiration cytology of breast lesions: a cytomorphological comparison of SurePath(R) liquid-based preparations and conventional smears. *Acta Cytol* 2013; 57: 391-9.
 68. Silva E, Meschter S, Tan MP. Breast biopsy techniques in a global setting-clinical practice review. *Transl Breast Cancer Res* 2023; 4: 14.
 69. Chauhan D, Sahu N, Sahoo SR, Senapati U. Accuracy of cytological grading in the carcinoma breast and its correlation with pathological prognostic parameters. *J Cancer Res Ther* 2023; 19: 1956-61.
 70. Bozzetti C, Nizzoli R, Guazzi A, et al. HER-2/neu amplification detected by fluorescence in situ hybridization in fine needle aspirates from primary breast cancer. *Ann Oncol* 2002; 13: 1398-403.
 71. Konofaos P, Kontzoglou K, Georgoulakis J, et al. The role of ThinPrep cytology in the evaluation of estrogen and progesterone receptor content of breast tumors. *Surg Oncol* 2006; 15: 257-66.
 72. Durgapal P, Mathur SR, Kalamuddin M, et al. Assessment of Her-2/neu status using immunocytochemistry and fluorescence in situ hybridization on fine-needle aspiration cytology smears: experience from a tertiary care centre in India. *Diagn Cytopathol* 2014; 42: 726-31.
 73. Vohra P, Buelow B, Chen YY, et al. Estrogen receptor, progesterone receptor, and human epidermal growth factor receptor 2 expression in breast cancer FNA cell blocks and paired histologic specimens: a large retrospective study. *Cancer Cytopathol* 2016; 124: 828-35.
 74. Torous VF, Cuda JM, Manucha V, et al. Cell blocks in cytology: review of preparation methods, advantages, and limitations. *J Am Soc Cytopathol* 2023; 12: 77-88.
 75. Jamidi SK, Li JJX, Aphivatanasiri C, et al. Papillary lesions of the breast: a systematic evaluation of cytologic parameters. *Cancer Cytopathol* 2021; 129: 649-61.
 76. van Essen HF, Verdaasdonk MA, Elshof SM, de Weger RA, van Diest PJ. Alcohol based tissue fixation as an alternative for formaldehyde: influence on immunohistochemistry. *J Clin Pathol* 2010; 63: 1090-4.
 77. Pinto D, Schmitt FC. Immunohistochemistry applied to breast cytological material. *Pathobiology* 2022; 89: 343-58.
 78. Dong J, Ly A, Arpin R, Ahmed Q, Brachtel E. Breast fine needle aspiration continues to be relevant in a large academic medical center: experience from Massachusetts General Hospital. *Breast Cancer Res Treat* 2016; 158: 297-305.
 79. Kumar SK, Gupta N, Rajwanshi A, Joshi K, Singh G. Immunohistochemistry for oestrogen receptor, progesterone receptor and HER2 on cell blocks in primary breast carcinoma. *Cytopathology* 2012; 23: 181-6.
 80. Puccetti M, Ravaioli S, Tumedei MM, et al. Are fine-needle aspiration biopsy-derived cell blocks a useful surrogate for tissue samples in breast cancer? *Histopathology* 2018; 73: 801-8.
 81. Briffod M, Hacene K, Le Doussal V. Immunohistochemistry on cell blocks from fine-needle cytopunctures of primary breast carcinomas and lymph node metastases. *Mod Pathol* 2000; 13: 841-50.
 82. Singh S, Shukla S, Singh A, Acharya S, Kadu RP, Bhake A. Comparison of estrogen and progesterone receptor status in tumor mass and axillary lymph node metastasis in patients with carcinoma breast. *Int J Appl Basic Med Res* 2020; 10: 117-21.
 83. Baros IV, Tanaskovic N, Pellas U, Eri Z, Tadic Latinovic L, Tot T. Internodal HER2 heterogeneity of axillary lymph node metastases in breast cancer patients. *Bosn J Basic Med Sci* 2019; 19: 242-8.
 84. Pareja F, Murray MP, Jean RD, et al. Cytologic assessment of estrogen receptor, progesterone receptor, and HER2 status in metastatic breast carcinoma. *J Am Soc Cytopathol* 2017; 6: 33-40.
 85. Kuukasjarvi T, Kononen J, Helin H, Holli K, Isola J. Loss of estrogen receptor in recurrent breast cancer is associated with poor response to endocrine therapy. *J Clin Oncol* 1996; 14: 2584-9.
 86. Kane G, Fleming C, Heneghan H, et al. False-negative rate of ultrasound-guided fine-needle aspiration cytology for identifying axillary lymph node metastasis in breast cancer patients. *Breast J* 2019; 25: 848-52.
 87. Desai N, Connelly CF, Sung S, Cimic A, Baskota SU. Interobserver variability in HER-2 immunostaining interpretation of met-

- astatic HER2 low breast cancers in cytology specimens. *Diagn Cytopathol* 2024; 52: 722-30.
88. Pisapia P, Pepe F, Sgariglia R, et al. Next generation sequencing in cytology. *Cytopathology* 2021; 32: 588-95.
 89. Rekhtman N, Roy-Chowdhuri S. Cytology specimens: a goldmine for molecular testing. *Arch Pathol Lab Med* 2016; 140: 1189-90.
 90. Vishnubhotla PS. Molecular testing of cytology specimens: are we ready for the new era? *Cancer Cytopathol* 2016; 124: 9-10.
 91. Symmans WF, Ayers M, Clark EA, et al. Total RNA yield and microarray gene expression profiles from fine-needle aspiration biopsy and core-needle biopsy samples of breast carcinoma. *Cancer* 2003; 97: 2960-71.
 92. Roy-Chowdhuri S, Chen H, Singh RR, et al. Concurrent fine needle aspirations and core needle biopsies: a comparative study of substrates for next-generation sequencing in solid organ malignancies. *Mod Pathol* 2017; 30: 499-508.
 93. Park HE, Han D, Lee JS, et al. Comparison of breast fine-needle aspiration cytology and tissue sampling for high-throughput proteomic analysis and cancer biomarker detection. *Pathobiology* 2024; 91: 359-69.
 94. Hoshino A, Oana Y, Ohi Y, et al. Using the DNA integrity number to analyze DNA quality in specimens collected from liquid-based cytology after fine-needle aspiration of breast tumors and lesions. *Acta Cytol* 2024; 68: 145-52.
 95. Akahane T, Isochi-Yamaguchi T, Hashiba-Ohnuki N, et al. Cancer gene analysis of liquid-based cytology specimens using next-generation sequencing: a technical report of bimodal DNA- and RNA-based panel application. *Diagn Cytopathol* 2023; 51: 493-500.
 96. Aydin Mericoz C, Eren OC, Kulac I, Firat P. Fusion of old and new: employing touch imprint slides for next generation sequencing in solid tumors. *Diagn Cytopathol* 2024; 52: 264-70.
 97. Martelotto LG, De Filippo MR, Ng CK, et al. Genomic landscape of adenoid cystic carcinoma of the breast. *J Pathol* 2015; 237: 179-89.
 98. D'Alfonso TM, Mosquera JM, MacDonald TY, et al. *MYB-NFIB* gene fusion in adenoid cystic carcinoma of the breast with special focus paid to the solid variant with basaloid features. *Hum Pathol* 2014; 45: 2270-80.
 99. Farahani N, Parwani AV, Pantanowitz L. Whole slide imaging in pathology: advantages, limitations, and emerging perspectives. *Pathol Lab Med Int* 2015; 7: 23-33.
 100. Ren F, Li H, Yang W, et al. Viability of whole-slide imaging for intraoperative touch imprint cytological diagnosis of axillary sentinel lymph nodes in breast cancer patients. *Diagn Cytopathol* 2024; 53: 18-26.
 101. Liu Y, Kohlberger T, Norouzi M, et al. Artificial intelligence-based breast cancer nodal metastasis detection: insights into the black box for pathologists. *Arch Pathol Lab Med* 2019; 143: 859-68.
 102. Sandbank J, Bataillon G, Nudelman A, et al. Validation and real-world clinical application of an artificial intelligence algorithm for breast cancer detection in biopsies. *NPJ Breast Cancer* 2022; 8: 129.
 103. Binder A, Bockmayr M, Hagele M, et al. Morphological and molecular breast cancer profiling through explainable machine learning. *Nat Mach Intell* 2021; 3: 355-66.

Diagnosis of invasive encapsulated follicular variant papillary thyroid carcinoma by protein-based machine learning

Truong Phan-Xuan Nguyen¹, Minh-Khang Le², Sittiruk Roytrakul³, Shanop Shuangshoti^{1,4}, Nakarin Kitkumthorn⁵, Somboon Keelawat^{1,6}

Graphical abstract



Diagnosis of invasive encapsulated follicular variant papillary thyroid carcinoma by protein-based machine learning

Truong Phan-Xuan Nguyen¹, Minh-Khang Le², Sittiruk Roytrakul³, Shanop Shuangshoti^{1,4}, Nakarin Kitkumthorn⁵, Somboon Keelawat^{1,6}

¹Department of Pathology, Faculty of Medicine, Chulalongkorn University, Bangkok, Thailand

²Department of Pathology, University of Yamanashi, Chuo City, Japan

³Functional Proteomics Technology Laboratory, National Center for Genetic Engineering and Biotechnology, National Science and Technology Development Agency, Pathumthani, Thailand

⁴Chulalongkorn GenePRO Center, Faculty of Medicine, Chulalongkorn University, Bangkok, Thailand

⁵Department of Oral Biology, Faculty of Dentistry, Mahidol University, Bangkok, Thailand

⁶Precision Pathology of Neoplasia Research Group, Department of Pathology, Faculty of Medicine, Chulalongkorn University, Bangkok, Thailand

Background: Although the criteria for follicular-pattern thyroid tumors are well-established, diagnosing these lesions remains challenging in some cases. In the recent World Health Organization Classification of Endocrine and Neuroendocrine Tumors (5th edition), the invasive encapsulated follicular variant of papillary thyroid carcinoma was reclassified as its own entity. It is crucial to differentiate this variant of papillary thyroid carcinoma from low-risk follicular pattern tumors due to their shared morphological characteristics. Proteomics holds significant promise for detecting and quantifying protein biomarkers. We investigated the potential value of a protein biomarker panel defined by machine learning for identifying the invasive encapsulated follicular variant of papillary thyroid carcinoma, initially using formalin-fixed paraffin-embedded samples. **Methods:** We developed a supervised machine-learning model and tested its performance using proteomics data from 46 thyroid tissue samples. **Results:** We applied a random forest classifier utilizing five protein biomarkers (ZEB1, NUP98, C2C2L, NPAP1, and KCNJ3). This classifier achieved areas under the curve (AUCs) of 1.00 and accuracy rates of 1.00 in training samples for distinguishing the invasive encapsulated follicular variant of papillary thyroid carcinoma from non-malignant samples. Additionally, we analyzed the performance of single-protein/gene receiver operating characteristic in differentiating the invasive encapsulated follicular variant of papillary thyroid carcinoma from others within The Cancer Genome Atlas projects, which yielded an AUC >0.5. **Conclusions:** We demonstrated that integration of high-throughput proteomics with machine learning can effectively differentiate the invasive encapsulated follicular variant of papillary thyroid carcinoma from other follicular pattern thyroid tumors.

Keywords: Follicular pattern thyroid tumors; Thyroid carcinoma; Machine learning, proteomics; Histological diagnosis

Received: July 23, 2024 **Revised:** September 11, 2024 **Accepted:** September 14, 2024

Corresponding Author: Nakarin Kitkumthorn, DDS, PhD

Department of Oral Biology, Faculty of Dentistry, Mahidol University, No. 6, Yothi Road, Ratchathewit, Bangkok 10400, Thailand

Tel: +66-868815947, Fax: +66-22564208, E-mail: nakarinkit@gmail.com

Corresponding Author: Somboon Keelawat, MD

Department of Pathology, Faculty of Medicine, Chulalongkorn University and Precision Pathology of Neoplasia Research Group, Department of Pathology, Faculty of Medicine, Chulalongkorn University, 1873 Rama IV Road, Pathum Wan, Bangkok 10330, Thailand

Tel: +66-891151963, Fax: +66-22564208, E-mail: trcsl@gmail.com, Somboon.Ke@chula.ac.th

This is an Open Access article distributed under the terms of the Creative Commons Attribution Non-Commercial License (<https://creativecommons.org/licenses/by-nc/4.0/>) which permits unrestricted non-commercial use, distribution, and reproduction in any medium, provided the original work is properly cited.

© 2025 The Korean Society of Pathologists/The Korean Society for Cytopathology

INTRODUCTION

Thyroid cancer is the most prevalent endocrine malignancy, with detection rates increasing significantly in recent years [1]. This increase is largely attributed to enhanced detection of papillary thyroid carcinoma (PTC), while other types, such as follicular, medullary, and anaplastic thyroid carcinomas, have maintained stable incidence rates [2,3].

The recent 5th edition of the World Health Organization (WHO) Classification of Endocrine and Neuroendocrine Tumors has refined the classification of thyroid tumors by integrating more detailed pathological, molecular, and behavioral characteristics [4]. This has led to the reclassification of invasive encapsulated follicular variant of papillary thyroid carcinoma (IEFVPTC) as its own entity rather than a subtype of PTC. IEFVPTC has a RAS-like mutational profile similar to those of follicular adenoma (FA), follicular thyroid carcinoma (FTC), and other classifications such as non-invasive follicular thyroid neoplasm with papillary-like nuclear features (NIFTP) and well-differentiated tumor of uncertain malignant potential (WDT-UMP). Despite their genetic resemblance, IEFVPTC differs from FA/FTC in terms of nuclear features (score 0–1). It shares morphological traits with NIFTP and WDT-UMP, such as the presence of a fibrous capsule and nuclear characteristics similar to PTC (score 2–3) [4–6]. Crucially, IEFVPTC can demonstrate capsular/vascular invasion and metastasis, necessitating aggressive treatment including complete thyroidectomy and adjuvant therapy. In contrast, NIFTP and WDT-UMP are considered low-risk neoplasms, typically managed with lobectomy and close monitoring [6,7].

Proteins play crucial roles in all biological processes and shape the phenotypes of cells and organisms. They are pivotal as diagnostic biomarkers and targets for therapy. Proteomics presents a viable analytic technique, especially through improvements in mass spectrometry (MS), increasing detection and quantification of a wide range of proteins and facilitating differentiation of various thyroid tumors through their proteomic signatures [8,9]. Although research has been conducted to differentiate FA and FTC [10–12], no study has focused on molecular markers that specifically distinguish IEFVPTC from lower-risk tumors (NIFTP, WDT-UMP). Our goal was to explore the applications and potential of machine learning, combined with protein profiling, in diagnosing and classifying IEFVPTC from follicular thyroid nodules. In this study, we improved the accuracy of techniques for distinguishing malignant

follicular thyroid tumors and identified potential immunohistochemistry markers for diagnosing IEFVPTC.

MATERIALS AND METHODS

Study subjects

Thyroid tumor tissue and nontumor tissue samples were obtained from the Department of Pathology, Chulalongkorn University. The present study was performed using the same cohort and tissue samples (13 IEFVPTC, 11 NIFTP, 12 WDT-UMP, 12 normal thyroid specimens) as in our recent study investigating proteomics profiles [13].

Protein preparation and shotgun liquid chromatography tandem mass spectrometry analysis

Tissue samples were prepared for proteomic analysis as previously described [13]. Two pathologists (T.PX.N. and S.K.) independently evaluated samples and reached consensus based on the 5th edition of the WHO Classification of Tumors of Endocrine Organs [4].

Protein was extracted from formalin-fixed paraffin-embedded (FFPE) specimens using 0.5% sodium dodecyl sulfate, incubated at 50°C for 60 minutes, and then centrifuged at 10,000 rpm for 30 minutes. Protein concentration was determined using the bicinchoninic acid method. Five micrograms of each protein sample were reduced with 5 mM dithiothreitol in 10 mM AMBIC at 60°C for 1 hour, alkylated with 15 mM iodoacetamide in 10 mM AMBIC at room temperature for 45 minutes in the dark, and then digested with sequencing-grade porcine trypsin (1:20 ratio) for 16 hours at 37°C. The proteins were dried in a speed vacuum concentrator and reconstituted in 0.1% formic acid for nano-liquid chromatography tandem mass spectrometry (nanoLC-MS/MS) analysis.

LC-MS/MS data were collected using an Ultimate3000 Nano/Capillary LC System (Thermo Scientific, Loughborough, UK) connected to a Hybrid quadrupole Q-ToF impact II (Bruker Daltonics, Billerica, MA, USA) with a Nano-captive spray ion source. One microliter of the peptide digest was enriched on a μ -Precolumn 300 μ m i.d. \times 5 mm C18 Pepmap 100, 5 μ m, 100 \AA (Thermo Scientific) and separated on a 75 μ m I.D. \times 15 cm Acclaim PepMap RSLC C18, 2 μ m, 100 \AA , nanoViper (Thermo Scientific) column heated to 60°C. Solvents A and B, containing 0.1% formic acid in water and 0.1% formic acid in 80% acetonitrile, respectively, were used to elute proteins at a 5%–55% gradient of solvent B over 30 minutes at a flow rate of 0.30 μ L/

min. Electrospray ionization was performed at 1.6 kV. Nitrogen was used as the drying gas at a flow rate of approximately 50 L/hr and to obtain collision-induced dissociation spectra. MS and MS/MS spectra were recorded in positive-ion mode at 2 Hz across the m/z range of 150–2,200, with the collision energy set to 10 eV based on the m/z value. Protein quantification for each sample was conducted using MaxQuant ver. 2.2.0.0, which uses the Andromeda search engine to match MS/MS spectra with the Uniprot *Homo sapiens* database.

LC-MS/MS analysis

An overview of our study design is depicted in Fig. 1. After preprocessing and filtering to include only proteins present in more than 40% of samples within each group, we identified a total of 1,398 proteins from the 46 proteomic data files.

We aimed to devise a machine-learning model that could differentiate between IEFVPTC and non-IEFVPTC specimens. The non-IEFVPTC samples included NIFTP, WDT-UMP, and normal thyroid tissue.

The entire set of samples (n = 46) was partitioned into training (n = 36) and internal testing (n = 10) subsets. The training

samples underwent peptide/protein screening, model selection, and model development. Conversely, the testing samples were used for model evaluation and sensitivity analysis. The patient characteristics of the corresponding training and internal testing samples are compared in Table 1.

Protein screening

Our screening process was composed of three steps: differentially expressed proteins (DEPs) of IEFVPTC (Supplementary Table S1), unsupervised screening, and supervised screening (Fig. 1). First, we selected 181 significant proteins based on the DESeq2 results between IEFVPTC and non-IEFVPTC. The second step of unsupervised protein screening involved computation of the variance to gauge differences in expression across samples. Only proteins with a variance greater than the 90th percentile were selected, effectively excluding those with no expression or constant expression across samples.

In the supervised screening phase, we restricted our analysis to proteins selected during unsupervised screening. For each protein, we built a logistic regression model and calculated the model univariate deviance (MUD). We then generated a

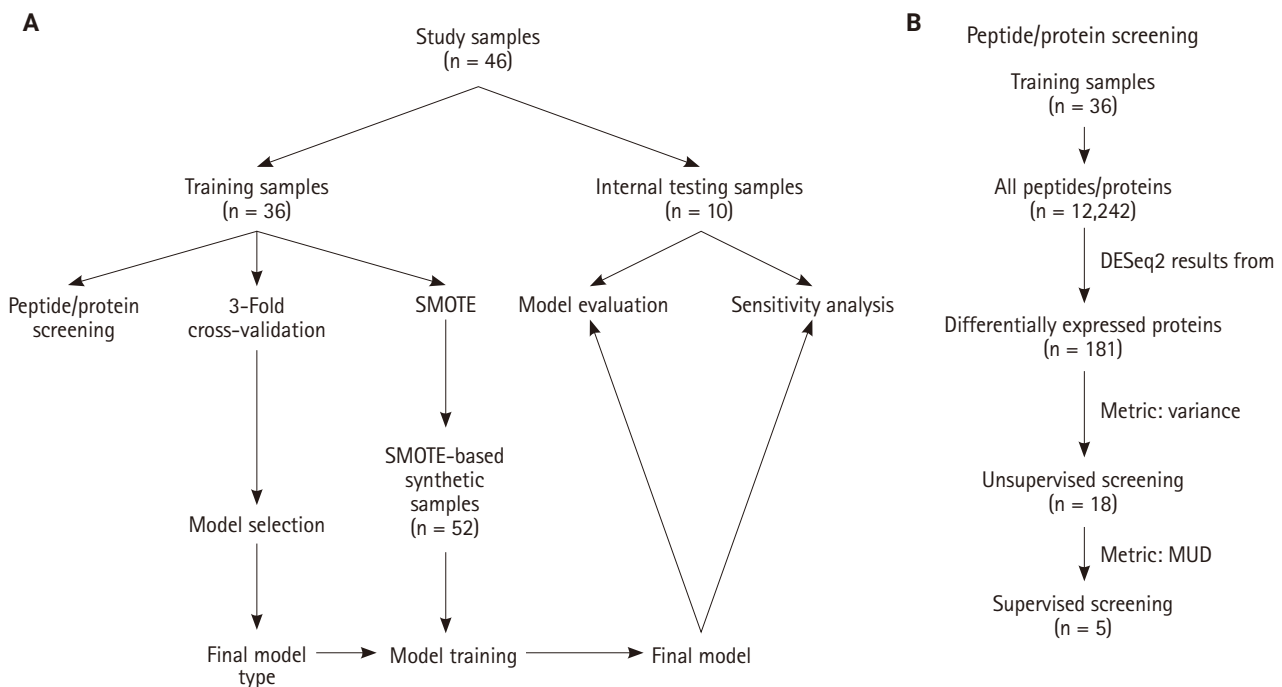


Fig. 1. (A) The study design, featuring the training and internal testing phases of our model. (B) The screening process used to pinpoint proteins that most effectively distinguish between IEFVPTC and non-IEFVPTC. IEFVPTC, invasive encapsulated follicular variant of papillary thyroid carcinoma; SMOTE, Synthetic Minority Oversampling Techniques; MUD, model univariate deviance.

Table 1. Characteristics of corresponding patients with the training and test samples

Variable	Train (n = 36)	Test (n = 10)	p-value
Age (yr)	42 (24–79)	52.5 (34–70)	.170
Sex			.987
Women	24 (66.7)	6 (60.0)	
Men	12 (33.3)	4 (40.0)	
Nuclear score			.421
2	6 (16.7)	2 (20.0)	
3	19 (52.8)	7 (70.0)	
No score	11 (30.6)	1 (10.0)	
Diameter (mm)	35 (15–84)	30 (22–70)	.922
Invasion			.498
No	9 (25.0)	2 (20.0)	
Capsular	6 (16.7)	2 (20.0)	
Vascular	4 (11.1)	1 (10.0)	
Unclear	6 (16.7)	4 (40.0)	
Normal tissue	11 (30.6)	1 (10.0)	
Diagnosis			.344
Normal tissue	11 (30.6)	1 (10.0)	
WDT-UMP	6 (16.7)	4 (40.0)	
NIFTP	9 (25.0)	2 (20.0)	
IEFVPTC	10 (27.8)	3 (30.0)	

Values are presented as median (range) or number (%). WDT-UMP, well-differentiated tumor of uncertain malignant potential; NIFTP, neoplasm with papillary-like nuclear features; IEFVPTC, invasive encapsulated follicular variant of papillary thyroid carcinoma.

deviance plot to determine the cut-off point for the number of peptides/proteins to be included.

Model selection and development

In this process, our aim was to pinpoint the supervised machine-learning model that exhibited the best performance. We carried out a three-fold cross-validation on the training samples. The models under consideration for selection encompassed logistic regression, generalized linear model with elastic net regularization, Naïve Bayes, support vector machine, decision tree, random forest, XGBoost, and multi-layer perceptron (MLP). The model that produced the highest accuracy score was ultimately selected. The 10 internal testing samples that we previously set aside were not involved in this process, and the cross-validation was performed by generating three training groups, each comprising 12 samples. A one-left-out testing approach was implemented to assess the accuracy of these models.

Prior to training the chosen model, we generated synthetic samples from the training set using the Synthetic Minority

Oversampling Techniques (SMOTE) method [14]. The total number of synthetic samples was n = 52, which encompassed 26 samples from each of the non-IEFVPTC and IEFVPTC categories. The selected model was subsequently trained on these SMOTE-created samples.

Model evaluation and sensitivity analysis

We conducted three analyses to evaluate the model. We first conducted a receiver operating characteristic (ROC) analysis and model calibration to evaluate model accuracy and stability under the probability score. Subsequently, we constructed a confusion matrix to assess the model's performance in the classification task. Since the model was constructed using a small dataset, sensitivity analyses were also performed. Typically, sensitivity analyses involve various methods to perturb the features of the test data and examine whether the performance can endure such data anomalies without a significant decrease. In this study, we induced data distortion by applying random masking and creating random missing values. We then employed the Multivariate Imputation by Chained Equations (MICE) algorithm [15] to impute the missing data, resulting in a new and distorted version of the original test samples. The intensity of data distortion escalates when we apply larger random masking as more information is lost. Taking this into account, we generated three masks with 30%, 40%, and 50% missing values.

External testing of The Cancer Genome Atlas dataset

We extracted PTC cases from The Cancer Genome Atlas Thyroid Cancer (TCGA-THCA) dataset, which included a total of 507 cases. Our focus was on cases diagnosed as PTC, follicular variant (ICD-0 3 8340/3, n = 107). In light of the recent reclassification of thyroid neoplasms, we aimed to revisit the histopathology of these cases. For this purpose, we selected cases that had available diagnostic whole slide images and gene expression data. These cases were subsequently re-evaluated by a pathologist (T.PX.N. and S.K) and reclassified, with a particular emphasis on IEFVPTC and non-IEFVPTC. The revised diagnoses comprised FTC (n = 5), non-invasive follicular neoplasm (n = 11), non-invasive follicular variant of papillary thyroid carcinoma (FVPTC) (n = 7), and invasive FVPTC (n = 24). Additionally, we identified other diagnoses (n = 60) that were considered irrelevant, including hyperplastic nodules, poorly differentiated thyroid carcinomas, Hürthle cell neoplasms, conventional PTC, adenomatous goiters, and cases with indeterminate morphology. Last, we reassigned cases with relevant diagnoses (n = 47) as

non-invasive FVPTC (n = 24) or non-IEFVPTC (n = 23) (Supplementary Table S2) as the external test set.

Given that the gene expression in the TCGA projects is based on sequencing technology for RNA quantification, it is not an appropriate input for our model, which was trained on LC-MS/MS protein expression data. Instead, we conducted a ROC analysis of protein expression in both the training and internal test sets. Additionally, we performed a ROC analysis of gene expression in the external test set. This approach allowed us to effectively utilize the available data and ensure the compatibility of genes or proteins in our model.

Statistical analyses

The descriptive statistics for continuous variables are represented by the median and range, while the number of samples and their respective percentages were used for categorical variables. To compare continuous and categorical variables between cohorts, Wilcoxon's and chi-square tests were employed, respectively. p-values less than .05 were considered significant in hypothesis testing. All analyses were conducted using ver. 4.3.2 of R software (R Foundation for Statistical Computing, Vienna, Austria).

RESULTS

Patient characteristics

Table 1 provides a summary of the study cohort characteristics, which are divided into training and internal testing cohorts. The average age of the patients was 43 years, ranging from 24 to 70, with a predominance of women (30 of 46, 65.2%). The most common samples were IEFVPTC (13 of 46, 28.3%), followed by normal tissue (12 of 46, 26.1%), NIFTP (11 of 46, 23.9%), and WDT-UMP samples (10 of 46, 21.7%). There were no significant differences in terms of age (p = .170), sex (p = .987), nuclear score (p = .421), diameter (p = .922), invasion (p = .498), and diagnosis (p = .344).

Protein screening

We conducted a three-layer screening process comprising differentially expressed proteins–unsupervised–supervised screening and listed the five resulting proteins with their metrics in Table 2. The optimal proteins were ZEB1, NUP98, C2C2L, NPAP1, and KCNJ3. The rationale for setting the cut-off at five proteins was the significant increase in MUD between the proteins with the 5th and 6th smallest values (Fig. 2A). This

heuristic is grounded in the balance between introducing an excessive number of predictive variables that overshadow the number of training samples and the potential reduction in machine learning accuracy. Another key consideration is that incorporating a greater number of predictive variables relative to the size of the training sample may result in overfitting. Finally, the expressions of these selected five proteins across the training samples were visualized as a heatmap (Fig. 2B).

Model selection

We summarized the results of cross-validation in Table 3. In this table, three one-left-out accuracy scores of each model were reported as fold 1, fold 2, and fold 3. The means and standard deviations of the accuracy scores of logistic regression, Generalized Linear Model with Elastic Net Regularization, Naïve Bayes, Support Vector Machine, Decision Tree, Random Forest, XGBoost, and MLP were 0.89 (±0.10), 0.92 (±0.09), 0.97 (±0.05), 0.97 (±0.05), 0.91 (±0.09), 1.00 (±0.00), 0.92 (±0.09), and 0.97 (±0.05), respectively. The random forest classifier model had the highest accuracy score and was selected to construct the final model.

Model evaluation and sensitivity analysis

Fig. 3 illustrates the outcomes of the model evaluation using both training and internal testing samples. The ROC analyses (Fig. 3A, B) and model calibration plots (Fig. 3C, D) exhibit the ROC curves and calibration for both the training and internal testing samples. Our model showed high ROC areas under the curve (AUCs) = 1.00 and good calibrations in the two groups. In the confusion matrices (Fig. 3E, F), the model accurately predicted all training samples without any errors and almost all testing samples. In the sensitivity analysis (Fig. 4), distortions of 30%, 40%, and 50% marginally reduced the model performance, with AUCs of 0.95, 1.00, and 0.88 and accuracies of 0.90, 0.90, and 0.80, respectively. Despite these distortions, the cali-

Table 2. Selected proteins after unsupervised and supervised screening

Protein	Variance	MUD
ZEB1	76.4	5.7×10^{-10}
NUP98	73.3	5.7×10^{-10}
C2C2L	54.6	5.7×10^{-10}
NPAP1	51.7	5.7×10^{-10}
KCNJ3	51.7	5.7×10^{-10}

MUD, model univariate deviance.

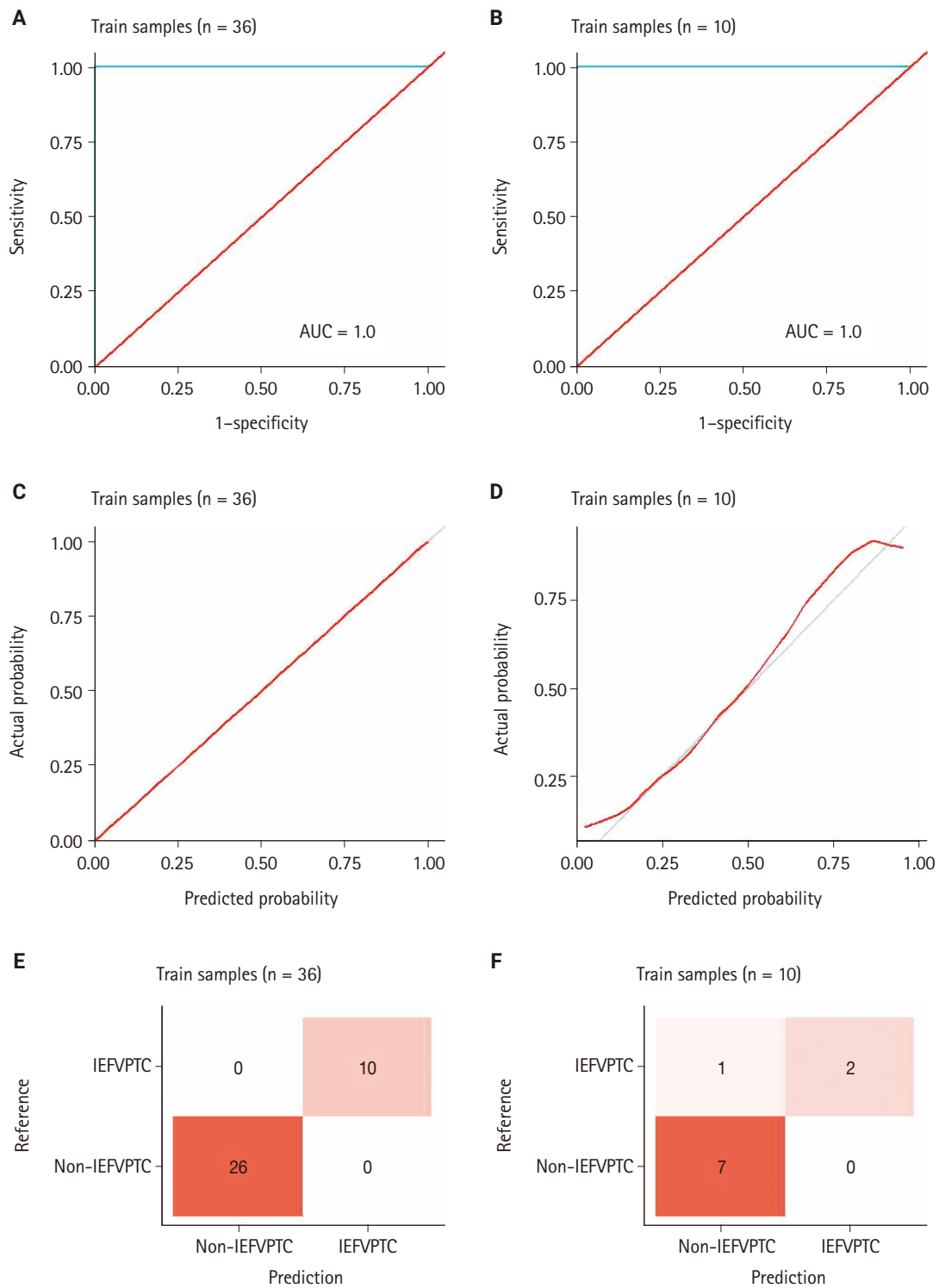


Fig. 3. Receiver operating characteristic analyses of our model for differentiating invasive encapsulated follicular variant of papillary thyroid carcinoma (IEFVPTC) from non-IEFVPTC in the training (A) and internal test (B) sets. This features the calibration plots of our model in both the training (C) and internal test (D) phases and the confusion matrices during the training (E) and internal testing (F) periods. AUC, area under the curve.

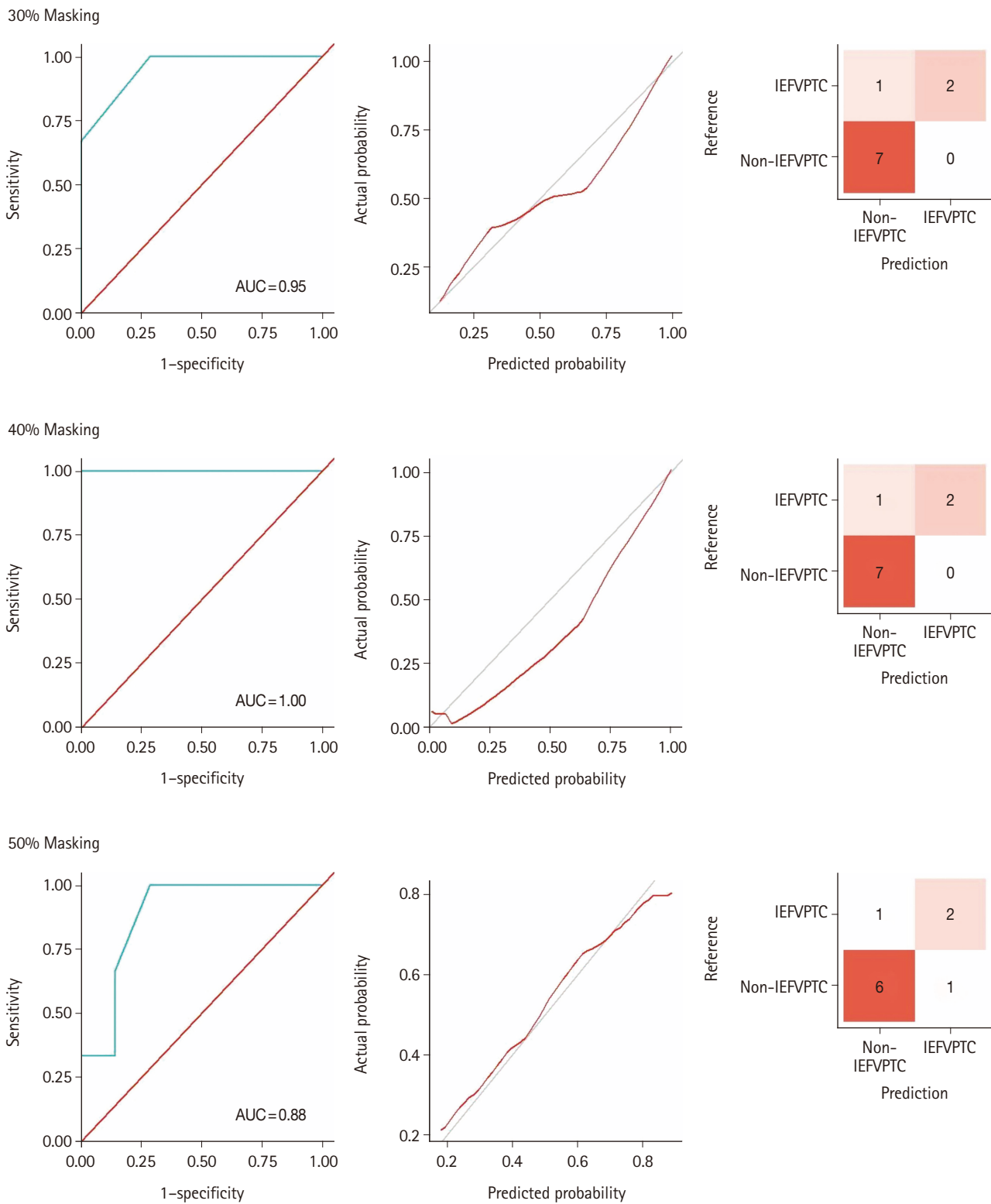


Fig. 4. Sensitivity analysis of our model when the input is disturbed by 30% (upper), 40% (middle), and 50% (lower). This indicates model robustness under different conditions. AUC, areas under the curve; IEFVPTC, invasive encapsulated follicular variant of papillary thyroid carcinoma.

Table 4. The area under the curve of receiver operating characteristics analysis in discriminating non-IEFVPTC and IEFVPTC of five proteins

Protein/Gene	Train	Internal test	External test
ZEB1	1.00	0.81	0.67
NUP98	0.98	0.83	0.67
C2C2L	0.99	1.00	0.57
NPAP1	1.00	0.83	0.60
KCNJ3	0.97	0.76	0.69

IEFVPTC, invasive encapsulated follicular variant of papillary thyroid carcinoma.

share similar nuclear features (2–3) but differ in capsular and vascular invasion characteristics. NIFTP lacks signs of capsular or vascular invasion, in contrast to IEFVPTC, which clearly exhibits such findings. WDT-UMP displays ambiguous patterns regarding capsular or vascular invasion [4].

According to the revised WHO classification, like FTC, IEFVPTC is recognized as malignant and is categorized into three subtypes: minimally invasive, encapsulated angioinvasive, and widely invasive. Minimally invasive tumors, considered low-risk, might only require local excision for treatment. In contrast, widely invasive or extensive vascular invasion (more than 4 foci) tumors often necessitate complete thyroidectomy and further therapy to prevent recurrence and/or distant metastasis. Such additional treatments are typically determined by individual clinical assessments, which might include factors like large tumor size (over 4 cm), extrathyroidal extension, or metastases [4,7]. On the other hand, NIFTP and WDT-UMP are classified as low-risk neoplasms. These tumors are considered borderline, displaying characteristics that fall between benign and malignant states. While the potential for metastasis exists in these neoplasms, such events are exceedingly rare. For patients with NIFTP and WDT-UMP, a lobectomy followed by vigilant monitoring is vital to prevent tumor progression [4]. Thus, precise diagnosis of IEFVPTC is crucial to avoid unnecessary or potentially detrimental surgical procedures.

The exploration of machine learning in medical fields is a burgeoning area of interest. Recent research has introduced new methods that enhance the diagnosis of follicular neoplasms. Sun et al. [10] utilized a machine learning model on data-independent acquisition MS, identifying a set of 31 proteins that effectively distinguish between FA and FTC. Their model achieved a high degree of precision, with an AUC of 0.963 and an accuracy rate of 91.7% in their test samples [10]. Addition-

ally, Li et al. [16] developed the Preoperative Risk Assessment Classifier for PTC, which incorporates clinical data, gene mutation details, immune indices, high-throughput proteomics, and machine learning technology to effectively stratify the preoperative risk of PTC, achieving an AUC of 0.925 and an accuracy of 0.844 [16]. This could reduce the incidence of unnecessary surgeries or excessive treatment.

In this study, we applied machine learning techniques, specifically using the random forest classifier, to analyze shotgun MS data to distinguish between IEFVPTC and non-IEFVPTC cases. Our analysis focused on identifying protein biomarkers within large proteomic datasets pertinent to thyroid cancers. We successfully identified the five proteins C2C2L, KCNJ3, NPAP1, NUP98, and ZEB1 that effectively differentiated malignant from benign conditions, achieving high AUCs and accuracy in training and test cohorts and demonstrating high sensitivity. Detecting the intensities of these five proteins with targeted MS-based proteomics assays combined with our model offers significant potential for clinical applications due to the high accuracy and rapid processing time [17].

Although there are no existing reports on the roles of these proteins in thyroid cancer, some have been implicated in carcinogenesis. KCNJ3 has been linked with increased disease progression in breast cancer [18]. NUP98 is an oncoprotein that contributes to malignant transformation and is associated with a broad range of hematopoietic malignancies [19]. ZEB1, a transcription factor, facilitates tumor invasion and metastasis by promoting epithelial-mesenchymal transition in carcinoma cells [20]. The roles of the remaining two proteins in cancer have not yet been explored and require further research. Further analysis of individual markers and validation on test data, alongside mRNA expression data from TCGA, revealed that these five proteins could potentially serve as immunohistochemistry markers to distinguish between IEFVPTC and non-IEFVPTC (Supplementary Fig. S1).

IEFVPTCs are RAS-driven lesions with a similar morphological pattern to FTCs, characterized by a follicular pattern and capsular or vascular invasion, but differing in nuclear features [5]. Like FTC, IEFVPTC also shows correlation between the extent of invasion and patient prognosis [21]. Huang et al. [11] indicated that FTC and FVPTC share proteotypes but are distinct from the benign tumor FA. In this study, we did not collect FTC and FA samples, so we could not perform further analysis to address this question. Instead, we analyzed the expressions of five proteins (ZEB1, NUP98, C2C2L, NPAP1, and KCNJ3)

using TCGA data (Supplementary Table S1). The expressions of these five proteins were similarly high in IEFVPTC and FTC (Supplementary Fig. S2).

Despite the valuable insights provided by our current research, it has certain limitations. First, we employed non-targeted proteomics to analyze peptide profiles in FFPE samples but did not perform validations on fine-needle aspiration (FNA) samples and other FFPE cohorts. Moreover, other follicular-patterned thyroid neoplasms such as FA and FTC were not included in this study and should be explored in future research. Although our sample size was small, this study represents a preliminary effort to identify potential protein markers for IEFVPTC. In the future, we plan to validate these five protein biomarkers (ZEB1, NUP98, C2C2L, NPAP1, and KCNJ3) using immunohistochemistry and to analyze the prognostic roles of these biomarker candidates to determine whether cancer is self-limiting and curable or lethal in a larger sample cohort including both FNA and FFPE samples.

In summary, our extensive proteomics analysis of thyroid tissue samples led to the identification of five proteins that can be utilized to diagnose IEFVPTC. Our findings contribute to the advancement of molecular diagnosis for follicular-patterned thyroid tumors and have the potential to enhance the diagnostic accuracy of existing molecular tests.

Supplementary Information

The Data Supplement is available with this article at <https://doi.org/10.4132/jptm.2024.09.14>.

Ethics Statement

The research was established according to the ethical guidelines of the Helsinki Declaration and was approved by the Institutional Review Board of Faculty of Medicine, Chulalongkorn University (COA.No. 1369/2023-IRB 0628/66). Written informed consent was obtained from all patients.

Availability of Data and Material

All data generated or analyzed and its supplementary information files during this study are included in this published article. The mass spectrometry proteomics data have been deposited to the PRIDE Archive (<http://www.ebi.ac.uk/pride/archive/>) via the PRIDE partner repository with the data set identifier PXD053567.

Code Availability

Not applicable.

ORCID

Truong Phan-Xuan Nguyen

<https://orcid.org/0000-0001-6965-5863>

Minh-Khang Le

<https://orcid.org/0000-0002-4571-0888>

Sittiruk Roytrakul

<https://orcid.org/0000-0003-3696-8390>

Shanop Shuangshoti

<https://orcid.org/0000-0003-3416-337X>

Nakarin Kitkumthorn

<https://orcid.org/0000-0003-0616-6039>

Somboon Keelawat

<https://orcid.org/0000-0002-4180-7914>

Author Contributions

Conceptualization: TPXN, SK, NK. Data curation: TPXN, MKL. Formal analysis: TPXN, MKL. Investigation: TPXN, SK. Methodology: TPXN, MKL. Project administration: SK, NK. Resources: TPXN. Supervision: SK, NK. Writing—original draft: TPXN, MKL. Writing—review & editing: TPXN, MKL, SR, SS, NK, SK. Approval of the final manuscript: all authors.

Conflicts of Interest

The authors declare that they have no potential conflicts of interest.

Funding Statement

This study was supported by Chulalongkorn's 90-year Scholarship Ratchadapisek Research and Ratchadapiseksompotch Fund, Graduate Affairs, Faculty of Medicine, Chulalongkorn University, grant number GA67/058. TPXN and SK are recipients. The funder had no role in the design of the study; the collection, analysis, and interpretation of data; the writing of the article; or the decision to submit the article for publication.

REFERENCES

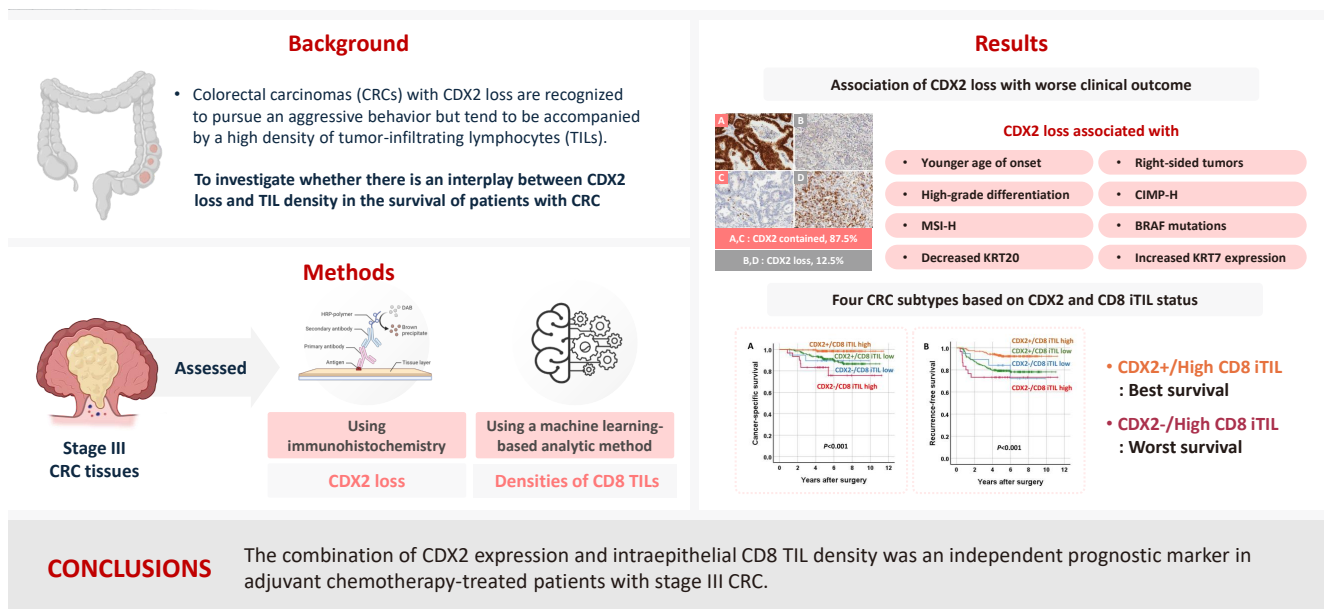
1. Sung H, Ferlay J, Siegel RL, et al. Global cancer statistics 2020: GLOBOCAN estimates of incidence and mortality worldwide for 36 cancers in 185 countries. *CA Cancer J Clin* 2021; 71: 209-49.
2. Miranda-Filho A, Lortet-Tieulent J, Bray F, et al. Thyroid cancer incidence trends by histology in 25 countries: a population-based study. *Lancet Diabetes Endocrinol* 2021; 9: 225-34.
3. Kitahara CM, Sosa JA. The changing incidence of thyroid cancer. *Nat Rev Endocrinol* 2016; 12: 646-53.
4. WHO classification of tumours of endocrine organs. 5th beta ed. [Internet]. Geneva: World Health Organization, 2022 [cited 2024].

- May 20]. Available from: <https://tumourclassification.iarc.who.int>.
- Baloch ZW, Asa SL, Barletta JA, et al. Overview of the 2022 WHO classification of thyroid neoplasms. *Endocr Pathol* 2022; 33: 27-63.
 - Na HY, Park SY. Noninvasive follicular thyroid neoplasm with papillary-like nuclear features: its updated diagnostic criteria, preoperative cytologic diagnoses and impact on the risk of malignancy. *J Pathol Transl Med* 2022; 56: 319-25.
 - Haugen BR, Alexander EK, Bible KC, et al. 2015 American Thyroid Association management guidelines for adult patients with thyroid nodules and differentiated thyroid cancer: the American Thyroid Association Guidelines Task Force on Thyroid Nodules and Differentiated Thyroid Cancer. *Thyroid* 2016; 26: 1-133.
 - Gillet LC, Leitner A, Aebersold R. Mass spectrometry applied to bottom-up proteomics: entering the high-throughput era for hypothesis testing. *Annu Rev Anal Chem (Palo Alto Calif)* 2016; 9: 449-72.
 - Kulyassov A, Fresnais M, Longuespee R. Targeted liquid chromatography-tandem mass spectrometry analysis of proteins: basic principles, applications, and perspectives. *Proteomics* 2021; 21: e2100153.
 - Sun Y, Li L, Zhou Y, et al. Stratification of follicular thyroid tumours using data-independent acquisition proteomics and a comprehensive thyroid tissue spectral library. *Mol Oncol* 2022; 16: 1611-24.
 - Huang D, Zhang H, Li L, et al. Proteotypic differences of follicular patterned thyroid neoplasms. *Front Endocrinol (Lausanne)* 2022; 13: 854611.
 - Suzuki A, Nojima S, Tahara S, et al. Identification of invasive subpopulations using spatial transcriptome analysis in thyroid follicular tumors. *J Pathol Transl Med* 2024; 58: 22-8.
 - Nguyen TP, Roytrakul S, Buranapraditkun S, Shuangshoti S, Kitkumthorn N, Keelawat S. Proteomics profile in encapsulated follicular patterned thyroid neoplasms. *Sci Rep* 2024; 14: 16343.
 - Chawla NV, Bowyer KW, Hall LO, Kegelmeyer WP. SMOTE: synthetic minority over-sampling technique. *J Artif Intell Res* 2002; 16: 321-57.
 - van Buuren S, Groothuis-Oudshoorn K. mice: multivariate imputation by chained equations in R. *J Stat Softw* 2011; 45: 1-67.
 - Li Y, Wu F, Ge W, et al. Risk stratification of papillary thyroid cancers using multidimensional machine learning. *Int J Surg* 2024; 110: 372-84.
 - Wenk D, Zuo C, Kislinger T, Sepiashvili L. Recent developments in mass-spectrometry-based targeted proteomics of clinical cancer biomarkers. *Clin Proteomics* 2024; 21: 6.
 - Rezania S, Kammerer S, Li C, et al. Overexpression of *KCNJ3* gene splice variants affects vital parameters of the malignant breast cancer cell line MCF-7 in an opposing manner. *BMC Cancer* 2016; 16: 628.
 - Chandra B, Michmerhuizen NL, Shirnekhi HK, et al. Phase separation mediates NUP98 fusion oncoprotein leukemic transformation. *Cancer Discov* 2022; 12: 1152-69.
 - Zhang P, Sun Y, Ma L. ZEB1: at the crossroads of epithelial-mesenchymal transition, metastasis and therapy resistance. *Cell Cycle* 2015; 14: 481-7.
 - Xu B, Wang L, Tuttle RM, Ganly I, Ghossein R. Prognostic impact of extent of vascular invasion in low-grade encapsulated follicular cell-derived thyroid carcinomas: a clinicopathologic study of 276 cases. *Hum Pathol* 2015; 46: 1789-98.

The combination of CDX2 expression status and tumor-infiltrating lymphocyte density as a prognostic factor in adjuvant FOLFOX-treated patients with stage III colorectal cancers

Ji-Ae Lee¹, Hye Eun Park², Hye-Yeong Jin^{3,4}, Lingyan Jin^{3,4}, Seung Yeon Yoo⁵, Nam-Yun Cho⁴, Jeong Mo Bae^{3,4}, Jung Ho Kim³, Gyeong Hoon Kang^{3,4}

Graphical abstract



The combination of CDX2 expression status and tumor-infiltrating lymphocyte density as a prognostic factor in adjuvant FOLFOX-treated patients with stage III colorectal cancers

Ji-Ae Lee¹, Hye Eun Park², Hye-Yeong Jin^{3,4}, Lingyan Jin^{3,4}, Seung Yeon Yoo⁵, Nam-Yun Cho⁴, Jeong Mo Bae^{3,4}, Jung Ho Kim³, Gyeong Hoon Kang^{3,4}

¹Department of Pathology, Seoul National University Bundang Hospital, Seongnam, Korea

²Department of Pathology, Seoul National University Boramae Hospital, Seoul, Korea

³Department of Pathology, Seoul National University College of Medicine, Seoul, Korea

⁴Laboratory of Epigenetics, Cancer Research Institute, Seoul National University College of Medicine, Seoul, Korea

⁵Pathology Center, Seegene Medical Foundation, Seoul, Korea

Background: Colorectal carcinomas (CRCs) with caudal-type homeobox 2 (CDX2) loss are recognized to pursue an aggressive behavior but tend to be accompanied by a high density of tumor-infiltrating lymphocytes (TILs). However, little is known about whether there is an interplay between CDX2 loss and TIL density in the survival of patients with CRC. **Methods:** Stage III CRC tissues were assessed for CDX2 loss using immunohistochemistry and analyzed for their densities of CD8 TILs in both intraepithelial (iTILs) and stromal areas using a machine learning-based analytic method. **Results:** CDX2 loss was significantly associated with a higher density of CD8 TILs in both intraepithelial and stromal areas. Both CDX2 loss and a high CD8 iTIL density were found to be prognostic parameters and showed hazard ratios of 2.314 (1.050–5.100) and 0.378 (0.175–0.817), respectively, for cancer-specific survival. A subset of CRCs with retained CDX2 expression and a high density of CD8 iTILs showed the best clinical outcome (hazard ratio of 0.138 [0.023–0.826]), whereas a subset with CDX2 loss and a high density of CD8 iTILs exhibited the worst clinical outcome (15.781 [3.939–63.230]). **Conclusions:** Altogether, a high density of CD8 iTILs did not make a difference in the survival of patients with CRC with CDX2 loss. The combination of CDX2 expression and intraepithelial CD8 TIL density was an independent prognostic marker in adjuvant chemotherapy-treated patients with stage III CRC.

Keywords: CD8 antigens; CDX2 transcription factor; Colorectal neoplasms; Prognosis; Lymphocytes, tumor-infiltrating

INTRODUCTION

Colorectal cancer (CRC) ranks third in cancer prevalence and second in cancer mortality worldwide [1]. The prognostication of patients with CRC is globally based on the tumor, node, metastasis (TNM) staging, which reflects the extent of the cancer. However, there is significant variation in survival among patients who have the same cancer stage [2,3]. Fluoropyrimi-

dine-oxaliplatin combination (FOLFOX) therapy is standard care after surgery for patients with stage III colon cancer. However, it is estimated that a considerable portion of patients with stage III colon cancer do not benefit from adjuvant FOLFOX therapy, and some patients suffer from unnecessary toxicity [4-7]. Thus, it is necessary to develop clinicopathological or molecular biomarkers that help to identify whether patients will benefit from adjuvant combination therapy.

Received: June 3, 2024 **Revised:** August 22, 2024 **Accepted:** September 26, 2024

Corresponding Author: Gyeong Hoon Kang, MD, PhD

Department of Pathology, Seoul National University College of Medicine, 103 Daehak-ro, Jongno-gu, Seoul 03080, Korea

Tel: +82-2-740-8263, Fax: +82-2-743-5530, E-mail: ghkang@snu.ac.kr

This is an Open Access article distributed under the terms of the Creative Commons Attribution Non-Commercial License (<https://creativecommons.org/licenses/by-nc/4.0/>) which permits unrestricted non-commercial use, distribution, and reproduction in any medium, provided the original work is properly cited.

© 2025 The Korean Society of Pathologists/The Korean Society for Cytopathology

Caudal-type homeobox 2 (CDX2) is a major regulator of intestine-specific genes involved in cell growth and differentiation. CDX2 is a gene that is only active in the small and large intestines and is detected in most CRCs (90%) [8-10]. Patients with CRC which has no CDX2 expression tend to have worse outcomes [8,11]. Although CDX2 loss has been shown to be a marker of poor prognosis in stage II colon cancer [12], CDX2 loss has been demonstrated to be a marker of chemotherapy sensitivity in stage II colon cancer patients, implying that adjuvant chemotherapy might be a treatment option for patients with stage II CDX2-deficient colon cancer [13]. However, another previous study has suggested that CDX2 loss may be a possible negative marker of chemotherapy response in CRC patients with metastases [14].

Regarding the cause of CDX2 loss in CRC, promoter CpG island hypermethylation has been suggested [11]. CDX2 loss is more frequent in CRCs with CpG island methylator phenotype (CIMP) than in CRCs without CIMP [8,15] and in CRCs with microsatellite instability (MSI) than in CRCs without MSI [8,11,12,16]. CIMP and MSI have been shown to be associated with enhanced tumor-infiltrating lymphocyte (TIL) density [17,18]. There is not much information about the TIL status in CRCs that lack CDX2 expression [8], but CRCs that lack CDX2 expression are likely to have higher TIL density than CRCs with retained CDX2 expression because of the relationship between CDX2 loss and MSI or CIMP. In terms of prognosis, it remains unclear whether patients with CDX2-deficient CRC show different clinical outcomes depending on TIL density status.

In the present study, we aimed to identify (1) whether CDX2 loss is associated with poor clinical outcome in adjuvant FOLFOX-treated patients with stage III CRC, (2) whether CDX2 loss is associated with an increased density of TILs, and (3) whether there is an interplay between CDX2 expression and TIL status in patient survival. To resolve the above issues, we performed CDX2 immunohistochemistry (IHC) of cancer tissue samples from stage III CRC patients treated with adjuvant FOLFOX and quantified CD3-positive TILs and CD8-positive TILs in both intraepithelial and stromal areas using a machine learning-based analytic method and then correlated CDX2 expression status with clinicopathological and molecular features. To investigate whether an interplay exists between CDX2 loss and TIL density in the survival of patients with CRC, we examined the combined CDX2 expression and TIL density statuses to understand their impact on survival characteristics.

MATERIALS AND METHODS

Samples

Archival tissue blocks of the surgical specimens from 505 patients with stage III CRC who received adjuvant FOLFOX after curative surgery (R0) at Seoul National University Hospital (SNUH) between April 2005 and December 2012 were available for construction of a tissue microarray (TMA). Whole-slide immunostaining of CD3 and CD8 was possible in 446 of the 505 patients. Patients were chosen for the present study based on the following criteria: they were over 18 years old, they had adenocarcinoma type of cancer, they had stage III CRC, they had their tumor removed completely with no cancer cells at the edges, and they finished at least six cycles of 5-fluorouracil plus oxaliplatin or four cycles of capecitabine plus oxaliplatin as adjuvant therapy. The present study did not include patients who met any of these criteria: having chemotherapy or radiotherapy before surgery, a genetic condition that causes many polyps in the colon and rectum, an idiopathic inflammatory bowel disease, or a previous diagnosis of any other cancer within 5 years. We reviewed electronic medical records and collected demographic and clinicopathological data, such as age, sex, tumor location, histological differentiation, lymphatic emboli or venous invasion, perineural invasion, and American Joint Committee on Cancer/International Union against Cancer (AJCC/UICC) cancer stage (7th edition).

Immunohistochemistry

One pathologist (S.Y.Y.) selected the paraffin tissue block most representative of the tumor, and whole-slide sections were subjected to IHC with antibodies against CD3 (clone F7.2.38, Dako, Carpinteria, CA, USA) and CD8 (clone SP57, Ventana Medical Systems, Tucson, AZ, USA) [19]. The TMA blocks received cores that were 2 mm across and taken from two separate regions of the tumor. TMA sections of 4- μ m thickness were stained with primary antibodies against KRT7 (cytokeratin 7 [CK7], clone OV-TL 12/30, Dako), KRT20 (CK20, clone Ks20.8, Dako), and CDX2 (clone EPR2764Y ready-to-use, Cell Marque, Rocklin, CA, USA). An Aperio AT2 slide scanner (Leica Biosystems, Wetzlar, Germany) was used to scan all the stained slides. To interpret the IHC results, the proportion of tumor cells that expressed KRT7 and KRT20 in their cytoplasm was measured. The threshold was based on scores of 10% and 50% for high KRT7 expression and low KRT20 expression, respectively, following a prior study [8]. To interpret CDX2 IHC

results, we used the H score to measure the intensity and extent of nuclear staining. The H score was calculated with this formula: $3 \times$ percentage of strongly stained nuclei + $2 \times$ percentage of moderately stained nuclei + $1 \times$ percentage of weakly stained nuclei. The cutoff value was set at an H score of 20, and an H score of <20 was called loss of expression [20]. The analytic pipeline used the virtual slide files of CD3 and CD8 IHC as input, and its detailed protocol can be found at <http://dx.doi.org/10.17504/protocols.io.yqvfww6> [21]. After a user marked the tumor area on a given image, the algorithm divided the area into tiles of $1 \text{ mm} \times 1 \text{ mm}$ and calculated the median density (number of cells/ mm^2) of TILs inside the epithelium (iTILs) and TILs in the stroma (sTILs).

DNA extraction, microsatellite instability analysis, and mutation analysis of *KRAS* and *BRAF*

Using a microscope, the parts of the tumor with typical histology and the most tumor cells were marked on glass slides, and the corresponding areas from the unstained tissue slides after deparaffinization were scraped from the glass slides. The tissues that were scraped off were transferred into microtubes with tissue lysis buffer and proteinase K and then left to incubate at 55°C for 24 hours. After centrifugation, the supernatant was transferred to a new tube and kept in a deep freezer. The fluorescent multiplex polymerase chain reaction (PCR) method with five microsatellite markers suggested by National Cancer Institute (BAT25, BAT26, D2S123, D5S346, and D17S250) was used to determine the MSI status of each tumor. Tumors were categorized as MSI-H (MSI-high, with ≥ 2 unstable markers out of 5) or MSS (microsatellite-stable, with 1 or no unstable marker) ($n = 503$). Real-time PCR-based allelic discrimination was used to examine *BRAF* mutations at codon 600 (V600E) ($n = 492$). Codons 12 and 13 of *KRAS* exon 2 were sequenced to determine their mutation statuses ($n = 486$).

Bisulfite modification and methylation analysis

Using an EZ DNA methylation kit (Zymo Research, Orange, CA, USA), genomic DNA underwent bisulfite conversion, and then the MethyLight assay was used to assess the methylation level of these CIMP-specific markers (*CACNA1G*, *CDKN2A* (*p16*), *CRABP1*, *IGF2*, *MLH1*, *NEUROG1*, *RUNX3*, and *SOC1*) ($n = 500$). The primer sequences and PCR conditions have been previously reported [22,23]. We performed the MethyLight assay three times and used the median value to show the methylation level of each marker. To determine the methylation status

of a specific marker, the percentage of methylated reference (PMR) was calculated, and a marker with a median PMR >4 was deemed to be methylated. Each tumor was assessed for CIMP status and grouped into CIMP-H (CIMP-high, ≥ 5 out of 8 methylated markers), CIMP-L (CIMP-low, 1–4 methylated markers), or CIMP-0 (no methylation) as previously reported [17].

Statistical analysis

The normality test was conducted to determine whether TIL density was normally distributed using the Shapiro-Wilks test. The null hypothesis that the TIL density is normally distributed was rejected because the p-value was below .05 for all four types of TILs, including intraepithelial CD3 TILs (CD3 iTILs), stromal CD3 TILs (CD3 sTILs), CD8 iTILs, and CD8 sTILs. Thus, comparison of the TIL density between subsets of CRCs with CDX2 loss and with CDX2 retention was performed using the nonparametric Mann-Whitney U test. Student's t test was used to compare the age distribution of two groups. For 2×2 contingency tables with a sample size of more than 5, a two-sided chi-square test was performed, while a Kruskal-Wallis test was applied for contingency tables with more than 2×2 dimensions. We measured the time from surgery to death by CRC as cancer-specific survival (CSS) time and the time from surgery to confirmed recurrence as recurrence-free survival (RFS) time. We censored the data from patients who did not die from CRC or relapse by the last follow-up visit for the CSS and RFS analyses, respectively. We used the Kaplan-Meier log-rank test to compare survival across groups. We estimated the hazard ratio with the Cox proportional hazard model and adjusted for baseline characteristics with a backward stepwise model that included the following covariates that were significant in univariate survival analysis: differentiation (high grade vs. low grade), venous invasion (present vs. absent), lymphatic emboli (present vs. absent), T category (T4 vs. T1–3), N category (N2 vs. N1), CK7 (expressed vs. not expressed), *KRAS* (mutant vs. wild type), CD3 sTIL, and CD8 sTIL.

RESULTS

The follow-up period for the 505 patients was a mean of 68.2 months (range, 4.1 to 134.8 months). Table 1 shows the demographic data. There were 303 males and 202 females. The tumor subsite was distributed as follows: 150 in the right colon, 289 in the left colon, and 66 in the rectum. CIMP-H and MSIH CRCs were present in 5.4% and 5.6% of stage III CRCs, respectively.

Table 1. Association of clinicopathological and molecular features between CRCs with and without CDX2 loss

Parameter	No.	CRCs with CDX2 loss	CRCs with retained CDX2	p-value
Sex				.681
Male	303	36 (42.9)	267 (39.6)	
Female	202	27 (57.1)	175 (60.4)	
Location				.049
Right colon	150	26 (41.3)	124 (28.1)	
Left colon	289	33 (52.4)	256 (57.9)	
Rectum	66	4 (6.3)	62 (14.0)	
Differentiation				<.001
Low	469	50 (79.4)	419 (94.8)	
High	36	13 (20.6)	23 (5.2)	
Venous invasion				.831
Absent	450	57 (90.5)	393 (88.9)	
Present	55	6 (9.5)	49 (11.1)	
Lymphatic emboli				.172
Absent	298	32 (50.8)	266 (60.2)	
Present	207	31 (49.2)	176 (39.8)	
Perineural invasion				.288
Absent	369	50 (79.4)	319 (72.2)	
Present	136	13 (20.6)	123 (27.8)	
T category				.018
T1	10	4 (6.3)	6 (1.4)	
T2	46	6 (9.5)	40 (9.0)	
T3	397	43 (68.3)	354 (80.1)	
T4	52	10 (15.9)	42 (9.5)	
N category				.313
N1	348	40 (63.5)	308 (69.7)	
N2	157	23 (36.5)	134 (30.3)	
CIMP				<.001
CIMP-L,0	473	51 (82.3)	422 (96.3)	
CIMP-H	27	11 (17.7)	16 (3.7)	
MSI				.001
MSS	475	53 (84.1)	422 (95.9)	
MSI-H	28	10 (15.9)	18 (4.1)	
KRAS				.642
Wild	346	39 (68.4)	307 (71.6)	
Mutant	129	18 (31.6)	122 (28.4)	
BRAF				<.001
Wild	475	51 (85.0)	424 (98.1)	
Mutant	17	9 (15.0)	8 (1.9)	
KRT20				<.001
Decreased	68	35 (55.6)	33 (7.5)	
Retained	437	28 (44.4)	409 (92.5)	
KRT7				<.001
Not expressed	474	52 (82.5)	422 (95.5)	
Expressed	31	11 (17.5)	20 (4.5)	

CRC, colorectal carcinoma; CDX2, caudal-type homeobox 2; CIMP, CpG island methylator phenotype; CIMP-L, CIMP-low; CIMP-0, no methylation; CIMP-H, CIMP-high; MSI, microsatellite instability; MSS, microsatellite-stable; MSI-H, MSI-high.

KRAS and BRAF mutations occurred in 28.8% and 3.5% of patients, respectively.

Relationships between decreased expression of CDX2 and clinicopathological features

Decreased expression of CDX2 (CDX2 loss) was found in 12.5% of stage III CRCs (Fig. 1). CDX2 loss was associated with a younger age of onset (56.1 vs. 59.8 years, Student's t test, p = .003). CDX2 loss was more frequent in the right colon than in the left colon and rectum, in CRCs with high-grade histological differentiation than in CRCs with low-grade histological differentiation, in CIMP-H CRCs than in CIMP-L,0 CRCs, in MSI-H CRCs than in MSS CRCs, in CRCs with BRAF mutations than in CRCs without BRAF mutation, in CRCs with decreased expression of KRT20 than in CRCs without decreased expression of KRT20, and in CRCs with KRT7 expression than in CRCs without KRT7 expression (Table 1). CRCs with CDX2 loss showed a higher density of CD8 iTILs and sTILs than CRCs without CDX2 loss (Fig. 2). The significance of the difference was higher in the density of CD8 iTILs than in that of CD8 sTILs. However, the densities of CD3 iTILs and sTILs tended to be higher in CRCs with CDX2 loss than in CRCs with retained CDX2 expression, but the difference did not reach statistical significance (Fig. 2).

Association of CDX2 loss with worse clinical outcome

In univariate survival analysis, CDX2 loss was found to be significantly associated with shortened CSS but not RFS (Fig. 3A, B). In addition, several clinicopathological parameters, including tumor differentiation, T category, N category, lymphatic emboli, venous invasion, KRAS mutation, KRT7 expression, CD3 sTILs, CD8 iTILs (Fig. 3C, D), and CD8 sTILs, were found to be significant prognostic factors in the univariate analysis of CSS (Table 2).

Combination of CDX2 expression and CD8 iTIL density status as a prognostic parameter

The combination of CDX2 expression and CD8 iTIL density status generates four subsets of CRCs. In the analysis of CSS using the Kaplan-Meier log-rank test, a subset with retained CDX2 expression and a high density of CD8 iTILs showed the best clinical outcome, whereas subsets with CDX2 loss exhibited worse clinical outcomes, regardless of CD8 iTIL status, than a subset with retained CDX2 expression and a high density of CD8 iTILs (Fig. 4). Statistically, there was no significant sur-

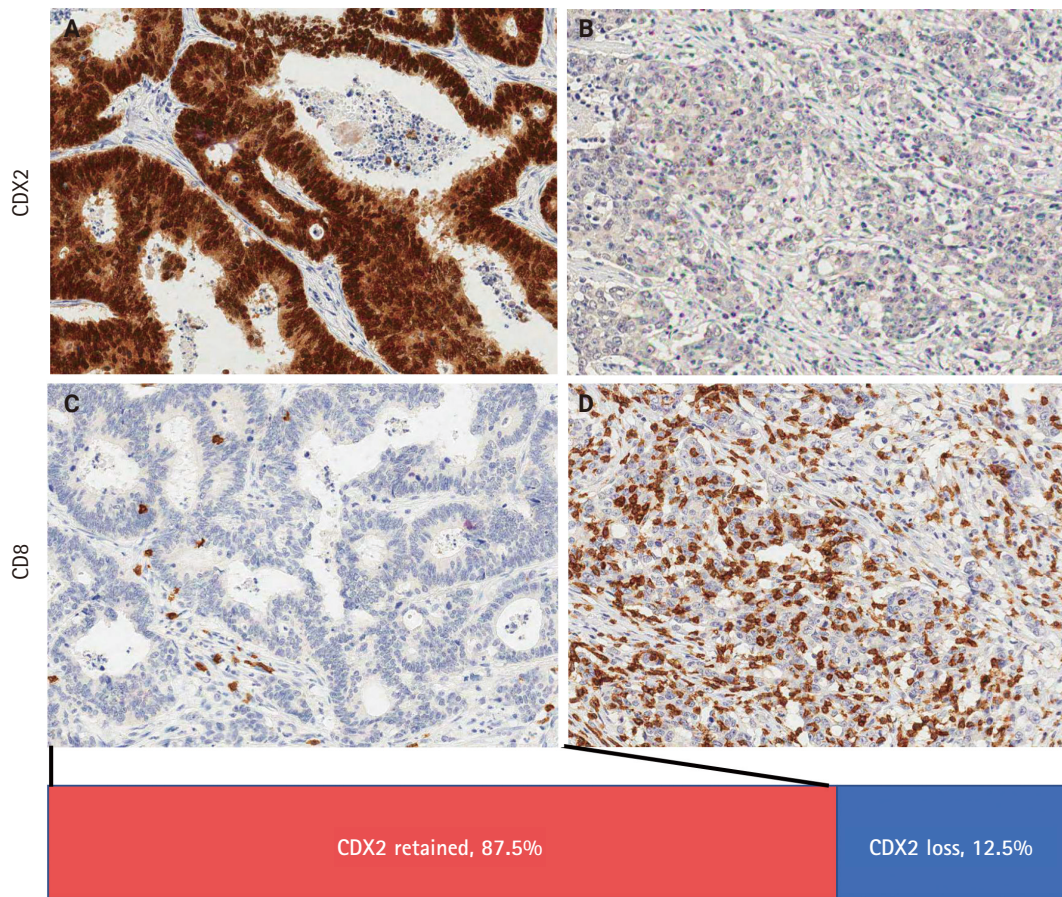


Fig. 1. Representative cases of colorectal carcinomas (CRCs) with retained caudal-type homeobox 2 (CDX2) expression and a low CD8 intraepithelial tumor-infiltrating lymphocyte (iTIL) density (A, C) and with CDX2 loss and a high CD8 iTIL density (B, D).

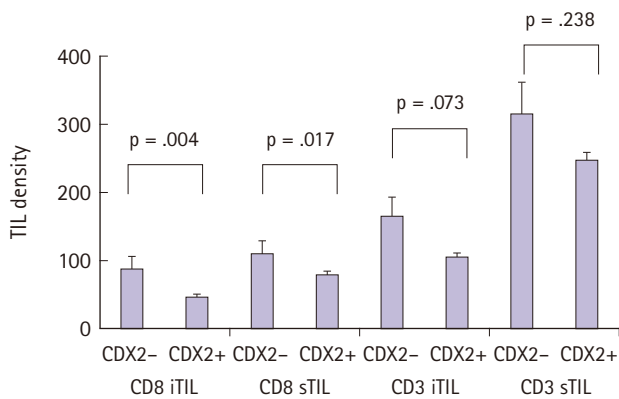


Fig. 2. Comparison of intraepithelial or stromal tumor-infiltrating lymphocyte (iTIL or sTIL) density between colorectal carcinomas with and without CDX2 loss. CDX2-, expressional loss of CDX2; CDX2+, retained expression of CDX2.

vival difference between a subset with CDX2 loss and a high density of CD8 iTILs and a subset with CDX2 loss and a low density of CD8 iTILs ($p = .384$ and $p = .501$, CSS and RFS, respectively). In the multivariate analysis, the combination of CDX2 expression and CD8 iTILs was found to be an independent prognostic parameter (Table 3).

DISCUSSION

In the present study, we analyzed a cohort of adjuvant FOLF-OX-treated patients with stage III CRC regarding whether CDX2 loss was associated with a shortened survival, whether CDX2 expression status was associated with the intraepithelial or stromal TIL density, and whether there was an interplay between CDX2 expression and TIL density in patient survival. The findings demonstrated that CDX2 loss was a prognostic factor heralding poor prognosis in patients with stage III CRC

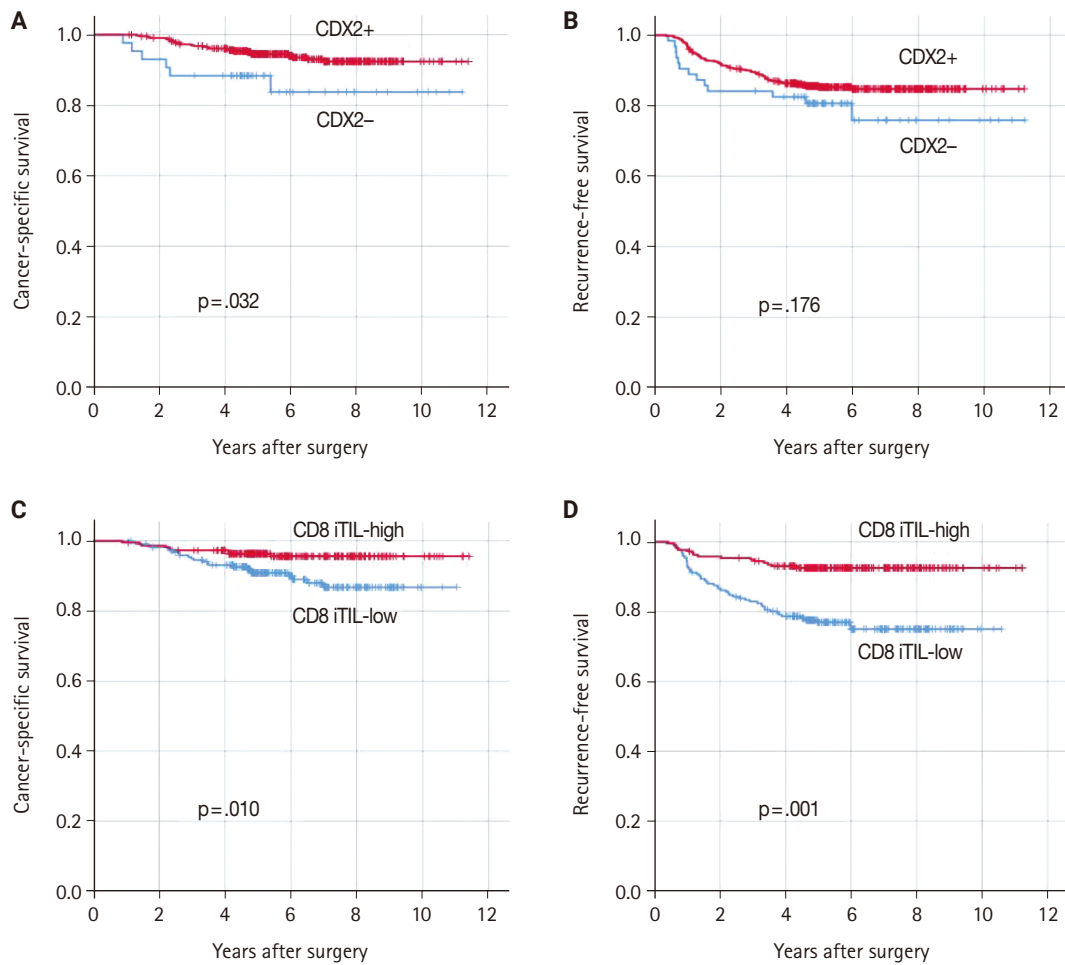


Fig. 3. Kaplan-Meier curves of cancer-specific survival (A, C) and recurrence-free survival (B, D) in adjuvant FOLFOX-treated patients with stage III colorectal carcinoma (CRC) according to caudal-type homeobox 2 (CDX2) expression status (A, B) and CD8 intraepithelial tumor-infiltrating lymphocyte (iTIL) density status (C, D). CDX2+ (retained expression, n = 442) and CDX2- (loss of expression, n = 63); CD8 iTIL-high (n = 223) and CD8 iTIL-low CRC (n = 223).

treated with adjuvant FOLFOX, CDX2 loss was accompanied by increased infiltration of CD8 iTILs and sTILs, and a combined status of CDX2 expression and CD8 iTIL density was an independent prognostic parameter in FOLFOX-treated patients with stage III CRC.

In the present study, CRCs with CDX2 loss showed higher densities of CD8 iTILs and sTILs than CRCs with retained CDX2 expression. However, in terms of prognosis, CDX2 loss might collide with an increased density of CD8 iTILs because CDX2 loss and an increased density of CD8 iTILs were associated with worse and better survival, respectively (Table 2, Fig. 3). Of the four subsets generated by the combination of CDX2 expression and CD8 iTIL density statuses, a subset of CRCs with

retained CDX2 expression and high CD8 iTIL density showed the best clinical outcome, which is in accordance with Derangere et al.'s study [24] in which stage III colon cancers harboring high CDX2 expression and a high CD3 TIL were associated with a good prognosis. However, in the present study, the worst clinical outcome was observed in a subset of CRCs with CDX2 loss and high CD8 iTIL density, in contrast to Derangere et al.'s study [24], which showed the worst prognosis in stage III colon cancers with low CDX2 expression and a low CD3 TIL density. The reason for such a discrepancy might be related to the different cutoff values set for CDX2 expression and TIL density for dichotomization. In Derangere et al.'s study [24], three-fourths of colon cancers were classified into tumors with low CDX2

Table 2. Univariate analysis of cancer-specific survival

Parameter	No.	HR (95% CI)	p-value
Differentiation			.014
Low grade	469	-	
High grade	36	2.997 (1.244–7.221)	
N category			<.001
N1	348	-	
N2	157	3.459 (1.759–6.803)	
T category			.001
T1-3	453	-	
T4	52	3.050 (1.567–5.936)	
Lymphatic emboli			<.001
Absent	298	-	
Present	207	7.586 (3.149–18.272)	
Venous invasion			.004
Absent	450	-	
Present	55	3.050 (1.429–6.512)	
Perineural invasion			.089
Absent	369	-	
Present	136	1.818 (0.914–3.619)	
CIMP			.076
CIMP-L,0	473	-	
CIMP-H	27	2.577 (0.906–7.333)	
BRAF			.320
Wild	475	-	
Mutant	17	2.070 (0.494–8.678)	
KRAS			.007
Wild	346	-	
Mutant	129	2.724 (1.315–5.644)	
KRT7			.008
Not expressed	474	-	
Expressed	31	3.316 (1.377–7.989)	
KRT20			.717
Retained	437	-	
Decreased	68	0.839 (0.324–2.169)	
CDX2			.037
Retained	442	-	
Loss	63	2.314 (1.050–5.100)	
CD3 iTIL			.316
Low	224	-	
High	222	0.697 (0.344–1.412)	
CD3 sTIL			.026
Low	216	-	
High	230	0.428 (0.203–0.903)	
CD8 iTIL			.013
Low	223	-	
High	223	0.378 (0.175–0.817)	
CD8 sTIL			.028
Low	223	-	
High	223	0.433 (0.205–0.915)	
Combination of the CDX2 expression and CD8 iTIL density statuses			
CDX2 retained/CD8 iTIL-high	188	-	
CDX2 loss/CD8 iTIL-low	19	7.250 (1.211–43.401)	.030
CDX2 loss/CD8 iTIL-high	30	15.781 (3.939–63.230)	<.001
CDX2 retained/CD8 iTIL-low	209	6.686 (1.994–22.419)	.002

HR, hazard ratio; CI, confidence interval; CIMP, CpG island methylator phenotype; CIMP-L, CIMP-low; CIMP-O, no methylation; CIMP-H, CIMP-high; iTIL, intraepithelial tumor-infiltrating lymphocyte; sTIL, stromal tumor-infiltrating lymphocyte; CDX2, caudal-type homeobox 2.

expression, and two-thirds of colon cancers were classified into tumors with a low CD3 TIL density, whereas in our study, one-eighth of CRCs were classified into tumors with CDX2 loss, and one-half of CRCs were classified into tumors with a low CD8 iTIL density.

Because a high CD8 iTIL density is associated with good prognosis, it was expected that tumors with CDX2 loss and a low CD8 iTIL density would be associated with the worst survival. Interestingly, the density of CD8 iTILs did not significantly impact the survival of patients with tumors exhibiting CDX2 loss. The underlying reason for this lack of effect remains challenging to explain. It can be speculated that CD8 iTILs might be not effective in fighting against cancers with CDX2 loss. However, little information is available to support this assumption, and thus, spatial transcriptomics at the single-cell level might provide clues to the explanation. Our result that the number of CD8 iTILs did not affect the survival of patients with tumors that had CDX2 loss seems to contradict the common belief of a better survival of patients with a high CD8 TIL number [25]. But in human cancer, renal cell carcinoma is the tissue type where many CD8 TILs are strongly related to bad clinicopathologic data and worse patient survival [26-28]. Furthermore, in pancreatic cancer, the role of CD8+ T cells is not directly associated with clinicopathological parameters [28]. Thus, loss of CDX2 expression in CRC may indeed indicate a reduction in intestinal differentiation, in which the prognostic role of CD8 TILs might differ from that in CRCs with retained CDX2 expression.

In our study, CDX2 loss was associated with increased infiltration of intraepithelial and stromal CD8-positive lymphocytes. However, the association between CDX2 loss and increased TIL density might be spurious because CDX2 loss was also associated with CIMP-H and MSI-H, which are known to be accompanied by increased TILs. Thus, to elucidate whether CDX2 loss is associated with increased TILs regardless of CIMP and MSI status, we analyzed the relationship between CDX2 loss and increased TIL density in CRCs which are negative for CIMP-H and MSI-H, namely, CIMP-L,0 and MSS CRCs (n = 396). An increased density of CD8 iTILs was found in CIMP-L,0 and MSS CRCs with CDX2 loss (n = 34) compared with CIMP-L,0 and MSS CRCs with retained CDX2 expression (n = 362) (Supplementary Fig. S1). Such a finding indicates that the increased density of CD8 iTILs might be related to CDX2 loss itself.

In summary, we found that in patients with stage III CRC,

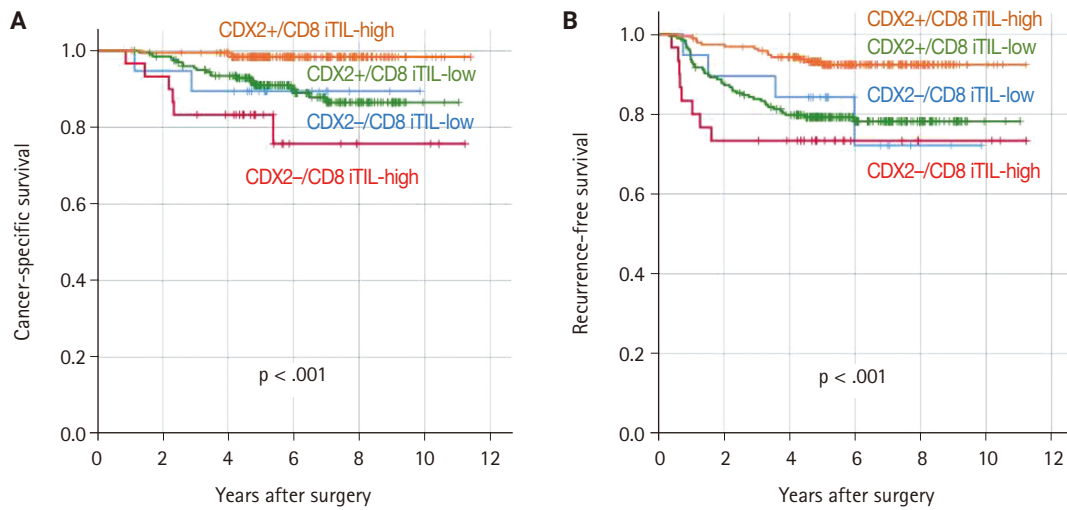


Fig. 4. Kaplan-Meier survival curves of cancer-specific survival (A) and recurrence-free survival (B). Kaplan-Meier survival analysis with the log-rank test was performed in adjuvant FOLFOX-treated patients with stage III colorectal carcinoma according to the combination of caudal-type homeobox 2 (CDX2) expression and CD8 intraepithelial tumor-infiltrating lymphocyte (iTIL) density. CDX2+ (CDX2 retained)/CD8 iTIL-high (n = 188); CDX2+/CD8 iTIL-low (n = 209); CDX2- (CDX2 loss)/CD8 iTIL-high (n = 30); CDX2-/CD8 iTIL-low (n = 19).

Table 3. Multivariate survival analysis (cancer-specific survival)

Parameter	HR (95% CI)	p-value
Differentiation		
High grade vs. low grade	1.733 (0.559–5.368)	.341
T category		
T4 vs. T1-3	1.934 (0.769–4.867)	.161
N category		
N2 vs. N1	1.943 (0.901–4.187)	.090
Lymphatic emboli		
Present vs. absent	4.432 (1.779–11.041)	.001
Venous invasion		
Present vs. absent	1.618 (0.646–4.053)	.304
KRAS		
Mutant vs. wild	2.318 (1.115–4.819)	.024
KRT7		
Expressed vs. not expressed	1.984 (0.734–5.360)	.177
CD3 sTIL		
High vs. low	0.438 (0.178–1.077)	.072
CD8 sTIL		
High vs. low	0.685 (0.182–2.584)	.577
Combination of the CDX2 expression and CD8 iTIL density statuses		
CDX2 retained/CD8 iTIL-high	-	
CDX2 loss/CD8 iTIL-low	8.176 (1.137–58.783)	.037
CDX2 loss/CD8 iTIL-high	17.868 (3.429–93.100)	.001
CDX2 retained/CD8 iTIL-low	6.769 (1.542–29.703)	.011

HR, hazard ratio; CI, confidence interval; sTIL, stromal tumor-infiltrating lymphocyte; iTIL, intraepithelial tumor-infiltrating lymphocyte.

CDX2 loss was associated with increased infiltration of CD8 iTILs or sTILs, and the density of CD8 iTILs did not significantly impact the survival of patients with CRC exhibiting CDX2 loss. The combination of CDX2 expression and intraepithelial CD8 iTIL density was found to be an independent prognostic marker in adjuvant chemotherapy-treated patients with stage III CRC.

Supplementary Information

The Data Supplement is available with this article at <https://doi.org/10.4132/jptm.2024.09.26>.

Ethics Statement

The Institutional Review Board of Seoul National University Hospital approved this study (1811-061-983) and waived the requirement to obtain informed consent. This study followed the Declaration of Helsinki guidelines.

Availability of Data and Material

The datasets generated or analyzed during the study are available from the corresponding authors on reasonable request.

Code Availability

Not applicable.

ORCID

Ji-Ae Lee <https://orcid.org/0000-0003-1493-6208>
 Hye Eun Park <https://orcid.org/0000-0003-1048-2827>
 Seung Yeon Yoo <https://orcid.org/0000-0002-7881-9038>
 Nam-Yun Cho <https://orcid.org/0000-0002-5736-2956>
 Jeong Mo Bae <https://orcid.org/0000-0003-0462-3072>
 Jung Ho Kim <https://orcid.org/0000-0002-6031-3629>
 Gyeong Hoon Kang <https://orcid.org/0000-0003-2380-6675>

Author Contributions

Conceptualization: JMB, GHK. Formal analysis: JMB, GHK. Funding acquisition: GHK. Investigation: JAL, HEP, HYJ, LJ, SYY, JMB. Methodology: SYY, JMB. Project administration: NYC, JMB. Resources: JMB, JHK, GHK. Supervision: JMB, GHK. Visualization: JAL, GHK. Writing—original draft: JAL, GHK. Writing—review & editing: JAL, GHK. Approval of final manuscript: all authors.

Conflicts of Interest

J.H.K., a contributing editor of the *Journal of Pathology and Translational Medicine*, was not involved in the editorial evaluation or decision to publish this article. All remaining authors have declared no conflicts of interest.

Funding Statement

This study was supported by grants from the National Research Foundation of Korea (NRF) funded by the Korea Government (MSIT) (No. 2021R1A2C1003542, RS-2023-00218623, and RS-2024-00450408).

REFERENCES

1. Sung H, Ferlay J, Siegel RL, et al. Global cancer statistics 2020: GLOBOCAN estimates of incidence and mortality worldwide for 36 cancers in 185 countries. *CA Cancer J Clin* 2021; 71: 209-49.
2. Cunningham D, Atkin W, Lenz HJ, et al. Colorectal cancer. *Lancet* 2010; 375: 1030-47.
3. Bockelman C, Engelmann BE, Kaprio T, Hansen TF, Glimelius B. Risk of recurrence in patients with colon cancer stage II and III: a systematic review and meta-analysis of recent literature. *Acta Oncol* 2015; 54: 5-16.
4. Andre T, Boni C, Mounedji-Boudiaf L, et al. Oxaliplatin, fluorouracil, and leucovorin as adjuvant treatment for colon cancer. *N Engl J Med* 2004; 350: 2343-51.
5. Twelves C, Wong A, Nowacki MP, et al. Capecitabine as adjuvant

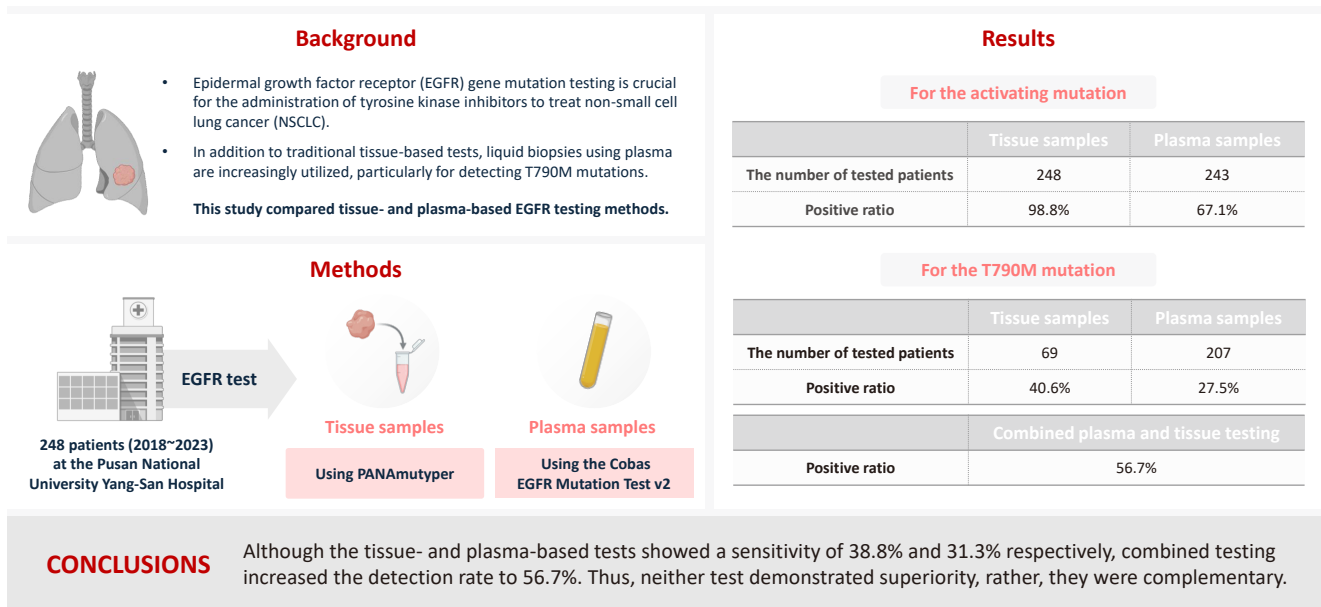
- treatment for stage III colon cancer. *N Engl J Med* 2005; 352: 2696-704.
6. Yothers G, O’Connell MJ, Allegra CJ, et al. Oxaliplatin as adjuvant therapy for colon cancer: updated results of NSABP C-07 trial, including survival and subset analyses. *J Clin Oncol* 2011; 29: 3768-74.
7. Schmoll HJ, Twelves C, Sun W, et al. Effect of adjuvant capecitabine or fluorouracil, with or without oxaliplatin, on survival outcomes in stage III colon cancer and the effect of oxaliplatin on post-relapse survival: a pooled analysis of individual patient data from four randomised controlled trials. *Lancet Oncol* 2014; 15: 1481-92.
8. Bae JM, Lee TH, Cho NY, Kim TY, Kang GH. Loss of CDX2 expression is associated with poor prognosis in colorectal cancer patients. *World J Gastroenterol* 2015; 21: 1457-67.
9. James R, Erler T, Kazenwadel J. Structure of the murine homeobox gene CDX-2: expression in embryonic and adult intestinal epithelium. *J Biol Chem* 1994; 269: 15229-37.
10. Li MK, Folpe AL. CDX-2, a new marker for adenocarcinoma of gastrointestinal origin. *Adv Anat Pathol* 2004; 11: 101-5.
11. Graule J, Uth K, Fischer E, et al. CDX2 in colorectal cancer is an independent prognostic factor and regulated by promoter methylation and histone deacetylation in tumors of the serrated pathway. *Clin Epigenetics* 2018; 10: 120.
12. Hansen TF, Kjaer-Frifeldt S, Eriksen AC, et al. Prognostic impact of CDX2 in stage II colon cancer: results from two nationwide cohorts. *Br J Cancer* 2018; 119: 1367-73.
13. Dalerba P, Sahoo D, Paik S, et al. CDX2 as a prognostic biomarker in stage II and stage III colon cancer. *N Engl J Med* 2016; 374: 211-22.
14. Zhang BY, Jones JC, Briggler AM, et al. Lack of caudal-type homeobox transcription factor 2 expression as a prognostic biomarker in metastatic colorectal cancer. *Clin Colorectal Cancer* 2017; 16: 124-8.
15. Baba Y, Noshio K, Shima K, et al. Relationship of CDX2 loss with molecular features and prognosis in colorectal cancer. *Clin Cancer Res* 2009; 15: 4665-73.
16. Konukiewitz B, Schmitt M, Silva M, et al. Loss of CDX2 in colorectal cancer is associated with histopathologic subtypes and microsatellite instability but is prognostically inferior to hematoxylin-eosin-based morphologic parameters from the WHO classification. *Br J Cancer* 2021; 125: 1632-46.
17. Bae JM, Kim JH, Kwak Y, et al. Distinct clinical outcomes of two CIMP-positive colorectal cancer subtypes based on a revised CIMP classification system. *Br J Cancer* 2017; 116: 1012-20.

18. Greenson JK, Huang SC, Herron C, et al. Pathologic predictors of microsatellite instability in colorectal cancer. *Am J Surg Pathol* 2009; 33: 126-33.
19. Jin HY, Yoo SY, Lee JA, et al. Combinatory statuses of tumor stromal percentage and tumor infiltrating lymphocytes as prognostic factors in stage III colorectal cancers. *J Gastroenterol Hepatol* 2022; 37: 551-7.
20. Lee JA, Seo MK, Yoo SY, et al. Comprehensive clinicopathologic, molecular, and immunologic characterization of colorectal carcinomas with loss of three intestinal markers, CDX2, SATB2, and KRT20. *Virchows Arch* 2022; 480: 543-55.
21. Yoo SY, Park HE, Kim JH, et al. Whole-slide image analysis reveals quantitative landscape of tumor-immune microenvironment in colorectal cancers. *Clin Cancer Res* 2020; 26: 870-81.
22. Weisenberger DJ, Siegmund KD, Campan M, et al. CpG island methylator phenotype underlies sporadic microsatellite instability and is tightly associated with BRAF mutation in colorectal cancer. *Nat Genet* 2006; 38: 787-93.
23. Ogino S, Cantor M, Kawasaki T, et al. CpG island methylator phenotype (CIMP) of colorectal cancer is best characterised by quantitative DNA methylation analysis and prospective cohort studies. *Gut* 2006; 55: 1000-6.
24. Derangere V, Lecuelle J, Lepage C, et al. Combination of CDX2 H-score quantitative analysis with CD3 AI-guided analysis identifies patients with a good prognosis only in stage III colon cancer. *Eur J Cancer* 2022; 172: 221-30.
25. Gooden MJ, de Bock GH, Leffers N, Daemen T, Nijman HW. The prognostic influence of tumour-infiltrating lymphocytes in cancer: a systematic review with meta-analysis. *Br J Cancer* 2011; 105: 93-103.
26. Nakano O, Sato M, Naito Y, et al. Proliferative activity of intratumoral CD8(+) T-lymphocytes as a prognostic factor in human renal cell carcinoma: clinicopathologic demonstration of antitumor immunity. *Cancer Res* 2001; 61: 5132-6.
27. Giraldo NA, Becht E, Pages F, et al. Orchestration and prognostic significance of immune checkpoints in the microenvironment of primary and metastatic renal cell cancer. *Clin Cancer Res* 2015; 21: 3031-40.
28. Blessin NC, Li W, Mandelkow T, et al. Prognostic role of proliferating CD8(+) cytotoxic T cells in human cancers. *Cell Oncol (Dordr)* 2021; 44: 793-803.

Comparison of tissue-based and plasma-based testing for EGFR mutation in non-small cell lung cancer patients

Yoon Kyung Kang¹, Dong Hoon Shin¹, Joon Young Park¹, Chung Su Hwang¹, Hyun Jung Lee¹, Jung Hee Lee¹, Jee Yeon Kim¹, JooYoung Na²

Graphical abstract



Comparison of tissue-based and plasma-based testing for *EGFR* mutation in non-small cell lung cancer patients

Yoon Kyung Kang¹, Dong Hoon Shin¹, Joon Young Park¹, Chung Su Hwang¹, Hyun Jung Lee¹, Jung Hee Lee¹, Jee Yeon Kim¹, JooYoung Na²

¹Department of Pathology, Pusan National University School of Medicine, Yangsan, Korea

²Department of Forensic Medicine, Pusan National University School of Medicine, Yangsan, Korea

Background: Epidermal growth factor receptor (*EGFR*) gene mutation testing is crucial for the administration of tyrosine kinase inhibitors to treat non-small cell lung cancer. In addition to traditional tissue-based tests, liquid biopsies using plasma are increasingly utilized, particularly for detecting T790M mutations. This study compared tissue- and plasma-based *EGFR* testing methods. **Methods:** A total of 248 patients were tested for *EGFR* mutations using tissue and plasma samples from 2018 to 2023 at Pusan National University Yangsan Hospital. Tissue tests were performed using PANAmutyper, and plasma tests were performed using the Cobas *EGFR* Mutation Test v2. **Results:** All 248 patients underwent tissue-based *EGFR* testing, and 245 (98.8%) showed positive results. Of the 408 plasma tests, 237 (58.1%) were positive. For the T790M mutation, tissue biopsies were performed 87 times in 69 patients, and 30 positive cases (38.6%) were detected. Plasma testing for the T790M mutation was conducted 333 times in 207 patients, yielding 62 positive results (18.6%). Of these, 57 (27.5%) were confirmed to have the mutation via plasma testing. Combined tissue and plasma tests for the T790M mutation were positive in nine patients (13.4%), while 17 (25.4%) were positive in tissue only and 12 (17.9%) in plasma only. This mutation was not detected in 28 patients (43.3%). **Conclusions:** Although the tissue- and plasma-based tests showed a sensitivity of 37.3% and 32.8%, respectively, combined testing increased the detection rate to 56.7%. Thus, neither test demonstrated superiority, rather, they were complementary.

Keywords: ErbB receptors; Lung cancer; Liquid biopsy

INTRODUCTION

Non-small cell lung cancer (NSCLC) is a major cause of cancer-related mortality globally [1,2]. However, the patients' prognosis and quality of life have significantly improved with the introduction of targeted therapies, including tyrosine kinase inhibitors (TKIs), which act against mutations in the epidermal growth factor receptor (*EGFR*). Despite their initial effectiveness, resistance to first- or second-generation TKIs often develops within months or years owing to various mechanisms, with the T790M mutation in the *EGFR* gene accounting for approximately 50% of these resistance cases [3,4]. To counter this, third-generation TKIs such as osimertinib have been developed

to target this specific mutation, making detection of the T790M mutation crucial for patients with NSCLC who have developed resistance to previous TKIs [3-9]. However, this detection can be challenging, especially in patients with small, hard-to-reach tumors, or when tissue biopsy is not an option.

Recent developments have underscored the potential of liquid biopsy as either an alternative or a supplementary approach to tissue biopsy for molecular diagnostics, including the detection of the T790M mutation in blood samples [5-9]. This method is particularly appealing because of its noninvasive nature, feasibility of repeated testing, fast turnaround time, and potential to reflect changes in tumor burden through serial monitoring. Unlike tissue biopsies, which only reveal mutations at the

Received: June 26, 2024 **Revised:** September 25, 2024 **Accepted:** September 30, 2024

Corresponding Author: Dong Hoon Shin, MD, PhD

Department of Pathology, Pusan National University School of Medicine, 49 Busandaehak-ro, Mulgeum-eup, Yangsan 50612, Korea

Tel: +82-55-360-1859, Fax: +82-55-360-1855, E-mail: donghshin@pusan.ac.kr

This is an Open Access article distributed under the terms of the Creative Commons Attribution Non-Commercial License (<https://creativecommons.org/licenses/by-nc/4.0/>) which permits unrestricted non-commercial use, distribution, and reproduction in any medium, provided the original work is properly cited.

© 2025 The Korean Society of Pathologists/The Korean Society for Cytopathology

sampling site, blood tests can detect all tumor DNA present in patient bloodstreams. Currently, the National Comprehensive Cancer Network guidelines recommend liquid biopsy as an alternative to tissue biopsy for initial T790M mutation testing [10]. The importance of accurately determining the sensitivity and specificity of liquid biopsies is paramount, given their broad applications. However, optimization of liquid biopsies is challenging, primarily because of the inability to directly quantify cell-free tumor DNA (ctDNA). This uncertainty in ctDNA levels complicates quality control compared with that of tissue biopsies [8,9]. In contrast, tissue biopsies allow pathologists to directly observe the number of tumor cells under a microscope, providing a clearer understanding of whether negative results stem from an insufficient amount of tumor DNA. Direct observation is not possible using liquid biopsies. Therefore, these differences may play a role in the diverse findings regarding the effectiveness of liquid biopsy for *EGFR* mutation detection, as reported in various studies [3-9].

In Korea, tissue-based tests are performed in the Department of Pathology, whereas blood-based tests are performed either in the Department of Pathology or the Department of Laboratory Medicine, depending on the institution [8,9,11]. However, this division may result in communication challenges between the two departments, potentially affecting the management of *EGFR* testing. The primary objective of our study was to evaluate the performance of tests performed independently in each department. Furthermore, we evaluated the effectiveness of *EGFR* assays conducted on both tissue and blood samples by examining a series of consecutive tests from each patient. This approach enabled us to ascertain the overall sensitivity and specificity on an individual basis, rather than limiting our evaluation to a per-test perspective. Consequently, our study also aimed to offer comprehensive insights into the detection of T790M mutations in both tissue and liquid biopsies. This was aimed at assisting clinicians in choosing the most appropriate testing approach for patients considering variables such as tumor burden and metastatic sites.

MATERIALS AND METHODS

Patients

Between 2018 and 2023, a total of 590 plasma *EGFR* mutation tests were conducted at Pusan National University Yangsan Hospital. Among these patients, those diagnosed with adenocarcinoma, squamous cell carcinoma, or NSCLC were selected.

Subsequently, only patients who also underwent an *EGFR* mutation test using tissue-based methods and tested positive for an *EGFR* mutation in either tissue or plasma at least once were included in the study. For analysis of T790M mutation, only the patient who received TKI treatment were considered. A comprehensive review of the longitudinal data of these patients was performed, including pathology reports with *EGFR* tests, the results of plasma *EGFR* tests, radiological imaging, and positron emission tomography scans.

Tissue *EGFR* test

The *EGFR* test in tissue was performed using the PANAMuytper, a peptide nucleic acid (PNA)-mediated, real-time polymerase chain reaction (PCR)-based assay. Mutant DNA was selectively amplified using wild-type DNA-specific PNA clamp probes, after which mutant-specific PNA detection probes were used to genotype the *EGFR* mutations using fluorescence melting curve analysis. This assay can detect and discriminate 47 types of *EGFR* mutations, including three G719X substitutions, 29 exon 19 deletions (Exon19del), one T790M substitution, one S768I substitution, 10 exon 20 insertions (Exon20ins), two L858R substitutions, and one L861Q substitution, with a high level of sensitivity [12].

Plasma *EGFR* test

Venous blood samples were collected from patients using 21G needles in a 10-mL Cell-Free DNA BCT tube (Streck, Omaha, NE, USA) per patient. For the 1-step centrifugation group, within 4 hours of room-temperature blood collection, blood samples were centrifuged at 1,600 ×g for 10 minutes, and 2 mL was dispensed into each Eppendorf tube. *EGFR* mutations were identified using the Cobas *EGFR* Mutation Test v2 on a Cobas z 480 analyzer (Roche Diagnostics, Pleasanton, CA, USA), according to the manufacturer's instructions [11]. This assay was designed to detect insertions and deletions in *EGFR*, such as deletions in exon 19 and insertions in exon 20, as well as nucleic acid substitutions, such as G719X, S768I, T790M, L858R, and L861Q.

Statistical analyses

Python software ver. 3.7.6 was used to perform all computation and analyses in this study. The Pandas library was used to perform basic statistical analysis of the data. All statistical tests were two-sided, and $p < .05$ was considered significant unless otherwise specified.

RESULTS

Clinical characteristics of patients

A total of 248 patients were enrolled for this analysis (106 males and 142 females) (Table 1). The average age at diagnosis was 67 years (range, 40 to 86 years). The pathological diagnoses included 238 cases of adenocarcinoma, eight of squamous cell carcinoma, and two of adenosquamous carcinoma. The distribution of patients according to stage was as follows: stage I, 16; stage II, 10; stage III, 39; and stage IV, 183. The most common sites of metastasis upon recurrence or progression were the lungs (136 patients), followed by the brain (n = 74), bone (n = 52), pleura (n = 31), lymph nodes (n = 19), liver (n = 15), and other organs (n = 10).

Activating EGFR mutation

All 248 enrolled patients underwent EGFR testing using tissue samples, including biopsy or resection, at the time of diagnosis or during the follow-up period. The results identified 245 (98.8%) positive and three (1.2%) negative cases (Table 2). For plasma EGFR testing, 408 tests were conducted across these patients, with 58 at the time of diagnosis and 350 following the initial diagnosis, showing 237 positive results (58.1%) and 171 negative results (41.9%). Of the patients tested, 163 (67.1%) tested positive and 80 (32.6%) tested negative in the plasma tests (Table 2). When both tissue- and plasma-based tests yielded positive results, they were consistent with exon 19 deletion, L858R, exon 20 insertion, and L861Q mutations. However,

Table 1. Characteristics of patients

Parameter	Value
Age (yr)	67 (40–86)
Sex	
Male	106 (42.7)
Female	142 (57.3)
Pathologic diagnosis	
Adenocarcinoma	238 (96.0)
Squamous cell carcinoma	8 (3.2)
Adenosquamous carcinoma	2 (0.8)
Stage	
I	16 (6.5)
II	10 (4.0)
III	39 (15.7)
IV	183 (73.8)

Values are presented as mean (range) or number (%). SCC, squamous cell carcinoma.

discrepancies were observed in compound mutations. In these instances, tissue tests identifying exon 19 deletion/L861Q, L861Q/G719S, G719S/S768, and L858R/T790M mutations were detected as exon 19 deletion, L861Q, G719S/L861Q, and L858R mutations, respectively, in the plasma-based tests. The tissue-based tests did not detect activating mutations in four of the samples. In one sample, the tumor cell count ranged from 200 to 500, while the other three samples had tumor cell counts exceeding 1,000. A repeated tissue biopsy conducted after 18 months in one case revealed an exon 19 deletion mutation. Additionally, three other cases were found to have mutations in plasma-based tests: one with an exon 19 deletion and the others with the L858R mutation.

T790M mutation

Of the 248 enrolled patients, 210 received TKI treatment. Among these, 69 underwent a tissue biopsy, 207 had a plasma test to detect the T790M mutation, and 66 underwent both tests. Tissue biopsies were performed 87 times in 69 patients to detect the T790M mutation, which resulted in 30 (34.1%) positive results. Of the 69 patients, 28 (40.6%) harbored the T790M mutation. Plasma tests for the T790M mutation were

Table 2. EGFR mutations detected in tissue and plasma

	Tissue	Plasma
Activating mutation		
Exon 19 deletion	139 (56.0)	102 (41.1)
L858R	87 (35.1)	53 (21.4)
L861Q	4 (1.6)	5 (2.0)
S768I	1 (0.4)	0
G719C	1 (0.4)	0
T790M	1 (0.4)	0
Exon 20 insertion	4 (1.6)	1 (0.4)
G719X/L861Q	3 (1.2)	1 (0.4)
19del/L861Q	2 (0.8)	0
L858R/ T790M	1 (0.4)	0
S768I/G719S	1 (0.4)	0
L858R/S768I	1 (0.4)	1 (0.4)
Negative	3 (1.2)	85 (34.3)
Total	248	248
Resistance mutation		
T790M	28 (40.6)	57 (27.5)
Negative	41 (59.4)	150 (72.5)
Total	69	207

Values are presented as number (%). EGFR, epidermal growth factor receptor.

conducted 333 times in 207 patients, with 62 positive results (18.6%). Of 271 negative test results, activating *EGFR* mutations were not detected in 148 patients. Among the 207 patients, 57 (27.5%) were confirmed to harbor the T790M mutation by plasma testing. Of these, 42 (20.3%) tested positive in the first plasma test, 10 out of 83 patients (12%) tested positive in the second test, and five out of 33 patients (15.2%) tested positive in the third test. Regarding tissue biopsies, 53 patients underwent the procedure once, 14 patients underwent it twice, and two patients underwent it thrice. For plasma tests during the treatment course, 124 patients were tested once, 50 patients twice, 24 patients thrice, eight patients four times, and one patient five times.

Sixty-six patients underwent both tissue- and plasma-based *EGFR* testing for T790M mutation (Table 3, Fig. 1). In nine (13.4%) of these patients, the T790M mutation was detected in both tests. The mutation was identified exclusively in the tissue samples of 17 patients (25.4%) and in the plasma samples of 12 patients (17.9%). In 28 patients (43.3%), neither test detected the T790M mutation. These cases are illustrated in Fig. 1.

Correlation of *EGFR* mutation detection with clinical parameters

In patients who underwent plasma *EGFR* testing at the time of histological diagnosis, a positive plasma test result for activating mutations was associated with the presence of nodal or distant metastases (Table 4). Conversely, the detection of the T790M mutation in the plasma did not exhibit a correlation with either nodal status or distant metastasis (Table 4).

DISCUSSION

Liquid biopsy is an emerging and highly valuable tool for detecting actionable mutations. Numerous studies have demonstrated its utility and yielded promising results [13-17]. One

of the most widely used liquid biopsy methods is the plasma-based *EGFR* test for patients with lung cancer, particularly to guide TKI treatment decisions. Therefore, evaluating the efficacy of this test is of paramount importance as it directly influences treatment choices. Although several studies have demonstrated that the plasma-based *EGFR* test is comparable to the tissue-based test, the reported detection rates of the T790M mutation in these studies vary, ranging from 19.2% to 47.1% [13-16]. In this comprehensive study, data from 248 patients who underwent both tissue- and plasma-based *EGFR* tests to detect *EGFR* mutations were analyzed. To identify T790M mutations, 333 plasma tests were performed on 207 patients treated with TKI, yielding positive results in 62 tests (18.6%) and confirming the T790M mutation in 57 patients (27.4%). Conversely, tissue-based tests were performed 87 times in 69 patients, resulting in 30 positive tests (34.1%), indicating the presence of the T790M mutation in 28 patients (38.6%). In 66 patients subjected to both tissue- and plasma-based *EGFR* tests, tissue-based tests demonstrated a marginally higher sensitivity, yielding positive results in 26 patients (38.8%) compared with 21 patients (31.3%) for plasma-based tests. Nevertheless, the sensitivity of both methods was relatively low considering the estimated prevalence of the T790M mutation in 50% of TKI resistance cases [3-6]. Interestingly, when the results from both tests were combined, the positive rate increased to 38 patients (56.7%), exceeding the expected prevalence of 50%. These findings suggest that tissue- and plasma-based tests complement each other.

In our study, 408 plasma assays were conducted to detect *EGFR*-activating mutations in a cohort of 248 patients with confirmed mutations. Of these, only 237 (58.1%) were positive. Remarkably, 85 of the 248 patients tested negative for these mutations in the plasma, despite the ability of plasma testing to facilitate repeated measurements. Furthermore, an examination of the 272 assays that were negative for the T790M muta-

Table 3. Patients who underwent both tissue- and plasma-based tests

	Activating <i>EGFR</i> mutation			T790M mutation		
	Tissue		p-value	Tissue		p-value
	Positive	Negative		Positive	Negative	
Plasma						
Positive	159 (65.4)	4 (1.6)	.371	9 (13.4)	12 (17.9)	.898
Negative	85 (31.6)	0		17 (25.4)	28 (43.3)	

Values are presented as number (%).
EGFR, epidermal growth factor receptor.

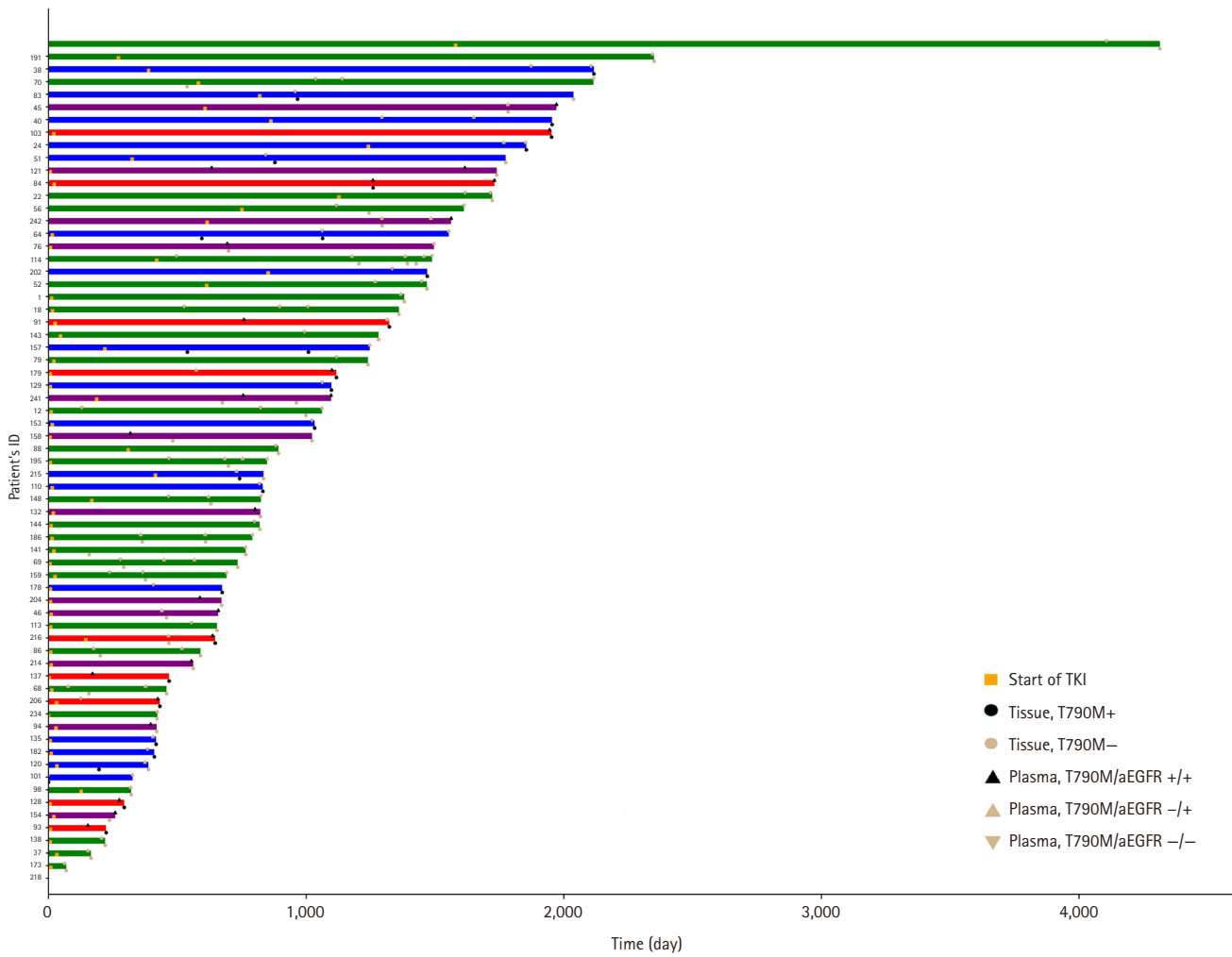


Fig. 1. Swimmer plot for test time points for enrolled patients. TKI, tyrosine kinase inhibitor; EGFR, epidermal growth factor receptor.

Table 4. Relationship between stage categories and plasma-based EGFR test results in patients

	Activating mutation		p-value	T790M		p-value
	Positive	Negative		Positive	Negative	
T category						
T1, T2	71	50	.052	27	75	.901
T3, T4	88	35		29	74	
N category						
N0	34	34	.013	42	111	.992
N1–N3	124	50		14	37	
M category						
M0	30	35	.012	13	45	.299
M1	133	50		44	5	

EGFR, epidermal growth factor receptor.

tion indicated that 148 (54.4%) failed to detect the activating mutation, suggesting that over half of the tests that failed to detect the activating *EGFR* mutation may not reliably indicate a true-negative result for the T790M mutation. Considering that there were no instances in which the T790M mutation was detected without the concurrent detection of the activating mutation, the presence of the activating mutation was a reliable indicator of ctDNA levels. Our findings suggest that ctDNA levels frequently fall below the detection threshold of the assay, indicating that liquid biopsies for other genes may also face similar challenges and thus require high sensitivity for effective clinical application.

The prevalent understanding is that significant tumor mass is crucial for the abundant presence of ctDNA in the bloodstream. Our study showed that higher N and M statuses at initial diagnosis were associated with the detection of activating *EGFR* mutations in the plasma, with a notably stronger correlation observed for M status. This relationship continues even after the initiation of TKI therapy, where the original M status significantly predicts the presence of activating mutations, suggesting that an increased tumor burden may lead to higher ctDNA levels. However, no significant link was found between T790M mutation detection and T, N, and M statuses. To explore the factors influencing the detection of the T790M mutation, we analyzed the organs that were predominantly affected as the cancer progressed. Our data showed that the lungs were the most affected organs, followed by the brain, bones, pleura, lymph nodes, liver, and other organs. Moreover, there was no association between the presence of the T790M mutation and specific organs affected by metastasis or the overall number of involved organs. While TNM status and the number of affected organs might reflect the patient tumor load, which is expected to correlate with ctDNA levels, the absence of a connection with the T790M mutation indicates a potential need for more sensitive detection techniques, such as digital droplet PCR or next-generation sequencing (NGS), or that factors other than tumor load might affect the detectability of the mutation in plasma. Regarding tissue-based T790M testing, among the 30 positive cases, 22 originated from the lungs or bronchi. In contrast, of the 60 negative cases, 33 samples were collected from these locations, suggesting that the biopsy site did not significantly affect the test results.

The primary advantage of plasma-based testing is its noninvasive nature, which allows for repeated testing and increases the likelihood of a positive result. In our investigation, initial

plasma screening revealed the T790M mutation in 42 of 207 patients, yielding a positivity rate of 20.2%. A subsequent plasma test of 83 patients identified 10 more individuals (12.0%) harboring this mutation. In the third round of testing involving 33 patients, the mutation was found in five individuals, resulting in a positivity rate of 15.2%. In contrast, the first round of tissue-based testing demonstrated a considerably higher positivity rate, with 25 of the 69 patients (35.7%) testing positive for the T790M mutation. However, a follow-up tissue-based assessment of 18 patients showed a reduced positivity rate of 11.1%, with just two patients testing positive. This trend suggests a decrease in positivity rates for both plasma- and tissue-based tests in subsequent rounds compared with initial testing. Owing to the noninvasive nature of plasma-based testing, it is recommended to start with this method for detecting the T790M mutation. If the initial plasma test result is negative, a tissue-based test should be considered owing to its higher success rate. In contrast to the ease of plasma testing, tissue biopsies offer additional advantages, including the ability to identify resistance mechanisms beyond the T790M mutation, such as histological transformation. The transition to small cell carcinoma is a well-established example of such a transformation.

Although a limitation of this study was that tissue- and plasma-based tests were performed on different platforms, previous studies have shown that both platforms have similar overall performance in terms of *EGFR* mutation detection [18]. In conclusion, this study suggests that both methods are complementary for detecting the T790M mutation, as neither method was completely satisfactory. Plasma-based tests frequently fail to detect activating mutations; therefore, clinicians should be aware of this drawback and perform tissue biopsy in such cases. Currently, the selection of test modalities, timing, and biopsy sites depends solely on the judgment of the clinician, with a lack of available tools to predict the outcome of these decisions. Recent advancements in highly sensitive techniques, including NGS and digital droplet PCR, have the potential to enhance the success rates of detecting T790M mutations in both tissue- and plasma-based tests.

Ethics Statement

This study was approved by the Institutional Review Board (IRB) of Pusan National University Yangsan Hospital (No. 2024-0021). The requirement for informed consent was waived by the IRB.

Availability of Data and Material

All data generated or analyzed during the study are included in this published article.

Code Availability

Not applicable.

ORCID

Yoon Kyung Kang	https://orcid.org/0009-0002-1746-6467
Dong Hoon Shin	https://orcid.org/0000-0002-4980-9295
Joon Young Park	https://orcid.org/0000-0002-4193-2520
Chung Su Hwang	https://orcid.org/0000-0001-9520-0301
Hyun Jung Lee	https://orcid.org/0000-0002-2995-6060
Jung Hee Lee	https://orcid.org/0000-0003-3003-2217
Jee Yeon Kim	https://orcid.org/0000-0002-0503-984X
JooYoung Na	https://orcid.org/0000-0003-1138-433X

Author Contributions

Conceptualization: DHS. Data curation: YKK. Formal analysis: YKK, JYP, CSH. Funding acquisition: DHS. Supervision: DHS. Writing—original draft: YKK, HJL. Writing—review & editing: JHL, JYK, JN, DHS. Approval of the final manuscript: all authors.

Conflicts of Interest

The authors declare that they have no potential conflicts of interest.

Funding Statement

This work was supported by a 2-year research grant of Pusan National University.

REFERENCES

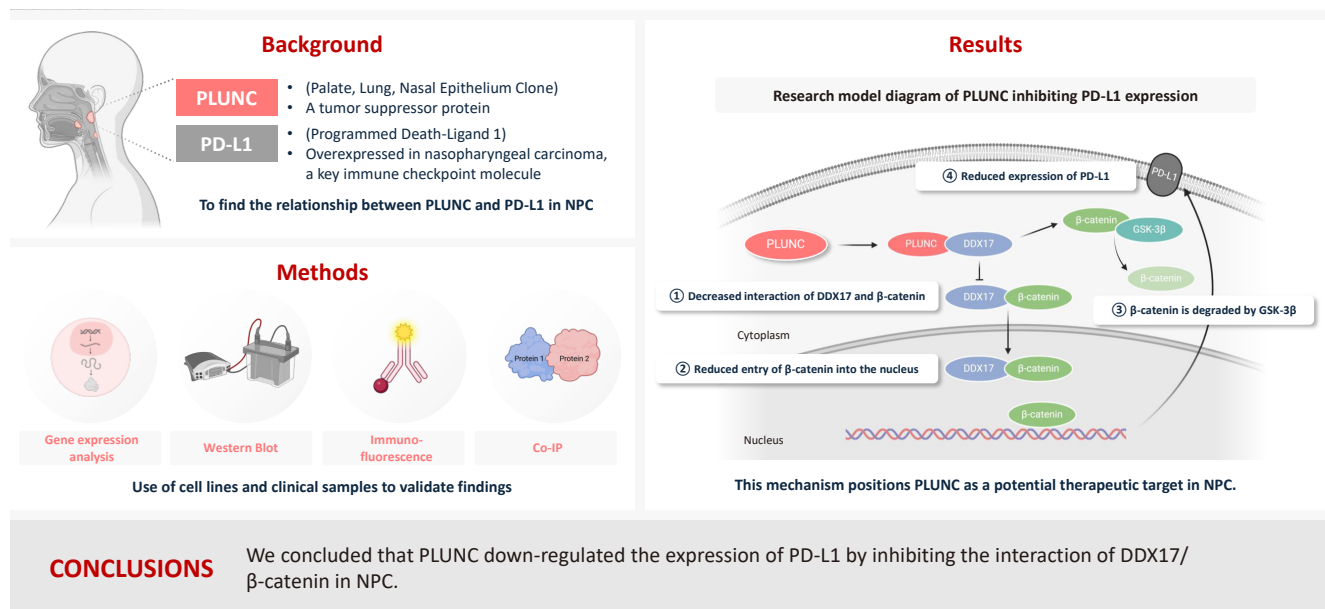
1. Wang M, Herbst RS, Boshoff C. Toward personalized treatment approaches for non-small-cell lung cancer. *Nat Med* 2021; 27: 1345-56.
2. Howlader N, Forjaz G, Mooradian MJ, et al. The effect of advances in lung-cancer treatment on population mortality. *N Engl J Med* 2020; 383: 640-9.
3. Wu YL, Tsuboi M, He J, et al. Osimertinib in resected *EGFR*-mutated non-small-cell lung cancer. *N Engl J Med* 2020; 383: 1711-23.
4. Vaclova T, Grazini U, Ward L, et al. Clinical impact of subclonal *EGFR* T790M mutations in advanced-stage *EGFR*-mutant non-small-cell lung cancers. *Nat Commun* 2021; 12: 1780.
5. Jenkins S, Yang JC, Ramalingam SS, et al. Plasma ctDNA analysis for detection of the *EGFR* T790M mutation in patients with advanced non-small cell lung cancer. *J Thorac Oncol* 2017; 12: 1061-70.
6. Naka G, Yokoyama T, Usui K, et al. Final report on plasma ctDNA T790M monitoring during *EGFR*-TKI treatment in patients with *EGFR* mutant non-small cell lung cancer (JP-CLEAR trial). *Jpn J Clin Oncol* 2022; 52: 791-4.
7. Rolfo C, Mack P, Scagliotti GV, et al. Liquid biopsy for advanced NSCLC: a consensus statement from the International Association for the Study of Lung Cancer. *J Thorac Oncol* 2021; 16: 1647-62.
8. Shin DH, Shim HS, Kim TJ, et al. Provisional guideline recommendation for *EGFR* gene mutation testing in liquid samples of lung cancer patients: a proposal by the Korean Cardiopulmonary Pathology Study Group. *J Pathol Transl Med* 2019; 53: 153-8.
9. Chang S, Hur JY, Choi YL, Lee CH, Kim WS. Current status and future perspectives of liquid biopsy in non-small cell lung cancer. *J Pathol Transl Med* 2020; 54: 204-12.
10. Ettinger DS, Wood DE, Aisner DL, et al. Non-small cell lung cancer, version 3.2022, NCCN Clinical Practice Guidelines in Oncology. *J Natl Compr Canc Netw* 2022; 20: 497-530.
11. Shin KH, Lee SM, Park K, et al. Effects of different centrifugation protocols on the detection of *EGFR* mutations in plasma cell-free DNA. *Am J Clin Pathol* 2022; 158: 206-11.
12. Lee J, Han YB, Kwon HJ, Lee SK, Kim H, Chung JH. Landscape of *EGFR* mutations in lung adenocarcinoma: a single institute experience with comparison of PANAMutyper testing and targeted next-generation sequencing. *J Pathol Transl Med* 2022; 56: 249-59.
13. Jung HA, Ku BM, Kim YJ, et al. Longitudinal monitoring of circulating tumor DNA from plasma in patients with curative resected stages I to IIIA *EGFR*-mutant non-small cell lung cancer. *J Thorac Oncol* 2023; 18: 1199-208.
14. Karlovich C, Goldman JW, Sun JM, et al. Assessment of *EGFR* mutation status in matched plasma and tumor tissue of NSCLC patients from a phase I study of rociletinib (CO-1686). *Clin Cancer Res* 2016; 22: 2386-95.
15. Mack PC, Miao J, Redman MW, et al. Circulating tumor DNA kinetics predict progression-free and overall survival in *EGFR* TKI-treated patients with *EGFR*-mutant NSCLC (SWOG S1403). *Clin Cancer Res* 2022; 28: 3752-60.
16. Kok PS, Lee K, Lord S, et al. Clinical utility of plasma *EGFR* mutation detection with quantitative PCR in advanced lung cancer: a

- meta-analysis. *Lung Cancer* 2021; 154: 113-7.
17. Minari R, Mazzaschi G, Bordi P, et al. Detection of *EGFR*-activating and T790M mutations using liquid biopsy in patients with *EGFR*-mutated non-small-cell lung cancer whose disease has progressed during treatment with first- and second-generation tyrosine kinase inhibitors: a multicenter real-life retrospective study. *Clin Lung Cancer* 2020; 21: e464-73.
 18. Han AL, Kim HR, Choi KH, et al. Comparison of cobas *EGFR* Mutation Test v2 and PANAMutyper-R-*EGFR* for detection and semi-quantification of epidermal growth factor receptor mutations in plasma and pleural effusion supernatant. *Ann Lab Med* 2019; 39: 478-87.

PLUNC downregulates the expression of PD-L1 by inhibiting the interaction of DDX17/ β -catenin in nasopharyngeal carcinoma

Ranran Feng^{1,2*}, Yilin Guo^{1,3*}, Meilin Chen^{4*}, Ziyang Tian^{1,5}, Yijun Liu^{1,5}, Su Jiang^{1,5}, Jieyu Zhou^{1,5}, Qingluan Liu^{1,5}, Xiayu Li⁶, Wei Xiong^{7,8}, Lei Shi⁹, Songqing Fan⁹, Guiyuan Li^{7,8}, Wenling Zhang^{1,5}

Graphical abstract



PLUNC downregulates the expression of PD-L1 by inhibiting the interaction of DDX17/ β -catenin in nasopharyngeal carcinoma

Ranran Feng^{1,2*}, Yilin Guo^{1,3*}, Meilin Chen^{4*}, Ziyang Tian^{1,5}, Yijun Liu^{1,5}, Su Jiang^{1,5}, Jieyu Zhou^{1,5}, Qingluan Liu^{1,5}, Xiayu Li⁶, Wei Xiong^{7,8}, Lei Shi⁹, Songqing Fan⁹, Guiyuan Li^{7,8}, Wenling Zhang^{1,5}

¹Department of Laboratory Medicine, The Third Xiangya Hospital, Central South University, Changsha, China

²Department of Laboratory Medicine, Reproductive and Genetic Hospital of CITIC-Xiangya, Changsha, China

³Department of Blood Transfusion, Children's Hospital Affiliated to Zhengzhou University, Henan Children's Hospital, Zhengzhou Children's Hospital, Zhengzhou, China

⁴The First Affiliated Hospital of Sun Yatsen University, Guangzhou, China

⁵Department of Medical Laboratory Science, Xiangya School of Medicine, Central South University, Changsha, China

⁶Hunan Key Laboratory of Nonresolving Inflammation and Cancer, Disease Genome Research Center, The Third Xiangya Hospital, Central South University, Changsha, China

⁷NHC Key Laboratory of Carcinogenesis, Hunan Cancer Hospital and the Affiliated Cancer Hospital of Xiangya School of Medicine, Central South University, Changsha, China

⁸The Key Laboratory of Carcinogenesis and Cancer Invasion of the Chinese Ministry of Education, Cancer Research Institute and School of Basic Medicine Sciences, Central South University, Changsha, China

⁹Department of Pathology, Second Xiangya Hospital, Central South University, Changsha, China

Background: Nasopharyngeal carcinoma (NPC) is characterized by high programmed death-ligand 1 (PD-L1) expression and abundant infiltration of non-malignant lymphocytes, which renders patients potentially suitable candidates for immune checkpoint blockade therapies. Palate, lung, and nasal epithelium clone (PLUNC) inhibit the growth of NPC cells and enhance cellular apoptosis and differentiation. Currently, the relationship between PLUNC (as a tumor-suppressor) and PD-L1 in NPC is unclear. **Methods:** We collected clinical samples of NPC to verify the relationship between PLUNC and PD-L1. PLUNC plasmid was transfected into NPC cells, and the variation of PD-L1 was verified by western blot and immunofluorescence. In NPC cells, we verified the relationship of PD-L1, activating transcription factor 3 (ATF3), and β -catenin by western blot and immunofluorescence. Later, we further verified that PLUNC regulates PD-L1 through β -catenin. Finally, the effect of PLUNC on β -catenin was verified by co-immunoprecipitation (Co-IP). **Results:** We found that PLUNC expression was lower in NPC tissues than in paracancer tissues. PD-L1 expression was opposite to that of PLUNC. Western blot and immunofluorescence showed that β -catenin could upregulate ATF3 and PD-L1, while PLUNC could downregulate ATF3/PD-L1 by inhibiting the expression of β -catenin. PLUNC inhibits the entry of β -catenin into the nucleus. Co-IP experiments demonstrated that PLUNC inhibited the interaction of DEAD-box helicase 17 (DDX17) and β -catenin. **Conclusions:** PLUNC downregulates the expression of PD-L1 by inhibiting the interaction of DDX17/ β -catenin in NPC.

Keywords: BPIFA1 protein; DEAD-box RNA helicases 17; Programmed cell death 1 ligand 1

INTRODUCTION

The 2020 Global Cancer Statistics report showed that there

were more than 133,000 new cases of nasopharyngeal cancer (NPC) worldwide [1]. NPC occurs mainly in East and South Asia. NPC is sensitive to radiotherapy, so radiotherapy is the

Received: June 13, 2024; **Revised:** October 31, 2024; **Accepted:** November 27, 2024

Corresponding Author: Wenling Zhang, MD

Department of Laboratory Medicine, The Third Xiangya Hospital, Central South University, 138 Tongzipo Road, Yuelu District Changsha, Hunan 410013, China
Tel, Fax: +86-0731-82650348, E-mail: zhangwenling73@126.com

*Ranran Feng, Yilin Guo, and Meilin Chen contributed equally to this work.

This is an Open Access article distributed under the terms of the Creative Commons Attribution Non-Commercial License (<https://creativecommons.org/licenses/by-nc/4.0/>) which permits unrestricted non-commercial use, distribution, and reproduction in any medium, provided the original work is properly cited.

© 2025 The Korean Society of Pathologists/The Korean Society for Cytopathology

preferred treatment. Radiotherapy plus adjuvant chemotherapy is the standard treatment for advanced NPC. However, 20%–30% of NPC patients will experience recurrence, with most recurrences occurring within the first 2 years after treatment [2]. Because of its unique immune environment, NPC is considered a highly immune-inflamed tumor. Massive lymphocytic infiltrations, high programmed death-ligand 1 (PD-L1) expression, and several key immune molecules that regulate the activation of T-cells (CD40, CD70, CD80, and CD86) are often observed in Epstein-Barr virus (EBV)-induced NPC [3]. Since NPC is characterized by high PD-L1 expression and significant non-malignant lymphocyte infiltration, patients may be suitable for immune checkpoint-blocking therapies [4]. Fortunately, anti-programmed death-1 (PD-1)/PD-L1 treatment has made certain progress in metastatic or recurrent metastatic NPC as a promising method to prolong the survival rate of patients [5]. Therefore, understanding the regulatory mechanism of PD-L1 is of great significance for the immunotherapy of NPC.

Palatal, lung, and nasal epithelial clone (PLUNC) protein is encoded by a 300-KB gene segment on chromosome 20, which is specifically expressed in the upper airway and nasopharyngeal regions and is involved in host defense [6,7]. PLUNC contributes to the overall surface tension of airway epithelial secretions, and this activity may interfere with the formation of biofilms in airway pathogens [8,9]. In innate immune defense, the PLUNC protein is involved in antimicrobial activity and can directly kill *Escherichia coli* and *Acinetobacter haemolyticus* through cell wall permeability [10]. In patients with chronic sinusitis, reduced levels of PLUNC expression are associated with repeated sinus surgery and the amount of bacterial colonization [11]. In acute pulmonary exacerbations (AEs), PLUNC expression decreases sharply as inflammation increases. In stable patients, lower PLUNC expression correlates with an increased AE risk. Thus, the downregulation of PLUNC could predict AE at the early stages [12]. However, in gastric hepatoid adenocarcinoma, PLUNC expression may be an important factor that can indicate the tumor's malignant potential, as positive cases show vascular invasion and lymph node metastasis [13].

A previous study suggested that PLUNC was downregulated in NPC and related to the poor prognosis of NPC patients [14]. PLUNC can inhibit the tumor inflammatory microenvironment by regulating the Toll-like receptor 9/nuclear factor κ B signaling pathway, thereby reducing the inflammatory response of EBV-induced NPC cells [15]. PLUNC may be a tumor-suppressor gene in NPC; in previous research, it inhibited the

growth of NPC cells and promoted cellular apoptosis and differentiation [16,17]. Our results revealed that PD-L1 is highly expressed in nasopharyngeal carcinoma. However, the relationship between PLUNC and PD-L1 in NPC is unclear.

Wnt/ β -catenin signaling plays a crucial role in cancer. Abnormal Wnt/ β -catenin signaling had been found to be closely related to the occurrence, development, and malignant transformation of cancer [18]. β -catenin is highly expressed in NPC tissues, and its positive expression negatively correlates with the survival rate of NPC patients [19]. It had been reported that β -catenin promotes the proliferation and metastasis of NPC cells [20,21]. However, it is still unclear whether β -catenin regulates PD-L1 in NPC.

In our study, we found a negative correlation between PLUNC and PD-L1 expression in NPC, and PLUNC suppressed PD-L1 expression by downregulating β -catenin. Mechanically, PLUNC downregulated PD-L1 expression by inhibiting DEAD-box helicase 17 (DDX17)/ β -catenin interaction. In summary, our research will provide new ideas for immune checkpoint blockade therapy in NPC.

MATERIALS AND METHODS

Bioinformatic analysis

We conducted gene expression differential analysis using a t test based on data from head and neck cancer cases in the GEP-IA public database (<http://gepia.cancer-pku.cn/detail.php>). In addition, the differences in EBV infection between high- and low-expression groups of the PLUNC gene in the GSE102349 dataset from the Gene Expression Omnibus (GEO) database (<https://www.ncbi.nlm.nih.gov/geo/GEO>) were compared using the t test, and the correlation between EBV infection and PLUNC gene expression was analyzed using Pearson's correlation analysis.

Cell culture

NPC cell lines (5-8F, HNE2, S18, and HONE1) and the 293T cell line come from the Cancer Research Institute of Central South University. 5-8F, HNE2, S18, and HONE1 were used for the study of protein expression, localization, and signal transduction in nasopharyngeal carcinoma cells. 293T cells are the most commonly used cells in the study of protein interactions in articles. These cells were maintained at 37°C and 5% CO₂ in Dulbecco's modified Eagle medium supplemented with 10% fetal bovine serum (Biological Industries, Kibbutz Beit-Haemek,

Israel), 100 U/mL of penicillin, and 100 µg/mL of streptomycin (GE Healthcare, Waukesha, WI, USA).

Cell transfection

Transfection plasmids (including PLUNC overexpression), PLUNC control vectors, PLUNC/ β -catenin/activating transcription factor 3 (ATF3) small hairpin RNAs (shRNAs), and their negative controls were purchased from Shanghai Genechem (Shanghai, China). DDX17/ β -catenin/ATF3 lentiviral expression vectors were constructed by inserting expanded DDX17/ β -catenin/ATF3 cDNA fragments into a lentiviral shuttle vector. The cells were seeded into six-well plates, and, upon reaching 80% confluence, recombinant plasmids were transfected using Lipofectamine 2000 (Thermo Fisher Scientific, Waltham, MA, USA), following the manufacturer's protocol. The indicated cells infected with the recombinant lentiviral vectors were selected with puromycin or G418 for 2 weeks.

Co-immunoprecipitation assay

Cell lysis ice immunoprecipitation lysis buffer was supplemented with protease and phosphatase inhibitors for 15 minutes. Add immunoprecipitation lysis buffer containing protease inhibitors and phosphatase inhibitors to the cells and lyse on ice for 15 minutes. After cell lysis, centrifuge at 16,000 \times g for 10 minutes at 4°C and incubate the supernatant with antibodies. Following incubation, the cells were added into pre-washed agarose beads, coupled with protein G or protein A, and incubated at 4°C for 3 hours. The immune complex was purified on the magnet by extensive washing of the lysis buffer. The chemiluminescence signals were collected by a BIO-RAD Gel imaging analysis system scanner (Bio-Rad Laboratories, Hercules, CA, USA).

Western blot analysis

Cells were lysed with RIPA lysis buffer, and the protein concentration was measured using a bicinchoninic acid protein assay kit (KeyGen Biotech, Nanjing, China). Protein samples (30 µg/well) were loaded onto 10% sodium dodecyl sulfate–polyacrylamide gel electrophoresis and then transferred onto polyvinylidene difluoride membranes. After blocking with skim milk, membranes were incubated in primary antibodies at 4°C overnight and then in horseradish peroxidase–conjugated secondary antibodies for 1 hour at 37°C. Primary antibodies used for experiments included anti-PLUNC (ab131163, Abcam, Cambridge, UK), glyceraldehyde 3-phosphate dehydrogenase

(Abcam), anti- β -catenin, T-cell factor 4 (TCF4) (Cell Signaling Technology, Danvers, MA, USA), DDX17 (sc398168, Santa Cruz Biotechnology, Dallas, TX, USA), PD-L1 (28076-1-AP, Proteintech, Rosemont, IL, USA), ATF3 (ab254268, Abcam), glycogen synthase kinase 3 β (GSK-3 β ; 67329-1-Ig, Proteintech), and p-GSK-3 β (67558-1-Ig, Proteintech). Protein bands were imaged and captured using ECL reagent (Biosharp, Hefei City, China).

Immunofluorescence staining

Cells were seeded on coverslips, fixed with 4% paraformaldehyde, and then permeabilized with 0.2% Triton X-100. After blocking with 5% bovine serum albumin, the cells were incubated with a primary antibody (anti-ATF3 [Abcam]; anti-Plunc, anti- β -catenin, and anti-PD-L1 [Proteintech]; and anti-DDX17 [Santa Cruz Biotechnology]) overnight at 4°C, which was followed by incubation with an Alexa Fluor 488- or Alexa Fluor 594-conjugated secondary antibody (Abcam). DAPI was used to stain cell nuclei. Immunofluorescence images were captured with a fluorescence microscope (Olympus Corp., Tokyo, Japan).

Clinical NPC samples and immunohistochemistry

NPC samples and paired paracancer tissues were collected from 30 NPC patients at the Second Xiangya Hospital of Central South University (Changsha, China). The study was approved by the Joint Ethics Committee of the Central South University Health Authority, and informed consent was obtained from each participant.

For immunohistochemistry, tissue sections of formalin-fixed and paraffin-embedded NPC tissues were incubated with anti-PLUNC (10413-1-AP, Proteintech), β -catenin (51067-2-AP, Proteintech), PD-L1 (28076-1-AP, Proteintech), DDX17 (sc398168, Santa Cruz Biotechnology) or control IgG1 (1 µg/mL). After washing with phosphate buffered saline, the slides were reacted with the Prolink-2 Plus horseradish peroxidase rabbit polymer detection kit (Golden Bridge International, Bothell, WA, USA), and the images were scanned using Aperio ScanScope CS software (Aperio Technologies, Vista, CA, USA). Two independent pathologists evaluated and scored the slides based on the intensity and extent of staining (double-blinded). A staining index (values, 0–9) was obtained from the intensity of the positive staining (negative = 0 points, weak = 1 points, moderate = 2 points, strong = 3 points), and the proportion of positive cells of interest (<25% = 1 point, 25%–50% = 2 points, \geq 50% = 3 points) was calculated. The final results were then

designated and rescored as follows: 0 points = negative, 1–3 points = weak positive (1 point), 4–6 points = moderately positive (2 points), or 7–9 points = strongly positive (3 points). All sections were scored independently by two pathologists blinded to the clinicopathological features and the clinical course.

Statistical analysis

Data were analyzed using GraphPad Prism (GraphPad Software, La Jolla, CA, USA). Graphed data were presented as mean \pm standard error of the mean values, and statistical significance was determined using Student's *t* test. Pearson's chi-squared or Fisher's exact test was used to analyze clinicopathological parameters. Multivariable Cox proportional hazards modeling was performed to identify independent risk factors for the prognosis of NPC. $p \leq 0.05$ was considered statistically significant.

RESULTS

PLUNC negatively correlates with PD-L1 expression in NPC

In the GEPIA online database (<http://gepia.cancer-pku.cn/detail.php>), the expression of the PLUNC gene (*BPIFA1*) was low in head and neck squamous cell carcinoma, while that of the PD-L1 gene (*CD274*) was high (Fig. 1A). The X-axis represents the tumor group and the normal group, while the Y-axis uses \log_2 (TPM+1) values to represent gene-expression levels. Based on the information of 114 NPC patients represented in tissue microarrays (Superbiotek, Shanghai, China) (for relevant clinical information, see Supplementary Table S1), we conducted univariate logistic regression analysis according to the immunohistochemical staining score of PD-L1 (0–3 points; 0 points = negative, >0 points = positive) and found that PD-L1 is a risk factor affecting the prognosis of nasopharyngeal carcinoma patients (Fig. 1B, C). Considering the close correlation between NPC occurrence and EBV infection, we analyzed the effect of EBV on PLUNC gene expression. The results showed no difference in the degree of EBV infection in NPC with high and low expression of PLUNC (Supplementary Fig. S1A). Moreover, there was no correlation between EBV infection and PLUNC gene-expression level ($R = -0.16$, $p = 0.083$) (Supplementary Fig. S1B). To investigate the correlation between PLUNC and PD-L1, we collected paraffin sections from 30 NPC patients in the Second Xiangya Hospital of Central South University for immunohistochemical staining. The results showed that the expression of PLUNC was low in NPC and high in paracancer

tissues, while the expression of PD-L1 was opposite to that of PLUNC (Fig. 1D). The statistical analysis of PD-L1 scores in tumor tissues and adjacent tissues of 30 NPC patients is presented in Supplementary Fig. S1C, indicating that the expression of PD-L1 was significantly greater in tumor tissues than in paracancer tissues. The negative and positive control results of immunohistochemical staining are shown in Supplementary Fig. S1D. Next, we validated the relationship between PLUNC and PD-L1 in NPC cells. In the HNE2 and 5-8F cell lines, we overexpressed PLUNC and found that PD-L1 was downregulated (Fig. 1E). However, when PLUNC was knocked down, the expression of PD-L1 was upregulated (Fig. 1F). Therefore, we considered a negative correlation to exist between the expression of PLUNC and PD-L1 in NPC.

β -catenin upregulates ATF3/PD-L1 expression

ATF3 is a transcription factor; as a member of the ATF/CREB family, it can regulate the expression of PD-L1 in melanoma cells [22]. We validated the regulation of PD-L1 by ATF3 in NPC cells. When we overexpressed ATF3 in 5-8F and S18 cells, the expression of PD-L1 was upregulated (Supplementary Fig. S2A, B). Conversely, when we knocked down ATF3, the expression of PD-L1 was downregulated (Supplementary Fig. S2C, D). The high expression of β -catenin is a risk factor for poor prognosis in NPC patients [23]. β -catenin is an upstream molecule of PD-L1 in glioblastoma [24]. However, whether β -catenin regulates PD-L1 in NPC remains unclear, so we validated the relationship between β -catenin and PD-L1 in NPC cells. When we overexpressed β -catenin in S18 cells and HNE2 cells, the expressions of ATF3 and PD-L1 were upregulated (Fig. 2A). Conversely, when we knocked down β -catenin in 5-8F and HONE1 cells, the expression of both PD-L1 and ATF3 was downregulated (Fig. 2B; statistical results are shown in Fig. 2C, D). Meanwhile, we validated the mRNA- and protein-expression levels of β -catenin after transfection with shRNA (Supplementary Fig. S3A, B). In addition, we also confirmed the expression of both ATF3 and PD-L1 through immunofluorescence experiments (Fig. 2E–H). Therefore, we confirmed that β -catenin upregulated the expression of PD-L1 and ATF3 in NPC cells.

PLUNC suppresses the β -catenin pathway

Since β -catenin could upregulate PD-L1 expression and PLUNC could downregulate PD-L1 expression, could PLUNC inhibit the β -catenin pathway? After overexpressing PLUNC in 5-8F and HNE2 cells (Supplementary Fig. S3C), we found

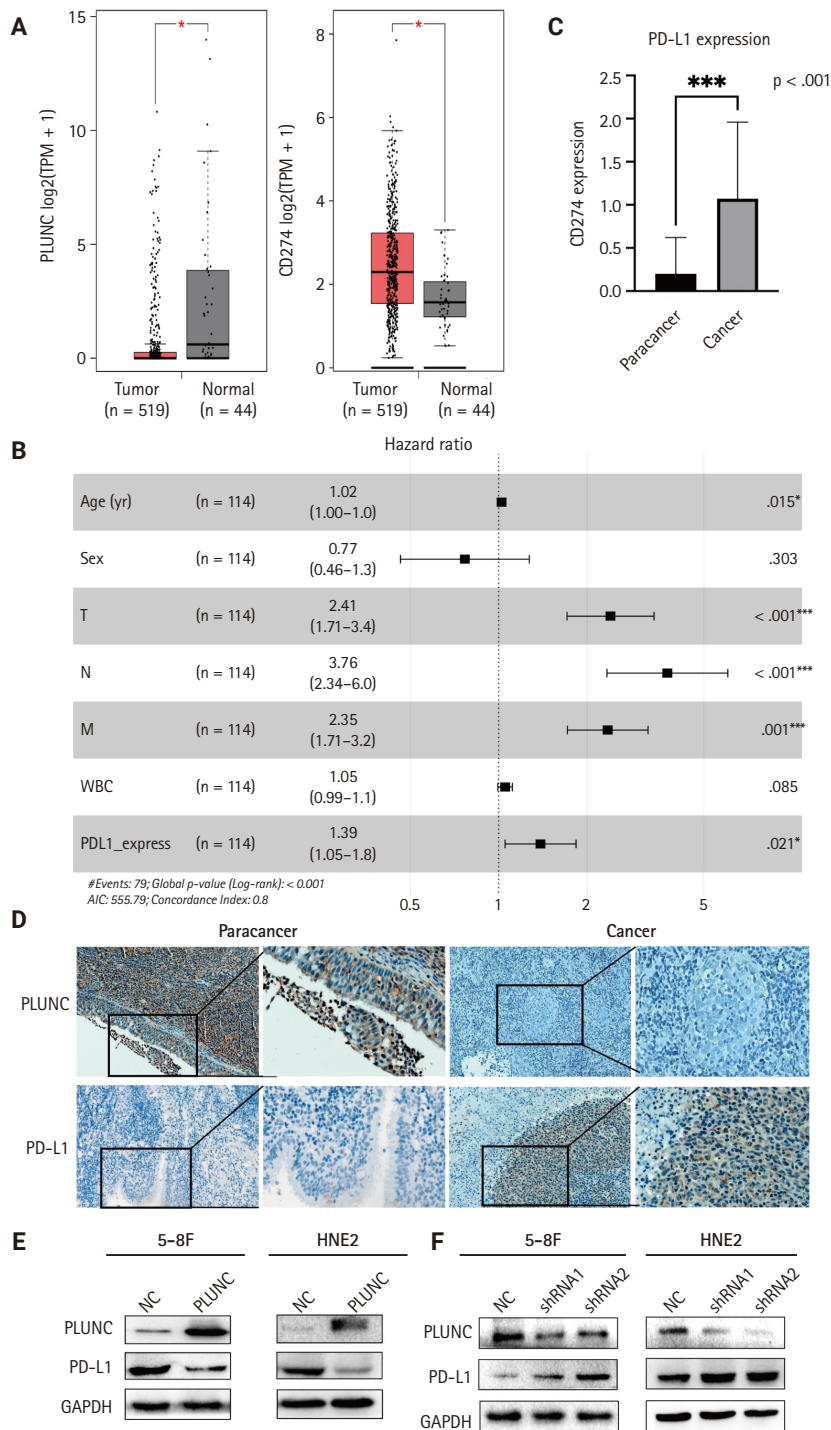


Fig. 1. Palatal, lung, and nasal epithelial clone (PLUNC) negatively correlates with programmed death-ligand 1 (PD-L1) expression in nasopharyngeal carcinoma (NPC). (A) PLUNC and PD-L1 gene expressions in the head and neck squamous cell carcinoma database. T represents tumor and N represents normal. (B) The forest map of risk factor analysis for NPC tissue chips, * $p < .05$, *** $p < .001$, with significant differences. (C) Detection of PD-L1 expression levels in NPC tissue and paracancer tissues using tissue chips. (D) Immunohistochemical staining was performed on paraffin sections of NPC and adjacent tissues to detect the expression levels of PLUNC and PD-L1. (E) Verification of PD-L1 expression in 5-8F and HNE2 cell lines after overexpression of PLUNC through western blot. (F) After transfection of PLUNC-shRNA in 5-8F and HNE2 cells, western blot was used to detect the expression of PD-L1. NC, negative control; GAPDH, glyceraldehyde 3-phosphate dehydrogenase; WBC, white blood cell; AIC, Akaike information criterion.

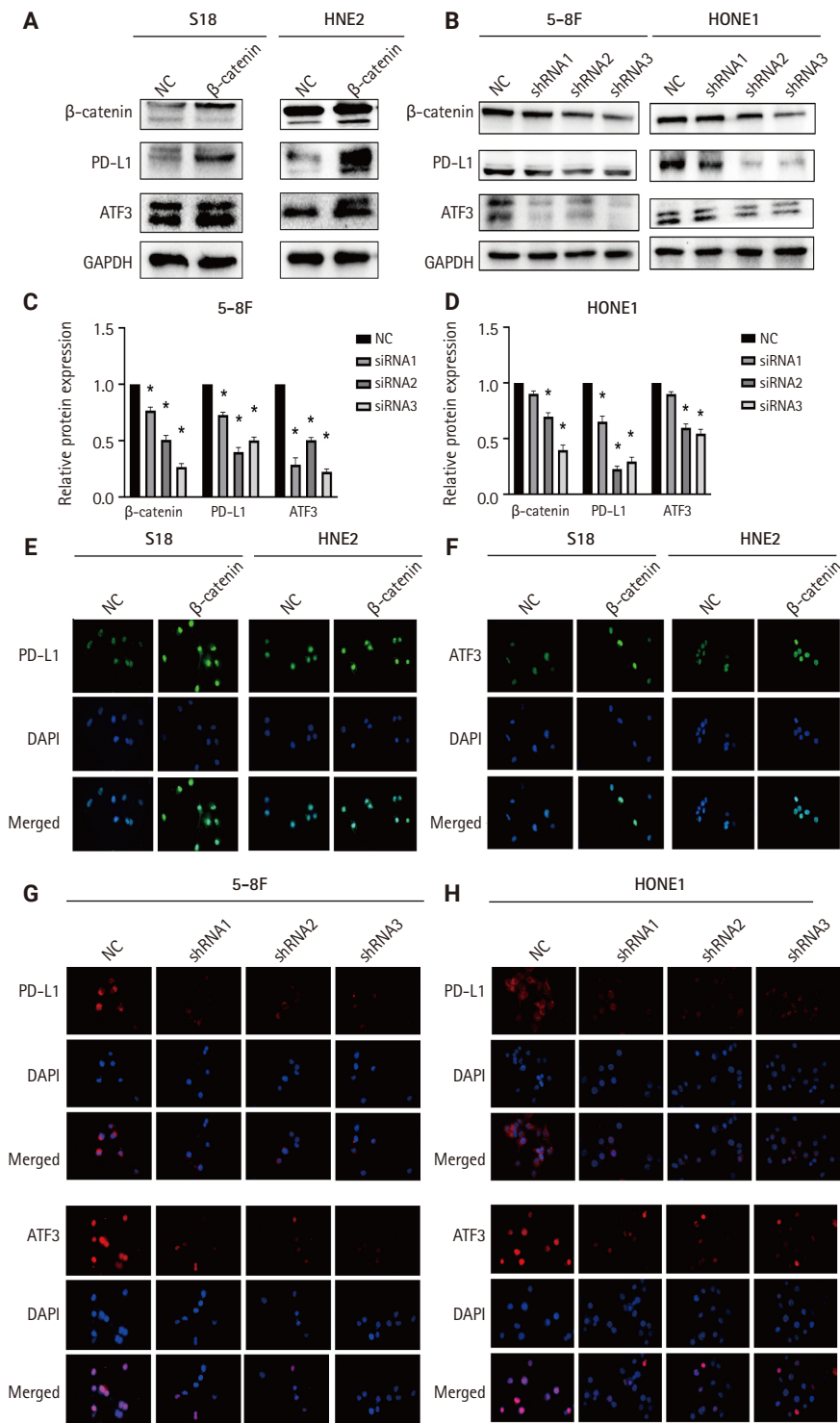


Fig. 2. β-catenin upregulates activating transcription factor 3 (ATF3)/programmed death-ligand 1 (PD-L1) expression. (A) Verification of PD-L1 and ATF3 expression in S18 and HNE2 cell lines by western blot after overexpression of β-catenin. (B) Verification of PD-L1 and ATF3 expression in 5-8F and HONE1 cell lines by western blot after transfection with β-catenin-shRNA. (C, D) Semi-quantitative analysis of the protein expressions of β-catenin, PD-L1, and ATF3 after overexpression and knockdown with β-catenin. *p < .05. (E, F) After overexpressing β-catenin, the expression of PD-L1 was verified by immunofluorescence. (G, H) After knocking down β-catenin, the expression of PD-L1 was verified by immunofluorescence. NC, negative control; GAPDH, glyceraldehyde 3-phosphate dehydrogenase.

that GSK-3 β (which promotes β -catenin ubiquitination degradation) [25] was upregulated. Conversely, phosphorylated GSK-3 β (its inactivated form) was upregulated. The expression of TCF4, which could interact with β -catenin to regulate downstream gene transcription [26], was also inhibited (Fig. 3A). The relative changes in β -catenin, GSK-3 β , p-GSK-3 β , TCF4, and ATF3 are shown in Fig. 3B and C. We also found that overexpression of PLUNC resulted in the downregulation of β -catenin expression by immunofluorescence experiments (Fig. 3D). On the contrary, knocking down PLUNC in HNE2 and 5-8F cells (Supplementary Fig. S3D) weakened the inhibition of the β -catenin pathway (Fig. 3E, F). Therefore, we considered that PLUNC could inhibit the β -catenin pathway.

PLUNC downregulates the expression of ATF3/PD-L1 through inhibiting the β -catenin pathway

After overexpressing PLUNC in 5-8F and HNE2 cells, we observed that the expression of ATF3/PD-L1 decreased (Fig. 4A–D). Conversely, when we knocked down PLUNC in 5-8F and HNE2 cells, we observed that the expression of both ATF3 and PD-L1 increased (Fig. 4E–H). After treating cells using XAV-939 as an inhibitor of the Wnt/ β -catenin pathway, the expression of β -catenin, p-GSK3 β , ATF3, and PD-L1 decreased. However, when PLUNC was knocked down in 5-8F and HNE2 cells, the expressions of β -catenin, p-GSK3 β , ATF3, and PD-L1 increased. When PLUNC-shRNA was combined with XAV-939, the expressions of β -catenin, p-GSK3 β , ATF3, and PD-L1 were weakened (Fig. 4I, J). Thus, we believed that PLUNC downregulated the expression of ATF3/PD-L1 through inhibiting the β -catenin pathway.

DDX17 interacts with β -catenin in NPC cells

However, the mechanism by which PLUNC downregulated β -catenin remains unclear. In 5-8F and HNE2 cells, PLUNC cannot bind directly to β -catenin, so we speculated that PLUNC may regulate β -catenin through another mechanism. The RNA helicase DDX17 is a member of a large family of highly conserved proteins that are involved in gene-expression regulation [27]. DDX17 acts as a co-activator or co-inhibitor of transcription factors of cell differentiation [28]. We explored the association of DDX17 with β -catenin in NPC cells. Just as seen in Fig. 5A–D, we confirmed DDX17 interactions with β -catenin by co-immunoprecipitation (Co-IP). Then, we demonstrated their co-localization by immunofluorescence experiments (Fig. 5E). Therefore, we further speculate whether PLUNC is related to

the combination of DDX17 and β -catenin.

PLUNC inhibits the interaction of DDX17 and β -catenin

In NPC cells, we confirmed the interactions between PLUNC and DDX17 by Co-IP (Fig. 6A, B). In addition, the co-localization of PLUNC and DDX17 was confirmed by immunofluorescence (Fig. 6C, D). Therefore, we speculate that PLUNC and β -catenin compete to combine with DDX17. We co-transfected PLUNC, β -catenin, and DDX17 plasmids in 293T cells and successfully validated their expression (Fig. 6E). Then, we used the DDX17 antibody to co-precipitate PLUNC and β -catenin. We found that, following transfection with PLUNC, the interaction of DDX17 and β -catenin decreased, while, after transfection with β -catenin, the interaction of PLUNC and DDX17 decreased (Fig. 6F). In addition, through immunofluorescence experiments, we found that, after transfection with PLUNC, the co-localization of β -catenin and DDX17 decreased (Fig. 6G, H). Therefore, the results confirmed that PLUNC inhibits the interaction of DDX17 and β -catenin.

PLUNC negatively correlates with DDX17 and β -catenin expression in NPC

In NPC tissue sections, we confirmed a negative correlation between PLUNC and the expressions of DDX17 and β -catenin. In NPC tissue, the expression of PLUNC was low, while those of DDX17 and β -catenin were high. However, in paracancer tissues, their expressions are exactly opposite (Fig. 7A). In addition, we present representative images with immunohistochemical scores in Supplementary Fig. S4.

Finally, we concluded that the interaction of PLUNC and DDX17 inhibited the interaction of β -catenin and DDX17, thereby promoting the degradation of β -catenin by GSK-3 β . However, the reduction of β -catenin's entry into the nucleus inhibited the expression of PD-L1, ultimately leading to a reduced expression of PLUNC (Fig. 7B).

DISCUSSION

EBV is closely related to the occurrence and development of NPC. It had been reported that EBV could upregulate the expression of PD-L1 in NPC cells [29–31]. Therefore, immunotherapy targeting PD-1/PD-L1 has become a new strategy for the treatment of NPC [32,33]. Our results indicated that high expression of PD-L1 is a risk factor for poor prognosis in pa-

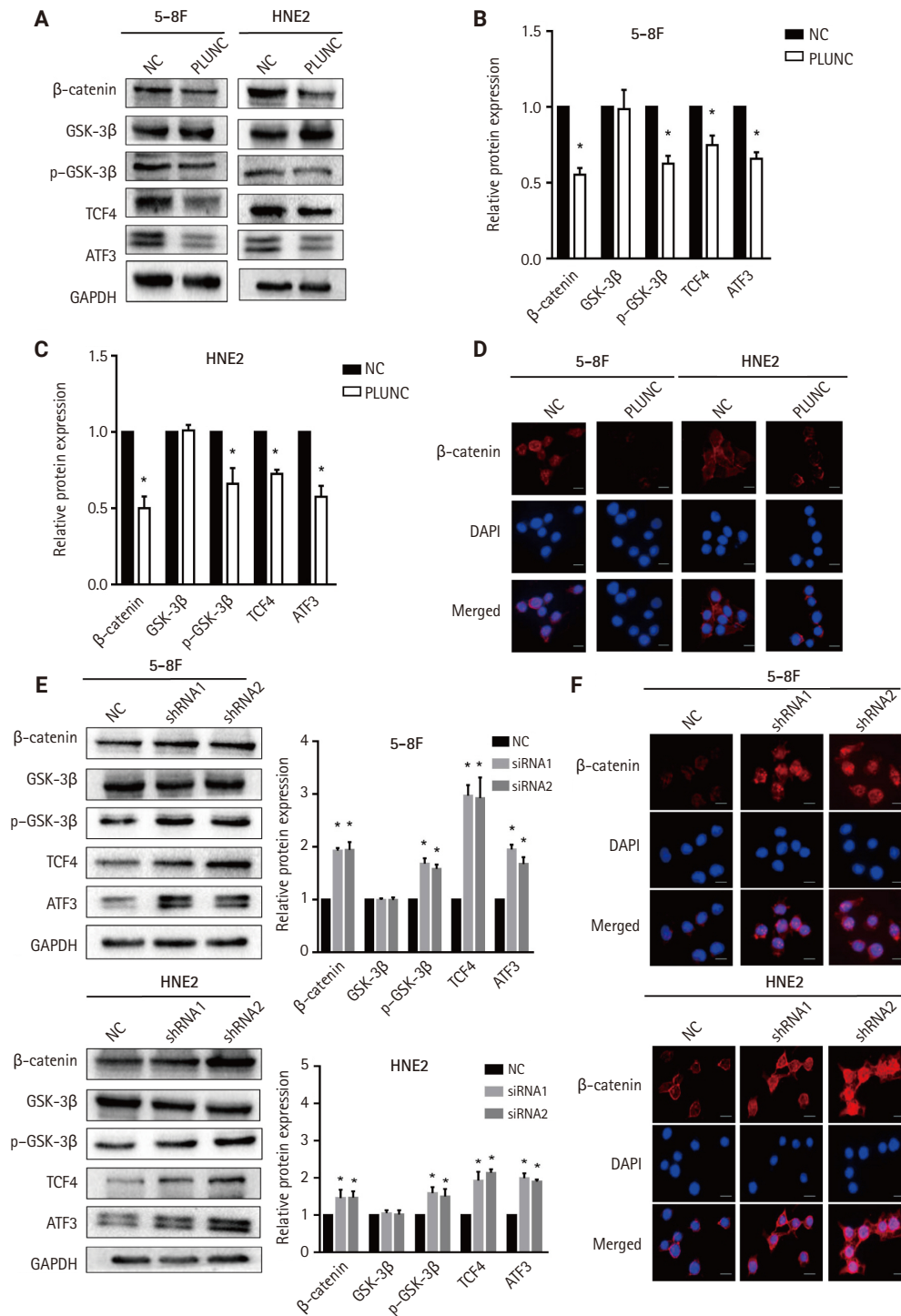


Fig. 3. Palatal, lung, and nasal epithelial clone (PLUNC) suppresses the β -catenin pathway. (A) Detection of the β -catenin pathway expression in 5-8F and HNE2 cell lines by western blot after overexpression of PLUNC. (B, C) Semi-quantitative analysis of the protein expressions of β -catenin, glycogen synthase kinase 3 β (GSK-3 β), p-GSK-3 β , T-cell factor 4 (TCF4), and activating transcription factor 3 (ATF3) after overexpression with PLUNC. * $p < .05$. (D) β -catenin expression in 5-8F and HNE2 cell lines by immunofluorescence after overexpression of PLUNC. (E) Detection of β -catenin pathway expression in 5-8F and HNE2 cell lines by western blot, and the semi-quantitative analysis of the protein expression after knocking down PLUNC. (F) β -catenin expression in 5-8F and HNE2 cell lines by immunofluorescence after knocking down PLUNC. NC, negative control; GAPDH, glyceraldehyde 3-phosphate dehydrogenase.

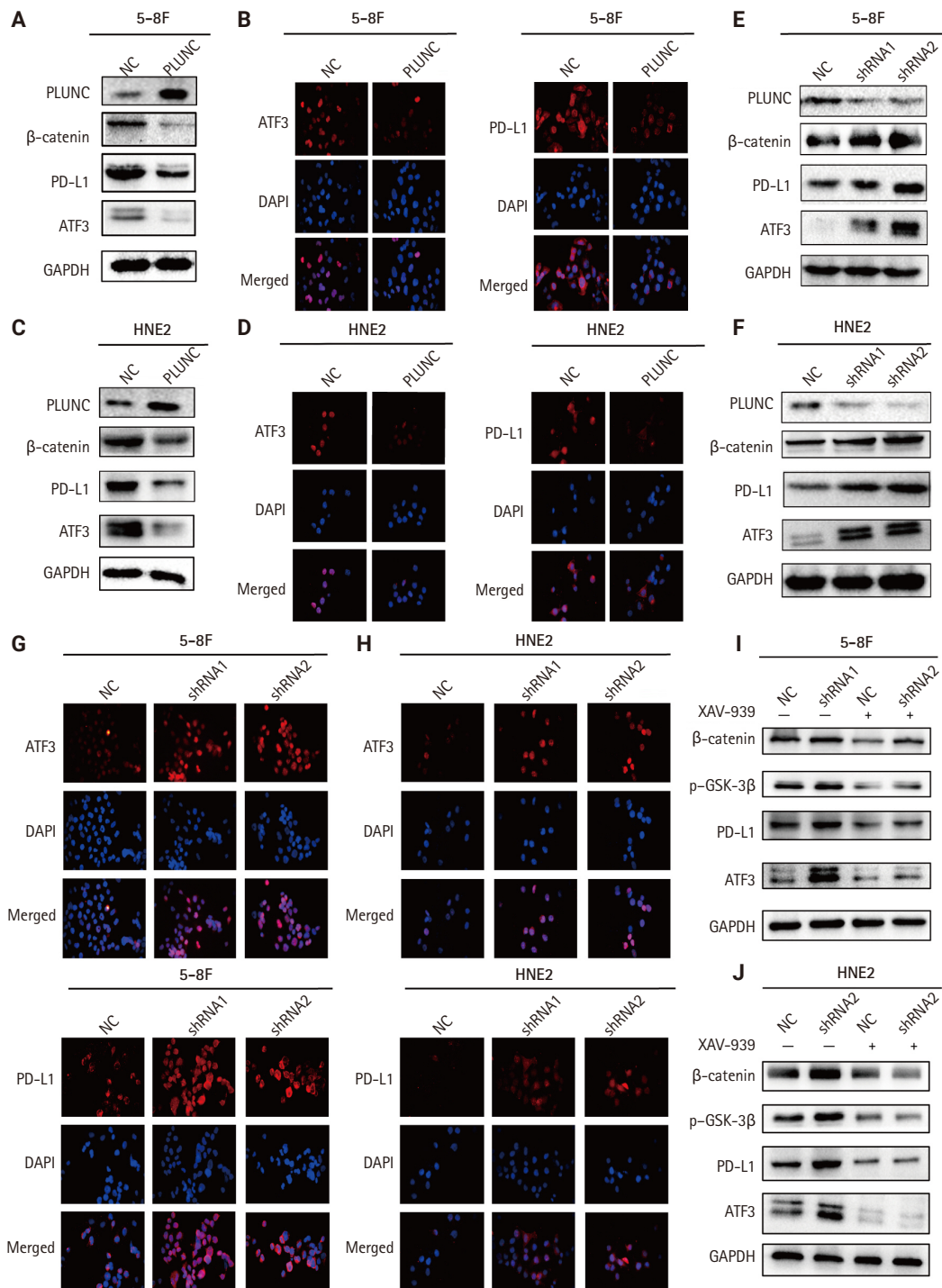


Fig. 4. Palatal, lung, and nasal epithelial clone (PLUNC) downregulates the expression of activating transcription factor 3 (ATF3)/programmed death-ligand 1 (PD-L1) by inhibiting the β-catenin pathway. (A, B) After overexpression of PLUNC in 5-8F cells, decreased ATF3 and PD-L1 expression was confirmed by western blot and immunofluorescence. (C, D) After overexpression of PLUNC in HNE2 cells, decreased ATF3 and PD-L1 expression was confirmed by western blot and immunofluorescence. (E-H) After knocking down of PLUNC in 5-8F and HNE2 cells, upregulated ATF3 and PD-L1 expression was confirmed by western blot and immunofluorescence. (I, J) After the cells were treated with PLUNC-shRNA and/or XAV-939, the expressions of β-catenin, phospho-glycogen synthase kinase 3β (p-GSK-3β), ATF3, and PD-L1 were verified by western blot. NC, negative control; GAPDH, glyceraldehyde 3-phosphate dehydrogenase.

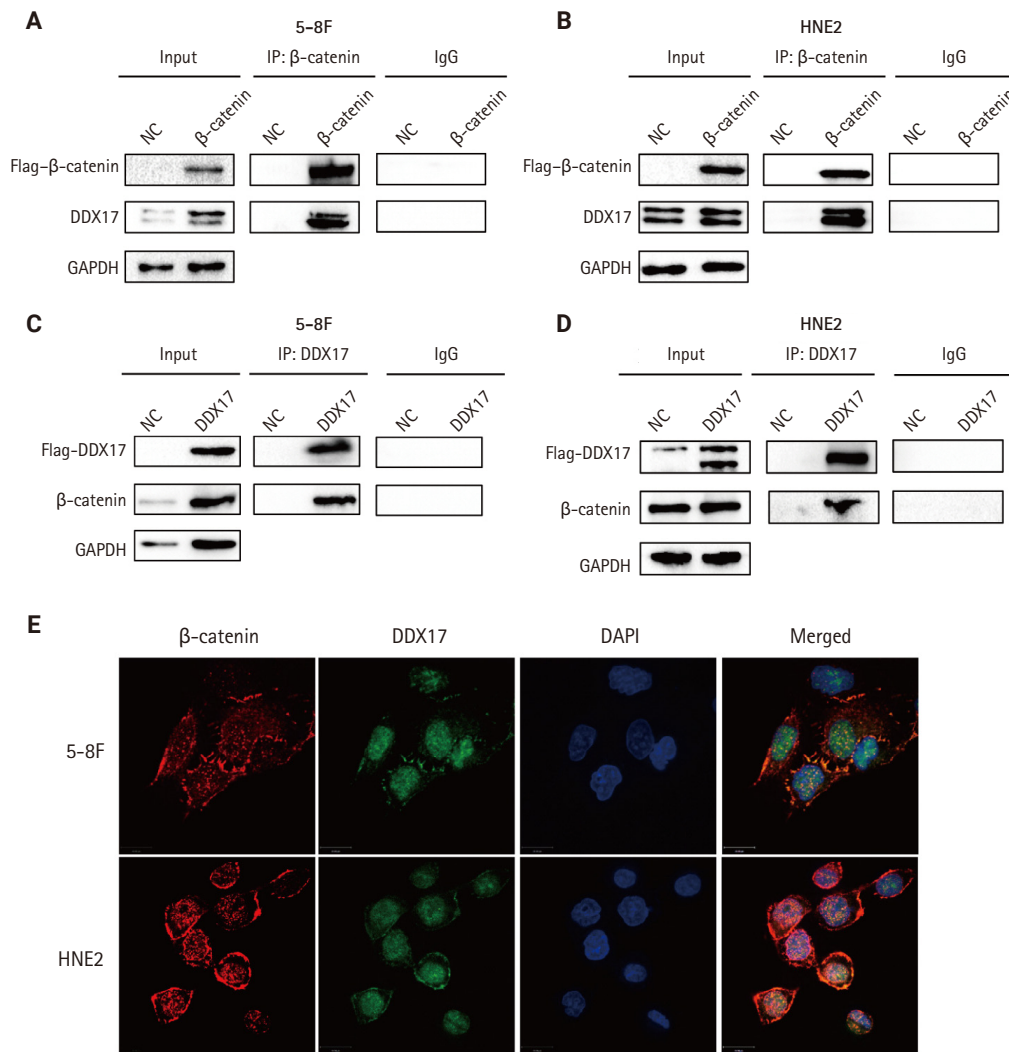


Fig. 5. DEAD-box helicase 17 (DDX17) interacts with β -catenin in nasopharyngeal carcinoma cells. (A–D) Co-immunoprecipitation (Co-IP) of DDX17 and β -catenin in 5-8F and HNE2 cells. (E) Co-localization of DDX17 and β -catenin by immunofluorescence (β -catenin: red, DDX17: green). NC, negative control; GAPDH, glyceraldehyde 3-phosphate dehydrogenase.

tients with NPC. Therefore, inhibiting the expression of PD-L1 will benefit patients with NPC.

PLUNC was originally identified in the trachea and bronchi [34]. It was originally called PLUNC, and its gene product was later renamed short PLUNC 1 (*SPLUNC1*), also known as *SPURT*, *LUNX*, *NASG*, or *BPIFA1*. The secreted protein encoded by *SPLUNC1* is abundant in human tracheobronchial secretions and saliva [35], nasal lavage [36], apical secretions of cultured human tracheobronchial epithelial cells [37,38], and specific granules of human neutrophils [39]. Previous research results from our group show that the poor prognosis of NPC patients closely relates to the low expression of PLUNC, which

may represent a candidate molecular marker for early diagnosis of NPC [14]. In recent years, immunotherapy has become a promising treatment for NPC and has made great progress [40]. Upregulation of the PD-1/PD-L1 pathway is one of the possible mechanisms of immune-evasion in EBV-associated NPC [41]. PD-1/PD-L1 immune checkpoint inhibitors were approved in China in 2021 for the treatment of relapsed or metastatic NPC. In our study, PLUNC could downregulate the expression of PD-L1 in NPC.

Under physiological conditions, Wnt/ β -catenin signaling is turned off. In the absence of Wnt signaling, a protein complex formed by AXIN, adenomatous polyposis coli (APC), serine/

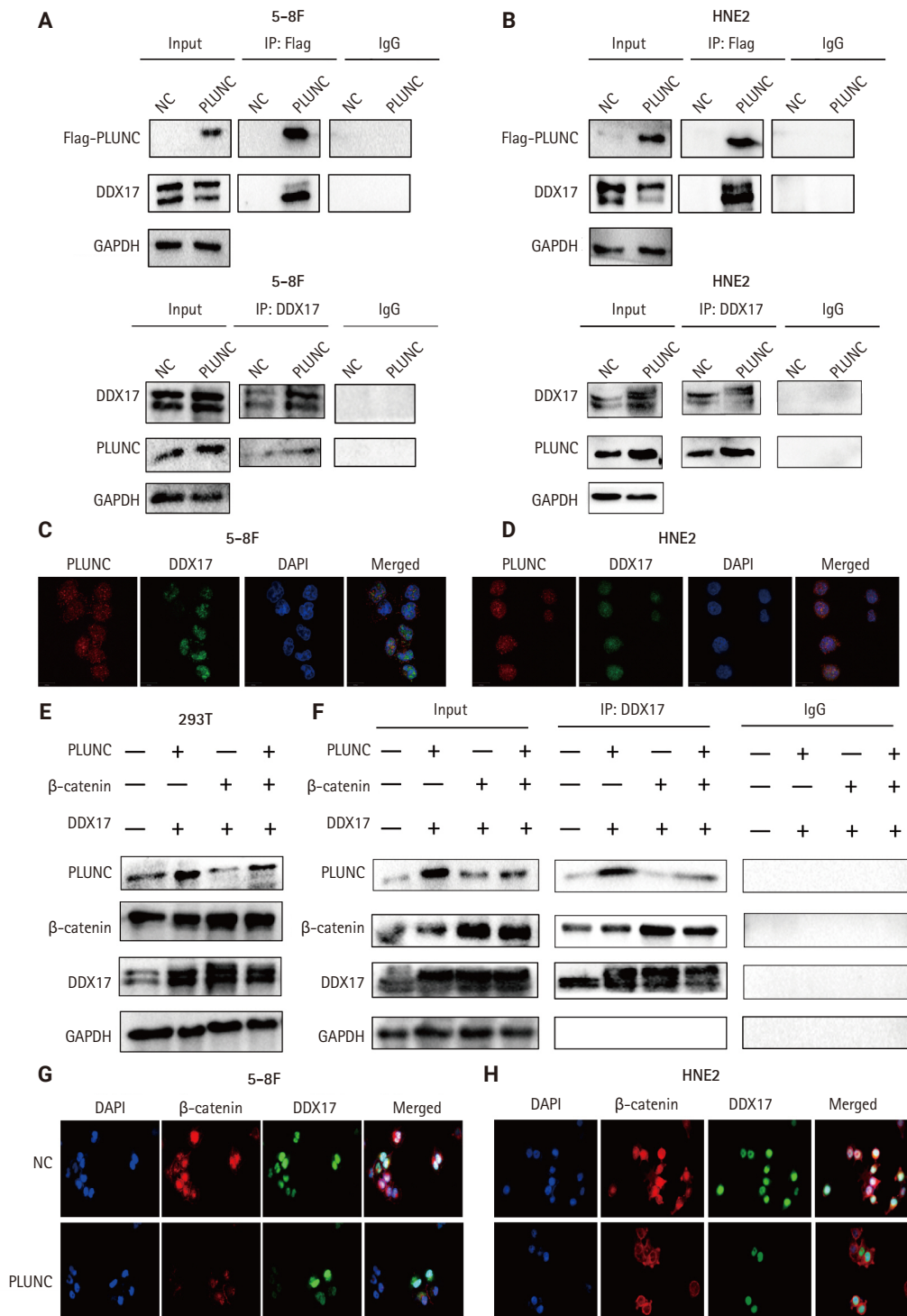


Fig. 6. Palatal, lung, and nasal epithelial clone (PLUNC) inhibits the interaction of DEAD-box helicase 17 (DDX17) and β -catenin. (A, B) Co-immunoprecipitation (Co-IP) of DDX17 and PLUNC in 5-8F and HNE2 cells. (C, D) Co-localization of DDX17 and PLUNC by immunofluorescence (PLUNC: red, DDX17: green). (E) Successful co-transfection of PLUNC, β -catenin, and DDX17 plasmids in 293T cells was verified through western blot. (F) Co-IP confirmed that PLUNC inhibited the interaction of DDX17 and β -catenin. (G, H) After overexpression of PLUNC in 5-8F and HNE2 cells, the co-localization of DDX17 and β -catenin was reduced (β -catenin: red, DDX17: green). NC, negative control; GAPDH, glyceraldehyde 3-phosphate dehydrogenase.

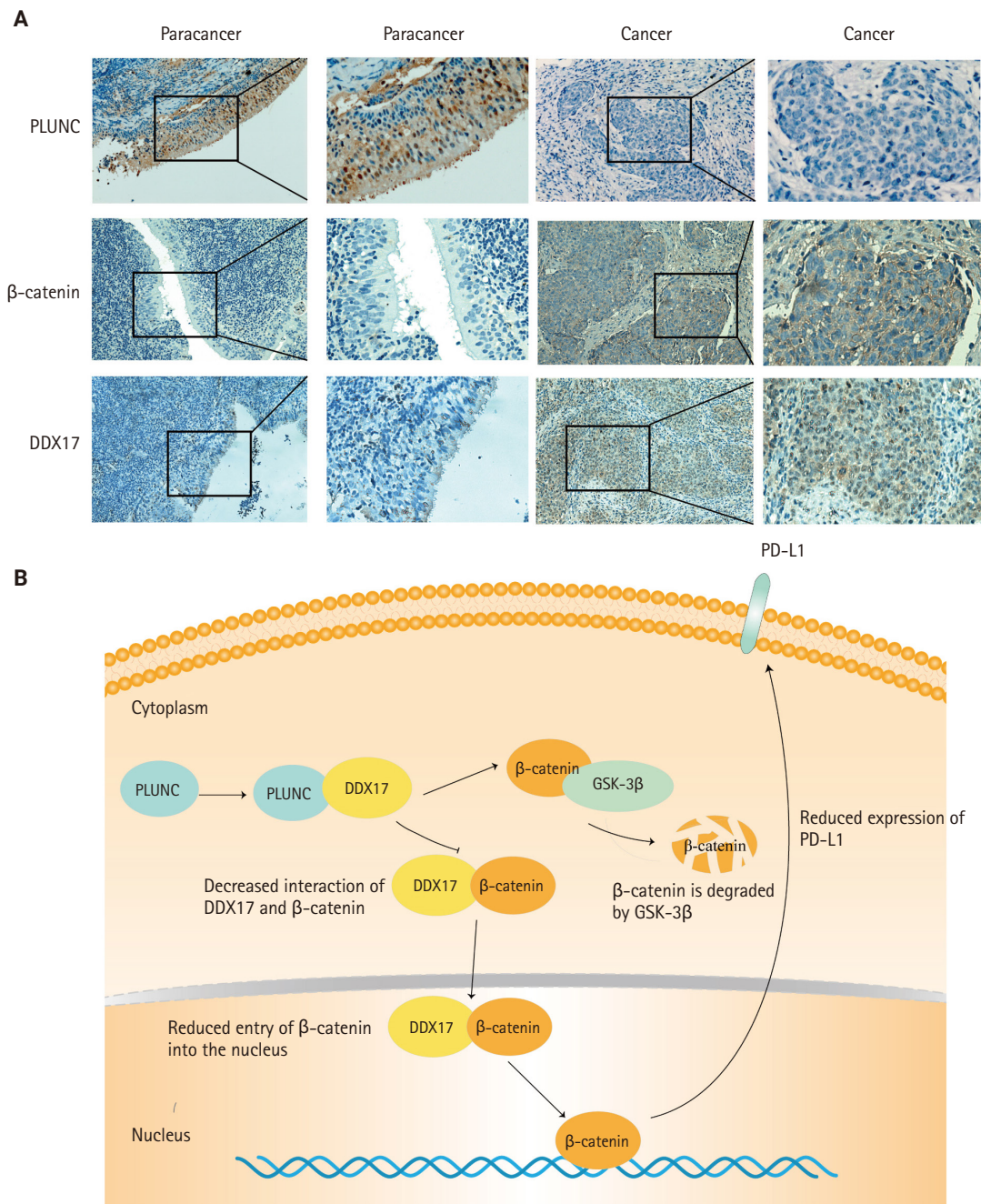


Fig. 7. Palatal, lung, and nasal epithelial clone (PLUNC) negatively correlates with DEAD-box helicase 17 (DDX17) and β -catenin expression in nasopharyngeal carcinoma (NPC). (A) Immunohistochemical staining results of PLUNC, DDX17, and β -catenin in NPC and paracancer. (B) Research model diagram of PLUNC inhibiting programmed death-ligand 1 (PD-L1) expression. GSK-3 β , glycogen synthase kinase 3 β .

threonine kinase GSK-3 β , CK1, and E3 ubiquitin ligase β -trcp degrades β -catenin [42]. Abnormal activation of Wnt/ β -catenin signaling is common in tumors. When Wnt signaling is activated, GSK-3 β is deactivated after phosphorylation, which leads to disassembly of the Axin/GSK3 β /APC complex, thereby inhibit-

ing the phosphorylation and degradation of β -catenin, and dephosphorylated β -catenin could be transported to the nucleus to regulate target genes [43]. Studies have shown that nuclear β -catenin can bind to the *CD274* promoter region, promoting PD-L1 transcription and upregulating PD-L1 expression in

nasopharyngeal carcinoma cells [44]. We also confirmed the expression of β -catenin in the nucleus and cytoplasm (Supplementary Fig. S3E, F). The results indicated that PLUNC could inhibit the expression of β -catenin in the nucleus and cytoplasm. However, the entry of β -catenin into the nucleus is reduced, leading to a decrease in the transcription of PD-L1 and ultimately downregulating the expression of PD-L1.

DDX17 (DEAD Asp-Glu-Ala-Asp) box helicase 17, also known as p72, is a typical member of the DEAD box family and is of interest for its role as an RNA helicase [45]. Among the DEAD-box RNA-binding proteins, DDX17 is a well-characterized cofactor of the Drosha/DGCR8 microprocessor, which mediates the recognition and processing of primary miRNAs (pri-miRNAs) to become mature miRNAs [46-48]. In addition, more and more studies are showing that DDX17 acts as a transcription factor-related protein that is associated with the function of transcription factors such as NFAT5, histone deacetylase 1, and SOX [49-52]. The abnormal expression of DDX17 could promote progression of various tumors [28,53,54]. Furthermore, DDX17 exerts its powerful oncogenic effects by acting as a co-activator or co-repressor of transcription factors, such as estrogen receptor α [55]. DDX17 could interact with β -catenin, while PLUNC could inhibit the β -catenin pathway. Therefore, we doubted whether PLUNC could regulate β -catenin through DDX17. Our experimental results also showed that PLUNC can directly interact with DDX17 and inhibited the interaction of DDX17 with β -catenin. After PLUNC knockdown, the expressions of both PD-L1 and β -catenin were increased.

ATF3 is a transcription factor that plays vital roles in modulating metabolism, immunity, and oncogenes that has sparked intense attention [56]. ATF3 could participate in the immune-regulation of the body and affect the occurrence, development, and treatment of tumors. Our results showed that β -catenin could upregulate ATF3 and PD-L1, while PLUNC can inhibit the Wnt/ β -catenin pathway, thereby inhibiting the expressions of ATF3 and PD-L1. However, our experimental results showed that ATF3 was indeed regulated by β -catenin, while PD-L1 was indeed regulated by ATF3, but whether β -catenin directly regulates PD-L1 expression or relies on ATF3 to regulate PD-L1 still requires further experimental verification.

In conclusion, this study confirmed that PLUNC could downregulate the expression of PD-L1 in NPC by inhibiting the interaction of DDX17/ β -catenin. This will provide new ideas for the immunotherapy of NPC.

Supplementary Information

The Data Supplement is available with this article at <https://doi.org/10.4132/jptm.2024.11.27>.

Ethics Statement

All procedures performed in the current study were approved by Xiangya Hospital of Central South University ethics committee (reference number: 202207389 Date:2022.07.05) in accordance with the 1964 Helsinki declaration and its later amendments. All specimens in this study had obtained informed consent from the patients.

Availability of Data and Material

The datasets generated or analyzed during the study are available from the corresponding author on reasonable request.

Code Availability

Not applicable.

ORCID

Ranran Feng	https://orcid.org/0000-0003-3830-3974
Yilin Guo	https://orcid.org/0009-0007-8410-2328
Meilin Chen	https://orcid.org/0009-0004-1384-4197
Ziyang Tian	https://orcid.org/0009-0003-9301-4961
Yijun Liu	https://orcid.org/0000-0002-1170-0470
Su Jiang	https://orcid.org/0009-0001-9559-3499
Jieyu Zhou	https://orcid.org/0009-0003-3368-7136
Qingluan Liu	https://orcid.org/0000-0002-4628-7727
Xiayu Li	https://orcid.org/0000-0003-3900-2145
Wei Xiong	https://orcid.org/0000-0002-3825-1679
Lei Shi	https://orcid.org/0000-0002-7438-2318
Songqing Fan	https://orcid.org/0000-0002-1486-9909
Guiyuan Li	https://orcid.org/0000-0002-1717-9305
Wenling Zhang	https://orcid.org/0000-0002-1586-6363

Author Contributions

Conceptualization: RF, YG, MC, WZ. Formal analysis: JZ. Funding acquisition: WZ. Investigation: YG, MC, YL, QL, ZT, SJ, LS, SF. Supervision: XL, WX, GL, WZ. Writing—original draft: RF. Writing—review & editing: RF, WZ. Approval of final manuscript: all authors.

Conflicts of Interest

The authors declare that they have no potential conflicts of interest.

Funding Statement

This work was funded by the National Natural Science Foundation of China (Grant No. 81672688) and the Hunan Province Natural Science Foundation (Grant No. 2020JJ4780).

Acknowledgments

We thank The Third Xiangya Hospital of Central South University and The Cancer Research Institute of Central South University for its technical support.

REFERENCES

- Sung H, Ferlay J, Siegel RL, et al. Global cancer statistics 2020: GLOBOCAN estimates of incidence and mortality worldwide for 36 cancers in 185 countries. *CA Cancer J Clin* 2021; 71: 209-49.
- Tang LQ, Li CF, Li J, et al. Establishment and validation of prognostic nomograms for endemic nasopharyngeal carcinoma. *J Natl Cancer Inst* 2016; 108: djv291.
- Xu JY, Wei XL, Wang YQ, Wang FH. Current status and advances of immunotherapy in nasopharyngeal carcinoma. *Ther Adv Med Oncol* 2022; 14: 17588359221096214.
- Chen YP, Chan AT, Le QT, Blanchard P, Sun Y, Ma J. Nasopharyngeal carcinoma. *Lancet* 2019; 394: 64-80.
- Adkins DR, Haddad RI. Clinical trial data of anti-PD-1/PD-L1 therapy for recurrent or metastatic nasopharyngeal Carcinoma: a review. *Cancer Treat Rev* 2022; 109: 102428.
- Bingle CD, Craven CJ. PLUNC: a novel family of candidate host defence proteins expressed in the upper airways and nasopharynx. *Hum Mol Genet* 2002; 11: 937-43.
- Geetha C, Venkatesh SG, Bingle L, Bingle CD, Gorr SU. Design and validation of anti-inflammatory peptides from human parotid secretory protein. *J Dent Res* 2005; 84: 149-53.
- Bartlett JA, Gakhar L, Penterman J, et al. PLUNC: a multifunctional surfactant of the airways. *Biochem Soc Trans* 2011; 39: 1012-6.
- Ben-Meir E, Perrem L, Shaw M, Ratjen F, Grasemann H. SPLUNC1 as a biomarker of pulmonary exacerbations in children with cystic fibrosis. *J Cyst Fibros* 2024; 23: 288-92.
- Liu H, Zhang X, Wu J, French SW, He Z. New insights on the palate, lung, and nasal epithelium clone (PLUNC) proteins: based on molecular and functional analysis of its homolog of YH1/SPLUNC1. *Exp Mol Pathol* 2016; 100: 363-9.
- Tsou YA, Peng MT, Wu YF, et al. Decreased PLUNC expression in nasal polyps is associated with multibacterial colonization in chronic rhinosinusitis patients. *Eur Arch Otorhinolaryngol* 2014; 271: 299-304.
- Khanal S, Webster M, Niu N, et al. SPLUNC1: a novel marker of cystic fibrosis exacerbations. *Eur Respir J* 2021; 58: 2000507.
- Osada M, Aishima S, Hirahashi M, et al. Combination of hepatocellular markers is useful for prognostication in gastric hepatoid adenocarcinoma. *Hum Pathol* 2014; 45: 1243-50.
- Zhang W, Zeng Z, Wei F, et al. SPLUNC1 is associated with nasopharyngeal carcinoma prognosis and plays an important role in all-trans-retinoic acid-induced growth inhibition and differentiation in nasopharyngeal cancer cells. *FEBS J* 2014; 281: 4815-29.
- Ou C, Sun Z, Zhang H, et al. SPLUNC1 reduces the inflammatory response of nasopharyngeal carcinoma cells infected with the EB virus by inhibiting the TLR9/NF-kappaB pathway. *Oncol Rep* 2015; 33: 2779-88.
- Liu H, Tang L, Gong S, et al. USP7 inhibits the progression of nasopharyngeal carcinoma via promoting SPLUNC1-mediated M1 macrophage polarization through TRIM24. *Cell Death Dis* 2023; 14: 852.
- Tang L, Peng L, Liu H, et al. SPLUNC1 regulates LPS-induced progression of nasopharyngeal carcinoma and proliferation of myeloid-derived suppressor cells. *Med Oncol* 2022; 39: 214.
- Yu F, Yu C, Li F, et al. Wnt/beta-catenin signaling in cancers and targeted therapies. *Signal Transduct Target Ther* 2021; 6: 307.
- Pang Q, Hu W, Zhang X, Pang M. Wnt/beta-catenin signaling pathway-related proteins (DKK-3, beta-catenin, and c-MYC) are involved in prognosis of nasopharyngeal carcinoma. *Cancer Biother Radiopharm* 2019; 34: 436-43.
- Hu Z, Meng J, Cai H, et al. KIF3A inhibits nasopharyngeal carcinoma proliferation, migration and invasion by interacting with beta-catenin to suppress its nuclear accumulation. *Am J Cancer Res* 2022; 12: 5226-40.
- Ou X, Zhang Y, Xu Y, et al. PICK1 inhibits the malignancy of nasopharyngeal carcinoma and serves as a novel prognostic marker. *Cell Death Dis* 2024; 15: 294.
- Liu N, Yan M, Tao Q, et al. Inhibition of TCA cycle improves the anti-PD-1 immunotherapy efficacy in melanoma cells via ATF3-mediated PD-L1 expression and glycolysis. *J Immunother Cancer* 2023; 11: e007146.
- Jin PY, Zheng ZH, Lu HJ, et al. Roles of beta-catenin, TCF-4, and survivin in nasopharyngeal carcinoma: correlation with clinicopathological features and prognostic significance. *Cancer Cell Int* 2019; 19: 48.
- Du L, Lee JH, Jiang H, et al. Beta-catenin induces transcriptional expression of PD-L1 to promote glioblastoma immune evasion. *J Exp Med* 2020; 217: e20191115.

25. Xue W, Yang L, Chen C, Ashrafizadeh M, Tian Y, Sun R. Wnt/ beta-catenin-driven EMT regulation in human cancers. *Cell Mol Life Sci* 2024; 81: 79.
26. Delgado-Bellido D, Zamudio-Martinez E, Fernandez-Cortes M, et al. VE-cadherin modulates beta-catenin/TCF-4 to enhance vasculogenic mimicry. *Cell Death Dis* 2023; 14: 135.
27. Yang S, Winstone L, Mondal S, Wu Y. Helicases in R-loop formation and resolution. *J Biol Chem* 2023; 299: 105307.
28. Zhao G, Wang Q, Zhang Y, et al. DDX17 induces epithelial-mesenchymal transition and metastasis through the miR-149-3p/ CYBRD1 pathway in colorectal cancer. *Cell Death Dis* 2023; 14: 1.
29. Wang J, Ge J, Wang Y, et al. EBV miRNAs BART11 and BART17-3p promote immune escape through the enhancer-mediated transcription of PD-L1. *Nat Commun* 2022; 13: 866.
30. Ge J, Wang J, Xiong F, et al. Epstein-Barr virus-encoded circular RNA CircBART2.2 promotes immune escape of nasopharyngeal carcinoma by regulating PD-L1. *Cancer Res* 2021; 81: 5074-88.
31. Kase K, Kondo S, Wakisaka N, et al. Epstein-Barr virus LMP1 induces soluble PD-L1 in nasopharyngeal carcinoma. *Microorganisms* 2021; 9: 603.
32. Wang FH, Wei XL, Feng J, et al. Efficacy, safety, and correlative biomarkers of toripalimab in previously treated recurrent or metastatic nasopharyngeal carcinoma: a phase II clinical trial (POLARIS-02). *J Clin Oncol* 2021; 39: 704-12.
33. Mai HQ, Chen QY, Chen D, et al. Toripalimab or placebo plus chemotherapy as first-line treatment in advanced nasopharyngeal carcinoma: a multicenter randomized phase 3 trial. *Nat Med* 2021; 27: 1536-43.
34. Weston WM, LeClair EE, Trzyna W, et al. Differential display identification of plunc, a novel gene expressed in embryonic palate, nasal epithelium, and adult lung. *J Biol Chem* 1999; 274: 13698-703.
35. Vitorino R, Lobo MJ, Ferrer-Correira AJ, et al. Identification of human whole saliva protein components using proteomics. *Proteomics* 2004; 4: 1109-15.
36. Ghafouri B, Kihlstrom E, Stahlbom B, Tagesson C, Lindahl M. PLUNC (palate, lung and nasal epithelial clone) proteins in human nasal lavage fluid. *Biochem Soc Trans* 2003; 31: 810-4.
37. Di YP, Harper R, Zhao Y, Pahlavan N, Finkbeiner W, Wu R. Molecular cloning and characterization of spurt, a human novel gene that is retinoic acid-inducible and encodes a secretory protein specific in upper respiratory tracts. *J Biol Chem* 2003; 278: 1165-73.
38. Campos MA, Abreu AR, Nlend MC, Cobas MA, Conner GE, Whitney PL. Purification and characterization of PLUNC from human tracheobronchial secretions. *Am J Respir Cell Mol Biol* 2004; 30: 184-92.
39. Bartlett JA, Hicks BJ, Schlomann JM, Ramachandran S, Nauseef WM, McCray PB Jr. PLUNC is a secreted product of neutrophil granules. *J Leukoc Biol* 2008; 83: 1201-6.
40. Huang H, Yao Y, Deng X, et al. Immunotherapy for nasopharyngeal carcinoma: current status and prospects (review). *Int J Oncol* 2023; 63: 97.
41. Johnson D, Ma BB. Targeting the PD-1/ PD-L1 interaction in nasopharyngeal carcinoma. *Oral Oncol* 2021; 113: 105127.
42. Liu J, Xiao Q, Xiao J, et al. Wnt/beta-catenin signalling: function, biological mechanisms, and therapeutic opportunities. *Signal Transduct Target Ther* 2022; 7: 3.
43. Wang D, Wu S, He J, et al. FAT4 overexpression promotes antitumor immunity by regulating the beta-catenin/STT3/PD-L1 axis in cervical cancer. *J Exp Clin Cancer Res* 2023; 42: 222.
44. Wang H, Luo K, Zhan Y, Peng S, Fan S, Wang W. Role of beta-catenin in PD-L1 expression of nasopharyngeal carcinoma. *Heliyon* 2023; 9: e18130.
45. Moy RH, Cole BS, Yasunaga A, et al. Stem-loop recognition by DDX17 facilitates miRNA processing and antiviral defense. *Cell* 2014; 158: 764-77.
46. Terrone S, Valat J, Fontrodona N, et al. RNA helicase-dependent gene looping impacts messenger RNA processing. *Nucleic Acids Res* 2022; 50: 9226-46.
47. Suthapot P, Xiao T, Felsenfeld G, Hongeng S, Wongtrakongate P. The RNA helicases DDX5 and DDX17 facilitate neural differentiation of human pluripotent stem cells NTERA2. *Life Sci* 2022; 291: 120298.
48. Zhou HZ, Li F, Cheng ST, et al. DDX17-regulated alternative splicing that produced an oncogenic isoform of PNX-AS1 to promote HCC metastasis. *Hepatology* 2022; 75: 847-65.
49. Li K, Mo C, Gong D, et al. DDX17 nucleocytoplasmic shuttling promotes acquired gefitinib resistance in non-small cell lung cancer cells via activation of beta-catenin. *Cancer Lett* 2017; 400: 194-202.
50. Germann S, Gratadou L, Zonta E, et al. Dual role of the ddx5/ ddx17 RNA helicases in the control of the pro-migratory NFAT5 transcription factor. *Oncogene* 2012; 31: 4536-49.
51. Wilson BJ, Bates GJ, Nicol SM, Gregory DJ, Perkins ND, Fuller-Pace FV. The p68 and p72 DEAD box RNA helicases interact with HDAC1 and repress transcription in a promoter-specific manner. *BMC Mol Biol* 2004; 5: 11.
52. Alqahtani H, Gopal K, Gupta N, et al. DDX17 (P72), a Sox2 binding partner, promotes stem-like features conferred by Sox2 in a small cell population in estrogen receptor-positive breast cancer.

- Cell Signal 2016; 28: 42-50.
53. Shin S, Rossow KL, Grande JP, Janknecht R. Involvement of RNA helicases p68 and p72 in colon cancer. *Cancer Res* 2007; 67: 7572-8.
 54. Liu X, Li L, Geng C, et al. DDX17 promotes the growth and metastasis of lung adenocarcinoma. *Cell Death Discov* 2022; 8: 425.
 55. Wortham NC, Ahamed E, Nicol SM, et al. The DEAD-box protein p72 regulates ERalpha-/oestrogen-dependent transcription and cell growth, and is associated with improved survival in ERalpha-positive breast cancer. *Oncogene* 2009; 28: 4053-64.
 56. Ku HC, Cheng CF. Master regulator activating transcription factor 3 (ATF3) in metabolic homeostasis and cancer. *Front Endocrinol (Lausanne)* 2020; 11: 556.

Primary renal *BCOR::CCNB3* sarcoma in a female patient: case report

Somang Lee¹, Binnari Kim^{1,2}

¹Department of Pathology, Ulsan University Hospital, Ulsan, Korea

²University of Ulsan College of Medicine, Ulsan, Korea

BCOR-rearranged sarcoma was classified by the World Health Organization in 2020 as a new subgroup of undifferentiated small round-cell sarcoma. It is known to occur very rarely in the kidney. This report presents the first case of a primary renal *BCOR::CCNB3* sarcoma in a 22-year-old woman. An 8-cm cystic mass was identified in the left kidney by abdominal pelvic computed tomography. Histopathologic examination revealed the mass to be composed of small round to oval or spindle cells with fibrous septa and a delicate vascular network. A *BCOR::CCNB3* fusion was detected by next-generation sequencing-based molecular testing. *BCOR::CCNB3* sarcoma presents diagnostic difficulties, highlighting the importance of recognizing its histological features. Immunohistochemical markers are helpful for diagnosis, but genetic molecular testing is necessary for accurate diagnosis. These tumors have a very poor and aggressive prognosis, and an optimal therapeutic regimen has not yet been defined. Therefore, further studies are needed.

Keywords: Adult; Biomarkers, tumor; Female; Gene fusion; Immunogistochemistry; Kidney; Sarcoma

INTRODUCTION

Ewing sarcoma (ES) and Ewing-like sarcoma are highly aggressive round-cell mesenchymal neoplasms [1]. Ewing-like sarcoma refers to tumors that histologically resemble ES but lack the characteristic fusion between the *EWSR1* gene and various members of the ETS family of transcription factors [1]. Recent advances in molecular techniques have revealed new entities in addition to ES, including round-cell sarcomas with *EWSR1* gene fusion with non-ETS family members, *CIC*-rearranged sarcomas, and *BCOR*-rearranged sarcomas [1].

BCOR::CCNB3 fusion is the most common *BCOR* gene abnormality and was first identified by Pierron et al. in 2012 [2] through RNA sequencing and subsequent reverse transcription polymerase chain reaction (RT-PCR) confirmation in a large series of sarcoma cases. *BCOR::CCNB3* fusion arises from a

paracentric inversion on the X chromosome between exon 15 (Xp11.4) of *BCOR* and exon 5 (Xp11.22) of *CCNB3* [3]. This fusion alters the complex associated with chromatin remodeling and histone modifications, impacting downstream gene regulation and contributing to sarcomatogenesis [3,4]. The 5-year survival rate for patients with *BCOR::CCNB3* sarcoma is similar to that of ES patients (72%–80%) and superior to that of *CIC*-rearranged sarcoma [3]. It is currently considered responsive to conventional ES therapy, although treatment guidelines are not firmly established due to the limited number of cases [3].

There have been few reports of primary renal *BCOR::CCNB3* sarcoma, with only 11 cases documented worldwide, all of which involved male patients [5]. Here, we present the first case of primary renal *BCOR::CCNB3* sarcoma in a 22-year-old woman, which posed diagnostic challenges.

Received: May 30, 2024 **Revised:** August 20, 2024 **Accepted:** September 30, 2024

Corresponding Author: Binnari Kim, MD, PhD

Department of Pathology, Ulsan University Hospital, 25 Daehakbyeongwon-ro, Dong-gu, Ulsan 44033, Korea
Tel: +82-52-250-8953, Fax: +82-52-250-8059, E-mail: 0734953@uuh.ulsan.kr

This is an Open Access article distributed under the terms of the Creative Commons Attribution Non-Commercial License (<https://creativecommons.org/licenses/by-nc/4.0/>) which permits unrestricted non-commercial use, distribution, and reproduction in any medium, provided the original work is properly cited.

© 2025 The Korean Society of Pathologists/The Korean Society for Cytopathology

CASE REPORT

A 22-year-old female patient with an unremarkable medical history visited the hospital complaining of lower back and lower abdominal pain that had persisted for several days. Physical examination revealed tenderness in the lower abdomen and percussion pain in the left flank. Abdominal pelvic computed tomography showed a large cystic lesion measuring 8 cm in diameter with peripheral and septal enhancement in the left kidney (Fig. 1A). Initially, a needle biopsy was attempted to rule out malignancy, but it was unsuccessful. Therefore, a laparoscopic radical nephrectomy was subsequently performed for both diagnostic and therapeutic purposes.

Macroscopic examination revealed that the kidney measured 12.5 cm × 9.0 cm × 7.5 cm and weighed 412 g. A well-demarcated, lobulated, solid, and firm tumor measuring 9.5 cm × 7.5 cm × 5.0 cm was identified in the renal pelvis (Fig. 1B). This tumor was closely adjacent to the renal capsule and extended into the perinephric fat tissue. The cut surface of the tumor displayed a predominantly tan and ivory color with multifocal areas of hemorrhage and necrosis.

Microscopic examination revealed that the mass was composed of solid sheets of small round to oval or spindle cells, interspersed with fibrous septa (Fig. 2A). The mass exhibited focal cystic change, hemorrhage, necrosis, and focal hyalinization (Fig. 2B, C). A delicate vascular network was observed with ex-

travasated red blood cells (Fig. 2D). At high-power magnification, the tumor cells exhibited vesicular nuclei, pale chromatin, and inconspicuous nucleoli (Fig. 2E). The nuclear membranes were indistinct and irregular, and the cytoplasm appeared clear to mildly eosinophilic. Frequent mitotic figures were identified, with up to 23 mitoses per 10 high-power fields (Fig. 2F).

Immunohistochemistry revealed diffusely strong nuclear positivity for TLE1 and focal nuclear positivity for cyclin D1 (Fig. 2G, H), diffuse cytoplasmic and membranous positivity for BCL2 (Fig. 2I), and membranous positivity for CD56 (Fig. 2J). The tumor cells were negative for CD99 (Fig. 2K). CD34 immunostaining showed extensive vascular proliferation within the tumor (Fig. 2L).

For more accurate diagnosis and treatment planning, next generation sequencing (NGS)-based molecular test was conducted using CancerScan V3.1 (Twist Biosciences, South San Francisco, CA, USA), a hybrid capture panel containing 407 genes along with introns of three genes for fusion hotspots. The panel also incorporates approximately 4,000 additional single-nucleotide polymorphisms distributed evenly across chromosomes for copy number variation purity correction and specific regions for microsatellite instability detection [6]. The quality of the NGS test was excellent, with a 98.86% on-target rate, mean depth = 612.45×, uniformity = 96.68%, and Q30 = 91.51%. In addition to detecting 15 single nucleotide variants and indels that were not clinically significant, the test identified

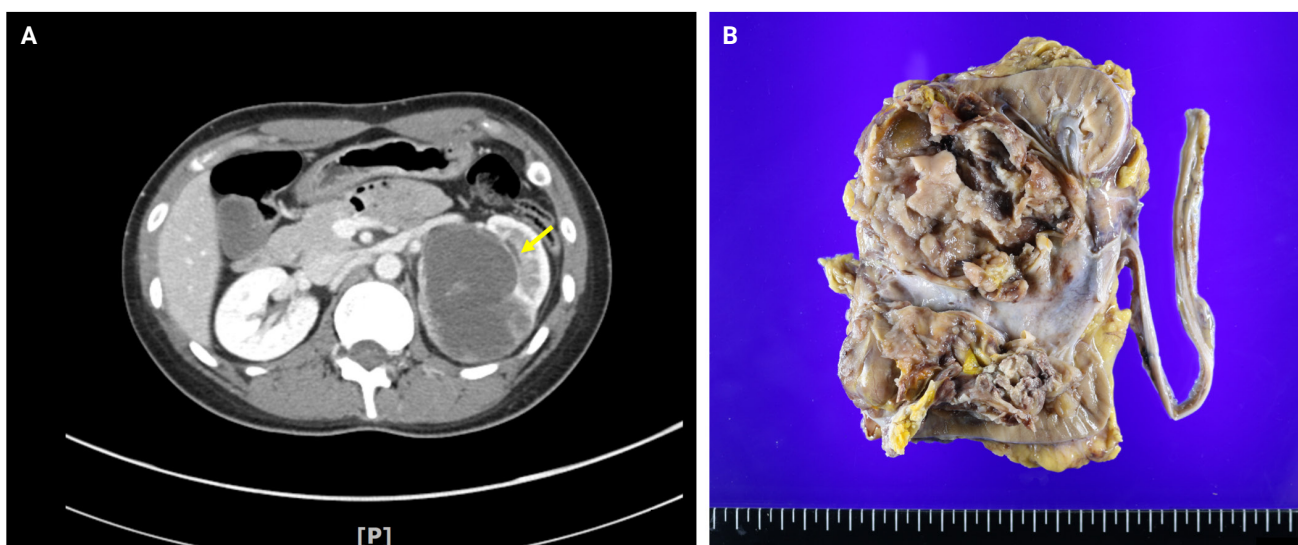


Fig. 1. Computed tomography image and gross findings. (A) Computed tomography scan reveals a well-defined, huge, solid-cystic tumor with focal enhancement (arrow). (B) A well-demarcated large solid tumor with cystic change in the renal pelvis.

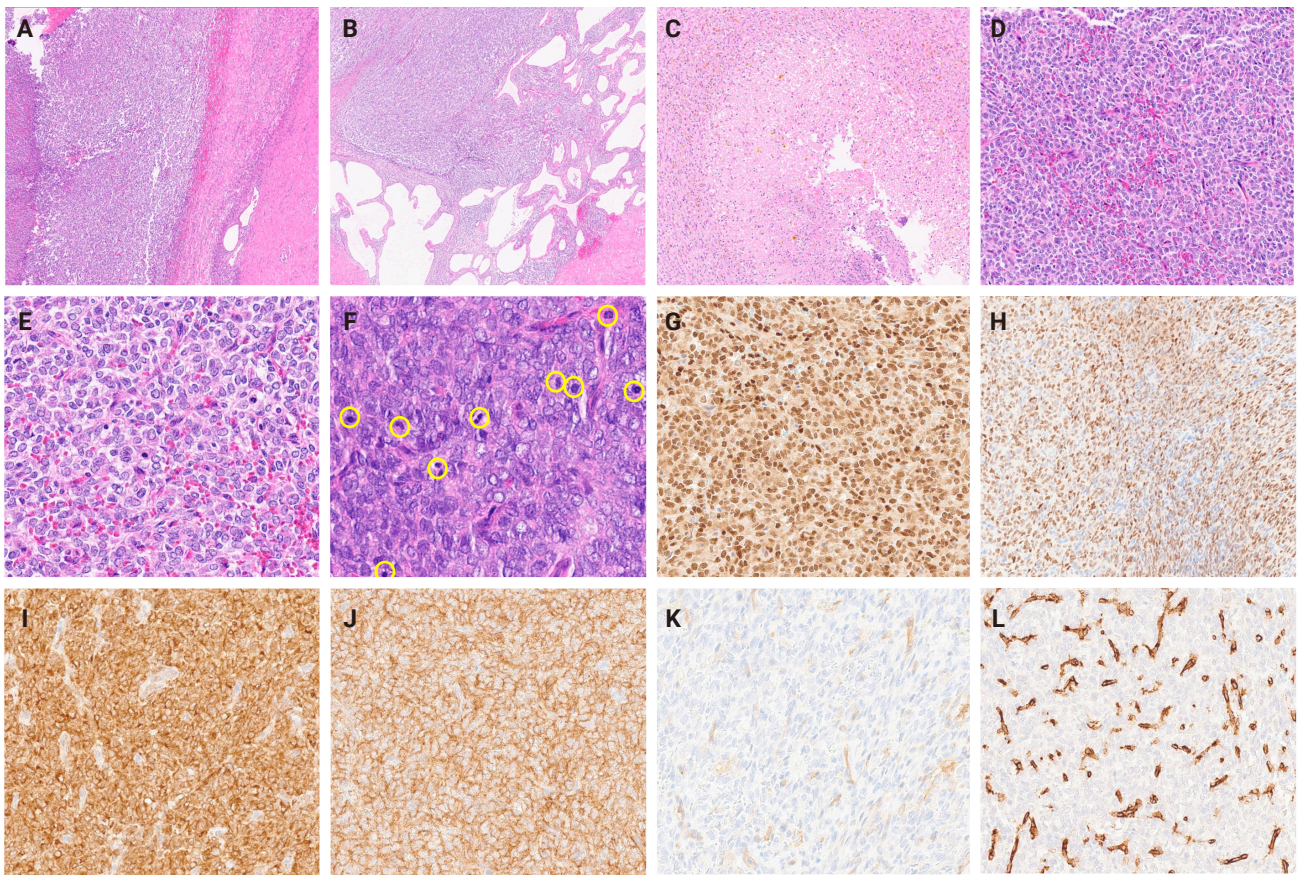


Fig. 2. Microscopic and immunohistochemistry findings of the tumor. (A) Solid growth pattern separated by fibrous septa. (B) Cystic change. (C) Necrosis. (D) Vascular networks with extravasated red blood cells. (E) Round to oval tumor cells with vesicular nuclei, irregular nuclear membrane, inconspicuous nucleoli, and clear to eosinophilic cytoplasm. (F) Increased mitotic activity (circles) up to 23/10 high-power field. (G) Diffuse strong nuclear positivity for TLE1. (H) Focal nuclear positivity for cyclin D1. (I) Diffuse cytoplasmic and membranous positivity for BCL2. (J) Diffuse membranous positivity for CD56. (K) No immunopositivity for CD99. (L) CD34 highlighted vascular networks.

a *BCOR::CCNB3* fusion, which was critical for diagnostic confirmation.

Although the tumor was completely removed with negative resection margins, the patient underwent postoperative chemotherapy using vincristine, adriamycin, cyclophosphamide alternating with ifosfamide, and etoposide (VAC/IE) to reduce recurrence potential. The patient remained stable for 10 months after postoperative chemotherapy, but the tumor recurred in the pelvis and left lower back skin. Subsequently, the patient underwent wide excisions for the recurrent tumors. Despite these procedures, the tumor metastasized to retroperitoneum and the lung. High-dose ifosfamide chemotherapy was administered, but metastatic tumors recurred five months later. Additional chemotherapy using irinotecan, gemcitabine, and docetaxel was attempted, but the patient expired 3 years after

the initial diagnosis. The clinical course following nephrectomy is depicted in Fig. 3.

DISCUSSION

BCOR-rearranged sarcoma is a rare tumor, particularly in the kidney [5]. It was first described by Pierron et al. in 2012 [2]. This newly recognized entity encompasses several variants, including *BCOR::CCNB3* sarcoma, sarcoma with *BCOR* variant fusions with a non-*CCNB3* partner, and sarcomas with internal tandem duplication of *BCOR* exon 15 (*BCOR* ITD) [5]. *BCOR* ITD is predominantly associated with clear-cell sarcomas of the kidney (CCSK), while *BCOR::CCNB3* fusion is identified in rare cases of renal sarcomas [5].

BCOR::CCNB3 sarcoma is relatively more common in bone

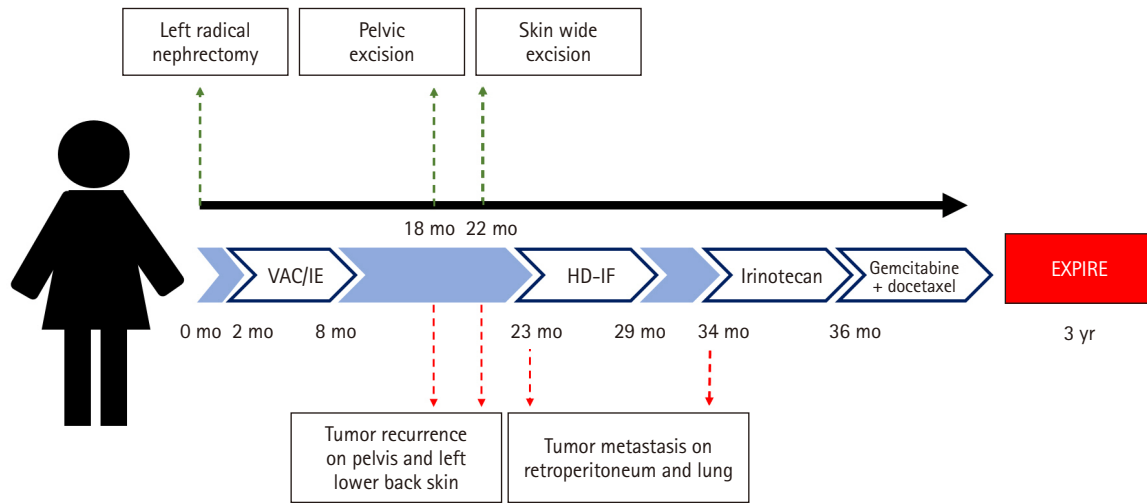


Fig. 3. Patient clinical course after left radical nephrectomy. VAC/IE, vincristine, adriamycin, cyclophosphamide alternating with ifosfamide and etoposide; HD-IF, high-dose ifosfamide.

than soft tissue, with a ratio of 1.5:1, and it tends to preferentially affect the pelvis, lower extremities, and paraspinal area. This type of sarcoma is most frequently seen in adolescents and young adults, with a male predominance; over 90% of patients are under 20 years old [4,7]. Only a small fraction (7.6%) of cases involve adults over 20 years old [8]. In contrast, sarcoma with *BCOR*-ITD mainly occurs in the soft tissues of the trunk, retroperitoneum, and head and neck, typically sparing the extremities [7]. Additionally, *BCOR*-ITD tumors often present within the first of year of life or even at birth, with 41% of cases diagnosed before the age of one [7,8].

To date, all 11 reported cases of primary renal *BCOR::CCNB3* sarcoma have occurred in male patients, with a mean age of 18 years (Table 1) [3,5,8-13]. The marked male predominance is thought to result from the *BCOR::CCNB3* fusion occurring during pericentric inversion of the X chromosome [13]. Clinical manifestations are nonspecific, with most patients presenting with abdominal pain. At the time of diagnosis, these tumors are usually large (3.2–27 cm), solid, and variably cystic [5]. The clinical manifestations in this case were similar to those reported in previously documented cases, aside from the sex. However, due to its rarity and nonspecific clinical findings, accurate preoperative diagnosis was not achieved [5].

Histopathological diagnosis is challenging even for experienced renal pathologists because *BCOR::CCNB3* sarcoma exhibits considerable morphological diversity and overlaps significantly with CCSK and synovial sarcoma in its histological and immunohistochemical features [5]. Key histological

features include a uniform proliferation of primitive small round to ovoid and plump spindle cells arranged in solid sheets, surrounded by abundant capillary networks [5]. Immunohistochemical markers such as SATB2, cyclin D1, TLE-1, *BCOR*, and *CCNB3* can be helpful for diagnosis [5]. In previous studies, *BCOR::CCNB3* sarcoma showed positivity for *CCNB3* (97%), *BCOR* (90%), TLE1 (84%), and SATB2 (84%). However, due to the insufficient sensitivity and specificity of these markers, molecular genetic analyses such as fluorescence in situ hybridization, RT-PCR, or RNA sequencing are currently the diagnostic gold standard for confirming the presence of *BCOR::CCNB3* fusion [4,5,7,9].

BCOR::CCNB3 sarcoma prognosis remains uncertain due to its rarity. However, some reports suggest a 5-year survival rate and a disease-free survival rate of approximately 72% and 68%, respectively, similar to those of CCSK and better than those of ES [5]. Other reports suggest the 5-year survival rate is comparable to that of ES [14,15]. A significant proportion of patients with *BCOR::CCNB3* sarcoma experiences metastases, most commonly to the lungs, followed by bone, soft tissue, and visceral sites [14,15]. Poor prognostic factors include axial location, local recurrence, and metastasis [14,15].

The optimal therapeutic regimen for *BCOR::CCNB3* sarcoma has not been established [5]. Since *BCOR::CCNB3* sarcoma was initially classified within the ES family of tumors, most patients have been treated according to ES-related chemotherapy protocols [14,15]. *BCOR::CCNB3* sarcoma has shown a histologic response to ES-based treatment, resulting in better outcomes

Table 1. Summary of primary renal *BCOR::CCNB3* sarcoma cases in the literature

Case No.	Age (yr)/ Sex	Clinical feature	Image finding	Gross finding (size)	Microscopic findings	IHC	Molecular study methods	Treatments	Follow-up
1 [9]	11/M	NA	NA	Cystic (27 cm)	Spindle to epithelioid, biphasic cord cell/septal pattern	BCOR, BCL2, CD56, SATB2, cyclin D1, TLE1 (+)	FISH	Resection	NA
2 [9]	12/M	NA	NA	Solid and cystic (13 cm)	Spindle, biphasic cord cell/septal cell pattern, high mitotic activity	Desmin, S100, AE1/3, CD34 (-) BCOR, BCL2, CD56, SATB2, cyclin D1, TLE1 (+)	FISH	Resection	Recurrence (15 mo)
3 [11]	8/M	NA	NA	NA	NA	Cyclin D1 (+) BCOR: not consistently	RT-PCR, Sanger sequencing	NA	NA
4 [8]	46/M	Incidentally detected	NA	NA (12 cm)	Spindle to oval, fascicular, vascular stroma, high mitotic activity	BCOR, SATB2, CCNB3, INI1, H3K27me3 (+) AE1/3, S100, SMA, desmin, myogenin, STAT6, MDM2 (-)	RNA sequencing, RT-PCR, Sanger sequencing	Resection	NED (54 mo)
5 [8]	26/M	Abdominal pain	NA	NA (16 cm)	Oval, fascicular, vascular stroma, high mitotic activity	BCOR, SATB2, CCNB3, INI1 (+) AE1/3, S100, SMA, desmin, myogenin, STAT6, MDM2, CDK4 (-)	FISH	Resection, chemotherapy	NED (1 mo)
6 [12]	10/M	Abdominal pain, dyspnea	Right renal mass with tumor thrombus extending through IVC into the right atrium	NA (8.1 cm)	Round to oval, spindle, network of capillary	Cyclin D1, NGFR5 (+)	RT-PCR, Sanger sequencing	Neoadjuvant chemotherapy, resection, and radiation therapy	NED (16 mo)
7 [12]	14/M	Back and abdominal pain	Left renal mass with tumor thrombus extending through IVC into the right atrium	NA (12.4 cm)	NA	Cyclin D1, CCNB3 (+)	RT-PCR, Sanger sequencing	Neoadjuvant chemotherapy, resection, and radiation therapy	NED (9 mo)
8 [10]	18/M	Hematuria	Left renal homogeneous solid mass with hemorrhage and IVC thrombus	A smooth lobulated pale pink-tan with hemorrhage (8.4 cm)	Oval to spindle nuclei, myxoid stroma, angulated thin-walled vessels, readily mitotic count	TLE1, cyclin D1, BCL2 (+) PAX8, AE1/AE3, CD34, CD31, STAT6, SMA, desmin, S100, CK7, WT-1, cathepsin-K (-)	RNA sequencing	Resection	NED (6 mo)
9 [5]	16/M	Abdominal discomfort, hematuria	Slightly enhanced, right renal solid mass with focal areas of hemorrhage and cystic change	A well-circumscribed, fleshy solid and cystic (11.3 cm)	Ovoid to spindle cell, solid sheets and vague fascicles, delicate vascular network, scattered mitotic figures	SATB2, cyclin D1, TLE1, PAX8 (focal), EMA (focal) (+) AE1/AE3, NKX2.2, CD99, WT1, CD34, S100 (-)	FISH, RT-PCR, Sanger sequencing	Resection	NED (12 mo)
10 [3]	14/M	Flank pain, hematuria	A well-circumscribed enhancing hypoechoic intrarenal lesion	Solid mass with hemorrhage and necrosis (3.2 cm)	Spindle, vague fascicular	Vimentin, BCL2 (+)	WES, RNA sequencing, GMA, miRNA sequencing	Resection, chemotherapy, and radiation therapy	NED (36 mo)
11 [13]	10/M	Hematuria	Complex solid-cystic, right renal hilar mass, with a filling defect in the right renal vein	A rounded, multilobular solid and cystic (5.5 cm)	Ovoid to spindle, subepithelial stroma, rare mitotic figures	Cyclin D1, WT1 (focal) (+) AE1/AE3, actin, desmin, CD34, BRAF (-)	NGS	Resection, chemotherapy	NA

IHC, immunohistochemistry; NA, not available; BCOR, BCL6 corepressor; BCL2, BCL2 apoptosis regulator; SATB2, SATB homeobox 2; FISH, fluorescence in situ hybridization; RT-PCR, reverse transcription polymerase chain reaction; CCNB3, cyclin B3; SMA, smooth muscle actin; NED, no evidence of disease; CDK4, cyclin dependent kinase 4; IVC, inferior vena cava; NGFR5, nerve growth factor receptor 5; WES, whole-exome sequencing; GMA, global methylation analysis; NGS, next generation sequencing.

[14,15]. Given the overlapping morphology and transcriptional profile of *BCOR::CCNB3* sarcoma and CCSK and the known sensitivity of CCSK to doxorubicin-based chemotherapy, there is a possibility that *BCOR::CCNB3* sarcoma may respond to similar treatments. However, it remains unclear whether these patients would benefit from a less toxic treatment protocol compared with current ES-based regimens [9,15]. Further studies on renal *BCOR::CCNB3* sarcoma are essential to define optimal treatment strategies and accurately predict prognosis for these patients.

Ethics Statement

The case report was approved by the Institutional Review Board of Ulsan University Hospital (UUH 2024-05-030). Informed consent was waived by the Institutional Review Board.

Availability of Data and Material

The datasets generated or analyzed during the study are available from the corresponding author on reasonable request.

Code Availability

Not applicable.

ORCID

Somang Lee <https://orcid.org/0009-0009-0208-0116>
Binnari Kim <https://orcid.org/0000-0002-0934-3056>

Author Contributions

Supervision: Kim B. Validation: Kim B. Visualization: Kim B. Writing—original draft: Lee S. Writing—review & editing: Kim B. Approval of final manuscript: all authors.

Conflicts of Interest

The authors declare that they have no potential conflicts of interest.

Funding Statement

No funding to declare.

REFERENCES

- Sbaraglia M, Righi A, Gambarotti M, Dei Tos AP. Ewing sarcoma and Ewing-like tumors. *Virchows Arch* 2020; 476: 109-19.
- Pierron G, Tirode F, Lucchesi C, et al. A new subtype of bone sarcoma defined by *BCOR-CCNB3* gene fusion. *Nat Genet* 2012; 44: 461-6.
- Hagoel TJ, Cortes Gomez E, Gupta A, et al. Clinicopathologic and molecular analysis of a *BCOR-CCNB3* undifferentiated sarcoma of the kidney reveals significant epigenetic alterations. *Cold Spring Harb Mol Case Stud* 2022; 8: a005942.
- Rekhi B, Kosemehmetoglu K, Ergen FB, et al. Spectrum of histopathological, immunohistochemical, molecular and radiological features in 12 cases of *BCOR::CCNB3*-positive sarcomas with literature review. *Int J Surg Pathol* 2023; 31: 1244-64.
- Zhao M, Zhang Q, He X, Zhang D. Primary renal *BCOR-CCNB3* fusion sarcoma: a case report and review of the literature. *Urol Int* 2022; 106: 644-8.
- Park S, Lee C, Ku BM, et al. Paired analysis of tumor mutation burden calculated by targeted deep sequencing panel and whole exome sequencing in non-small cell lung cancer. *BMB Rep* 2021; 54: 386-91.
- Choi JH, Ro JY. The 2020 WHO classification of tumors of soft tissue: selected changes and new entities. *Adv Anat Pathol* 2021; 28: 44-58.
- Yoshida A, Arai Y, Hama N, et al. Expanding the clinicopathologic and molecular spectrum of *BCOR*-associated sarcomas in adults. *Histopathology* 2020; 76: 509-20.
- Argani P, Kao YC, Zhang L, et al. Primary renal sarcomas with *BCOR-CCNB3* gene fusion: a report of 2 cases showing histologic overlap with clear cell sarcoma of kidney, suggesting further link between *BCOR*-related sarcomas of the kidney and soft tissues. *Am J Surg Pathol* 2017; 41: 1702-12.
- Setoodeh S, Palsgrove DN, Park JY, Pedrosa I, Kapur P, Jia L. Primary renal sarcoma with *BCOR-CCNB3* gene fusion in an 18-year-old male: a rare lesion with a diagnostic quandary. *Int J Surg Pathol* 2021; 29: 194-7.
- Wong MK, Ng CCY, Kuick CH, et al. Clear cell sarcomas of the kidney are characterised by *BCOR* gene abnormalities, including exon 15 internal tandem duplications and *BCOR-CCNB3* gene fusion. *Histopathology* 2018; 72: 320-9.
- Han H, Bertrand KC, Patel KR, et al. *BCOR-CCNB3* fusion-positive clear cell sarcoma of the kidney. *Pediatr Blood Cancer* 2020; 67: e28151.
- Dorwal P, Abou-Seif C, Ng J, Super L, Chan Y, Rathi V. Clear cell sarcoma of the kidney (CCSK) with *BCOR-CCNB3* fusion: a rare case report with a brief review of the literature. *Pediatr Dev Pathol* 2023; 26: 149-52.
- Cohen-Gogo S, Cellier C, Coindre JM, et al. Ewing-like sarcomas with *BCOR-CCNB3* fusion transcript: a clinical, radiological and pathological retrospective study from the Societe Francaise des

- Cancers de L'Enfant. *Pediatr Blood Cancer* 2014; 61: 2191-8.
15. Kao YC, Owosho AA, Sung YS, et al. *BCOR-CCNB3* fusion positive sarcomas: a clinicopathologic and molecular analysis of 36 cases with comparison to morphologic spectrum and clinical behavior of other round cell sarcomas. *Am J Surg Pathol* 2018; 42: 604-15.